DIMERIZATION OF THE NOTCH INTRACELLULAR DOMAIN RESULTS IN DISTINCT SIGNALING ACTIVITY

by

Jacob Jeffery Crow

A dissertation

submitted in partial fulfillment

of the requirements for the degree of

Doctor of Philosophy in Biomolecular Sciences

Boise State University

August 2020

BOISE STATE UNIVERSITY GRADUATE COLLEGE

DEFENSE COMMITTEE AND FINAL READING APPROVALS

of the dissertation submitted by

Jacob Jeffery Crow

Dissertation Title: Dimerization of the Notch Intracellular Domain Results in Distinct Signaling Activity

Date of Final Oral Examination: 12 August 2020

The following individuals read and discussed the dissertation submitted by student Jacob Jeffery Crow, and they evaluated their presentation and response to questions during the final oral examination. They found that the student passed the final oral examination.

Allan Albig, Ph.D.	Chair, Supervisory Committee
Julia Thom Oxford, Ph.D.	Member, Supervisory Committee
Kenneth A. Cornell, Ph.D.	Member, Supervisory Committee
Richard S. Beard, Ph.D.	Member, Supervisory Committee

The final reading approval of the dissertation was granted by Allan Albig, Ph.D., Chair of the Supervisory Committee. The dissertation was approved by the Graduate College.

DEDICATION

I'd like to dedicate this dissertation to my parents, Jeff and Maria Crow, who have always encouraged and nurtured academic excellence, never-wavering integrity, an intense work ethic, and a passion for whatever I set my sights on. They taught through example how to persevere and stay headstrong when life gets challenging and reminded that hard work eventually pays dividends. Little did I know back then, this type of tenacity is a much-needed skill in the sciences and one that I became am intimately familiar with.

Thank you.

ACKNOWLEDGMENTS

I'd like to thank Dr. Allan Albig for being my scientific mentor through my undergraduate and graduate careers. I have studied and researched under Allan's guidance for quite some time (nearly eight years!) and was even one of the first students Allan took on when he transitioned to Boise State University. During this time, I've experienced many changes within the Albig laboratory; from a plethora of students coming and going, a handful of grant turnovers, and even Allan's transition into associate professorship! One thing remaining constant, however, is his passion for science and mentorship. Through the thick and thin, you knew you could go to him for ideas, questions, and advice. Whether it was in his office or even while he was working alongside you in the lab (yes, this PI still works in the lab), he was always easily accessible, open to help, encouraging, and understanding. Finally, along with Dr. Albig and a special mention for Dr. Alison Miyamoto, I'd like to acknowledge all the past, present, and future Albig lab members. I couldn't have asked for a better group of people to work with. Thanks for putting up with my bitching.

ABSTRACT

The Notch signaling pathway is a core component of multicellularity; enabling cells to directly communicate with both their neighbors and the surrounding microenvironment. These signals are translated directly through the Notch proteins, where a fragment of Notch transitions into the nucleus to act as a co-transcription factor, setting into motion a host of physiological responses. Commonly involved in pathways that define a cell's identity and fate decisions, what appears to be a simplistic pathway instead exists in a state of high-tunability and strict control. Missteps in this pathway are generally embryonically lethal or lead to a suite of congenital disorders and cancers. Therefore, it's pertinent to understand the mechanisms of Notch that provide its flexibility and pleiotropic outcomes. One such property is its ability to homodimerize on DNA while within its transcriptional activation complex, resulting in an enhanced transcriptional signal of a select pool of Notch target genes. This dissertation reviews the general mechanics behind Notch signaling, discusses how the field of Notch dimerization came to be and where it stands currently, and finally, details my contributions to the understanding of this regulatory mechanism. Despite Notch's ubiquitous function in metazoan life, there are still many mysteries behind this signaling pathway. The work detailed here describes my time spent as a basic science researcher, where my findings contribute a couple of puzzle pieces to the expansive Notch signaling field.

TABLE OF CONTENTS

LIST OF TABLES

LIST OF FIGURES

LIST OF ABBREVIATIONS

ADAM	A Disintegrin And Metalloprotease
ANK	Ankyrin repeats
BP	Base Pairs
BTD	Beta-Trefoil Domain
ChIP	Chromatin Immunoprecipitation
ChIP-seq	Chromatin Immunoprecipitation with parallel DNA sequencing
Co-IP	Co-Immunoprecipitation
CSL	CBF-1/Suppressor of Hairless/Lag-1
CTCF	CCCTC-binding factor
CycC:CDK	Cyclin C/Cyclin-dependent kinase
DLL	Delta-like ligand
DSL	Delta/Serrate/LAG-2
EGF	Epidermal Growth Factor
EMSA	Electrophoretic Mobility Shift Assay
FBXW7	F-box/WD repeat-containing protein 7
FRET	Fluorescence Resonance Energy Transfer
GSK-3α or β	Glycogen synthase kinase-3α or β
HD	Heterodimerization domain
HEK293T	Human embryonic kidney cells with the SV40 large T antigen
Hes	Hairy and enhancer of split family members

Hey	Hairy/enhancer-of-split related with YRPW motif family members
HH or H-H	Head-to-Head
HT or H-T	Head-to-Tail
JAG	Jagged
LNR	Lin12/Notch Repeats
MAML	Mastermind-like family members
MNNL	Module at the N-terminus of Notch Ligands
NICD	Notch Intracellular Domain
NLS	Nuclear Localization Signal
NRR	Negative Regulatory Region
NTC	Notch transcriptional activation complex
PEST	Proline/Glutamic acid/Serine/Threonine
RAM	RBPJ associated module
RBPJ	Recombination signal Binding Protein for immunoglobulin kappa J region
RHR-N or -C	Rel-homology region, -N or -C for N- and C-Terminal domain
ROI	Region of Interest
SCF complex	Skp, Cullin, F-box containing complex
SpDamID	Split DNA adenine methyltransferase identification
SPS	Sequence-paired site
TAD	Transactivation domain
T-ALL	T-cell acute lymphoblastic leukemia
TM	Transmembrane

CHAPTER ONE: INTRODUCTION

Classical Notch Signaling

The Notch signaling system is a core component of multicellularity; utilized across the metazoan spectrum with components of the pathway found in even earlier common ancestors [1–3]. These ubiquitous signaling proteins engage in cell-to-cell contacts and through this mechanism, control processes such as differentiation, cell identity, and maintenance of tissue homeostasis. When dysregulated, either through direct Notch mutations or other indirect mechanisms, it can result in an assortment of genetic disorders and cancers (thoroughly reviewed by Siebel & Lendahl, (2017) [4]). Amusingly, phenotypic mutations within Notch signaling resulted in its initial identification, where over 100 years ago landmark studies first described 'Notches' in *Drosophila melanogaster* wings [5,6] (Figure 1.1A). As the field of genetics progressed, a Notch gene from fruit flies was first cloned, sequenced, and initially characterized in the 80s [7–10]. Finally, developments within the fields of cell and molecular biology have surged research on Notch signaling forward to where it is today (summarized in Figure 1.1B). This introductory chapter aims to summarize the field as it currently stands; including both Notch signaling at large and a specific signaling mechanism, the dimerization of the Notch intracellular domain. The following chapters within this dissertation detail my contributions to this ever-evolving field.

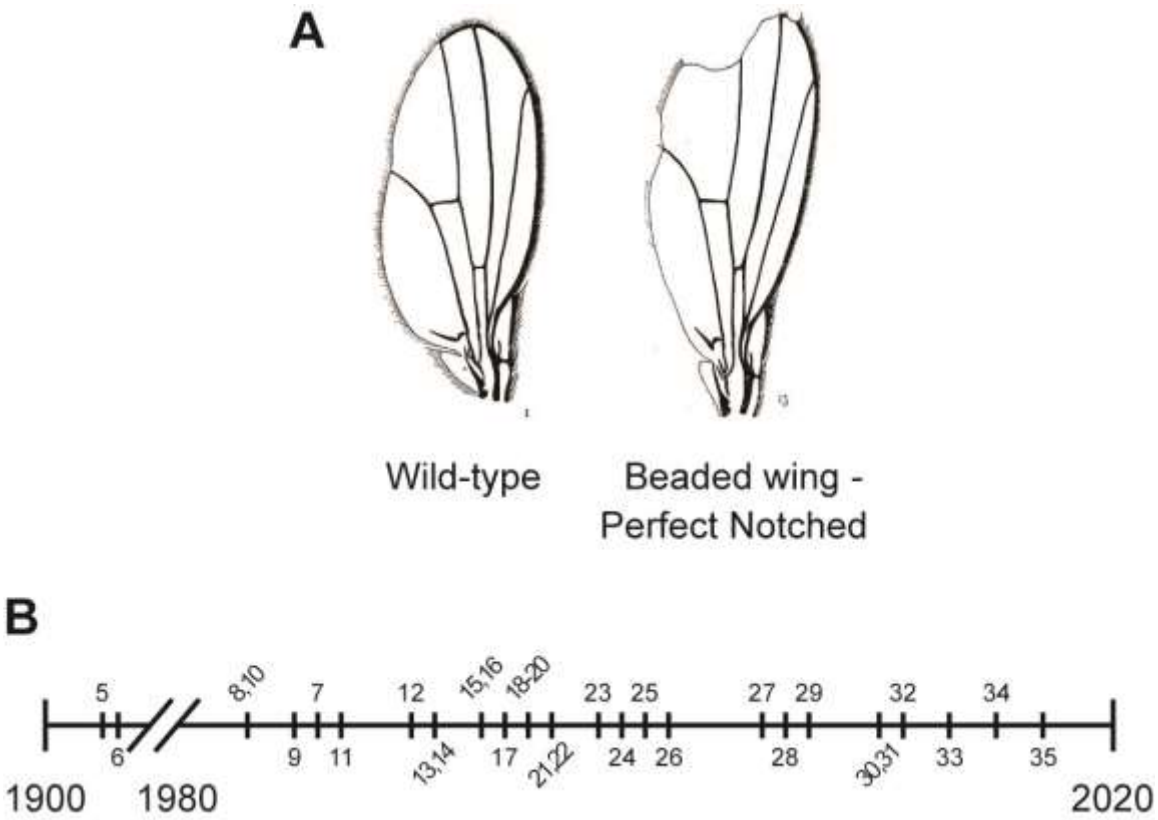

Figure 1.1: Landmark Studies Concerning Notch's Function and Dimerization

A) Adapted from his original manuscript, Dexter JS. (1914) The Analysis of a Case of Continuous Variation in Drosophila by a Study of its Linkage Relations. *The American Naturalist*. 48(576): 712-758., Dexter described a Beaded wing, *D. melanogaster* line, with "Perfect Notched" wings. This phenotypic observation is the namesake for the Notch signaling pathway. B) A timeline representing over a hundred years of Notch signaling research, emphasizing the last forty years of progress. Selected publications represent landmark studies with key findings of what the Notch protein is, identification of its structural domains, how it functions, and eventually, how it signals through NICD dimerization. The following table lists these breakthrough manuscripts and their key finding(s).

Authors (First and Last), Year Published, Reference Number	**Critical Finding, Emphasis on NICD Dimerization**
Hunt TH (1911) [5]	Notch Fly Phenotype
Dexter JS (1914) [6]	Notch Fly Phenotype
Kidd S, Young MW, et al. (1983) [8]	Notch Gene Identification (Fly)
Artavanis-Tsakonas S, Yedvobnick B, et al. (1983) [10]	Notch Gene Identification (Fly)
Wharton KA, Artavanis-Tsakonas S, et al. (1985) [9]	Sequence, Structure Prediction
Kidd S, Young MW, et al. (1986) [7]	Sequence, Structure Prediction
Breeden L and Nasmyth K (1987) [11]	Ankyrin Repeats Identification
Lux SE, Bennett V, et al. (1990) [12]	Ankyrin Repeats Identification
Rebay I, Artavanis-Tsakonas S, et al. (1991) [13]	Receptor/Ligand Activation
Weinmaster G, Lemke G, et al. (1991) [14]	Notch Gene Identification (Mammal, Rat)
Rebay I, Artavanis-Tsakonas S, et al. (1993) [15]	Extracellular = Regulatory, Intracellular = Activity
Lieber T, Young MW, et al. (1993) [16]	Ankyrin domain is necessary, NICD found in the nucleus
Tun T, Kawaichi M, et al. (1994) [17]	RBPJ DNA binding sequence
Jarriault S, Israel A, et al. (1995) [18]	Notch interacts with RBPJ, Interaction induces gene transcription
Bailey AM and Posakony JW (1995) [19]	Sequence-paired site Identification
Tamura K, Honjo T, et al. (1995) [20]	RBPJ and NICD's RAM interaction
Kato H, Honjo T, et al. (1996) [21]	Comparison of the Notch1-4 family members
Kopan R, Nye JC, et al. (1996) [22]	Canonical Activation
Schroeter EH, Kopan R, et al. (1998) [23]	Canonical Activation
Nellesen DT, Posakony JW, et al. (1999) [24]	Sequence-paired site Identification
Wu L, Griffin JD, et al. (2000) [25]	MAML1 interacts with NICD
Kitagawa M, Harigaya K, et al. (2001) [26]	MAML1 interacts with NICD
Cave JW, Caudy MA, et al. (2005) [27]	Sequence-paired site Identification
Ong C, Kopan R, et al. (2006) [28]	Sequence-paired site Identification, Thorough Promoter Analysis
Nam Y, Blacklow SC, et al. (2007) [29]	Ankyrin-mediated Dimerization Model
Arnett KL, Blacklow SC, et al. (2010) [30]	Ankyrin-mediated Dimerization Crystal
Liu H, Pear WS, et al. (2010) [31]	Dimerization's Physiological Relevance
Vasquez-Del Carpio R, Capobianco AJ, et al. (2011) [32]	Anti-parallel Dimerization Model
Castel D, Stunnenberg HG, et al. (2013) [33]	Sequence-paired site Identification
Hass MR, Kopan R, et al. (2015) [34]	Sequence-paired site Identification
Severson E, Aster JC, et al. (2017) [35]	Analysis of Cryptic SPSs, Sequence-paired site Identification

Protein Structure and Processing

As a transmembrane signaling protein, Notch can be readily split into two functional halves. The extracellular region interacts with neighboring cells to receive signals from their displayed ligands, while the intracellular region translates this signal into transcriptional responses. For a structural summary of the Notch1 receptor, refer to Figure 1.2, where each indicated subdomain will be discussed in the following sections.

The Extracellular Domain

Throughout its lifetime the Notch protein is continuously processed and cleaved to elicit or inhibit its transcriptional capabilities. The first cleavage event occurs during its initial maturation before it traffics to the plasma membrane, where within the trans-Golgi network it is cleaved by the convertase Furin (or Furin-like proteases) at the S1 cleavage site [36,37]. Interestingly, cleavage at this location is not necessary for normal Notch extracellular domain folding or further proteolysis, but instead is required for standard trafficking to the cell surface [38,39], though this mechanism is not well understood. As a mature protein, the extracellular and intracellular halves of Notch are held together by several interdomain non-covalent interactions. The first is through a region termed the heterodimerization domain (HD) which consists of hydrophobic and electrostatic interactions, rejoining the two Notch parts separated by S1 cleavage. Importantly, the HD contains an internal S2 cleavage site which is covered and protected by the other set of interdomain contacts, the three Lin12/Notch repeats (LNR) [40,41]. Altogether, these components and contacts form the negative regulatory region (NRR) and its activation will be further explored in the ‘Signaling Mechanism’ section.

Beyond this crucial regulatory region lies the Epidermal Growth Factor (EGF)-like repeats which make up the bulk of the extracellular domain. These repeats are heavily post-translationally modified by several forms of *O*-linked glycosylation and act to regulate Notch signaling through its interactions with partner ligands. This regulation is variable based on the EGF-like repeat composition of the different Notch receptors, what ligands are available to interact with, and even depends on cell-specific contexts which dictate how the EGFs are first modified (thoroughly reviewed by Harvey & Haltiwanger, (2018); Gordon et al., (2008) [42,43]).

The Intracellular Domain

Soon after the S2 site within the HD is a transmembrane-spanning domain, followed by the remainder of the Notch protein; the Notch Intracellular Domain (NICD). Located within the transmembrane-spanning region are the S3 and S4 cleavage sites, both cleaved by the presenilin/γ-secretase complex. The S3 cleavage site is near the cytosolic side of the plasma membrane [23], though the exact cleavage location and the resulting start of the N-terminus of the NICD are variable based on if the Notch protein goes through traditional ligand-induced activation or endosomal-mediated signaling [44,45]. The S4 cleavage site is found near the middle of the transmembrane spanning region and, when cleaved, results in the secretion of a small extracellular/intramembrane fragment [46,47].

Starting immediately after the S3 cleavage sites is the NICD, the transcriptionally active, "dissertation-relevant" portion of the Notch protein. It consists of three large domains with a plethora of other regulatory elements within. To be discussed in length in the upcoming 'Transcriptional Activation Complex' and 'Notch Intracellular Domain Dimerization' sections, Notch is a co-transcription factor which interacts with the DNA-

binding protein Recombination signal Binding Protein for immunoglobulin kappa J region (RBPJ), also commonly called CSL, for CBF-1/Suppressor of Hairless/Lag-1. This interaction with RBPJ is initiated through the first of NICD's large domains, the RBPJ associated module (RAM) domain [20,48].

The second large domain is composed of ankyrin repeat (ANK) motifs, which are individually made up of two antiparallel α-helices connected by a short loop, with tandem ankyrin repeats linked together by longer loops [49]. Notch contains seven of these ankyrin repeats, and this domain is essential for transcriptional activation of target genes by mediating protein-protein interactions [18,50]. Critically, when an active NICD molecule binds to a DNA-bound RBPJ protein, this complex further recruits a Mastermind-like (MAML) family member through interactions with both RBPJ and NICD's ankyrin domain [51].

The third large domain is the transactivation domain (TAD), which is the least characterized region within the Notch proteins. Its presence in Notch1 is a requirement for successful activation of target genes [52,53], yet its structural characteristics and interactions aren't well defined. Overall, it's thought to augment Notch1-induced transcription by playing roles in the assembly of the Notch1/RBPJ/MAML ternary transcription complex [54], and may also be involved in the recruitment of other transcriptional machinery, like histone acetyltransferases [55,56].

Beyond these large domains are several smaller structural features and a wide array of post-translational modifications. These modifications range from the assortment of glycosylations on the EGF-like repeats, to protein attachments (ubiquitination/sumoylation), and a plethora of other transient, amino-acid level

modifications (phosphorylations/acetylations/methylations/hydroxylations), all thoroughly reviewed in Antfolk et al., (2019) [57]. Other minor, yet critical, structural features include two nuclear localization signals (NLS) [50,58] and a Proline/Glutamic acid/Serine/Threonine (PEST) domain, which is involved in the Notch protein's rapid degradation [59,60]. An EP domain has also been described within the C-terminus of the ankyrin domain which recruits the histone acetyltransferase p300 [61,62]. However, whether it holds this specific function or if it just aids in the stability of the ankyrin domain, which itself has larger implications, is up for debate [63,64].

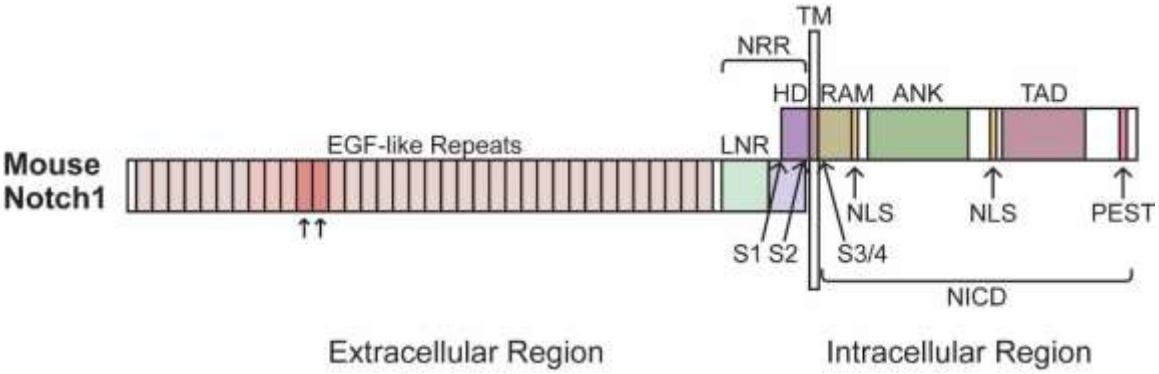

Figure 1.2: Structural Domains of Notch1

The functional domains of the mouse Notch1 protein. As a transmembrane (TM) receptor, Notch can be readily split into two functional regions: the extracellular region which receives signals from neighboring cells and the intracellular region, which translates these signals into transcriptional outputs. This diagram represents a Notch protein that has already been cleaved with Furin at the S1 site, reassembled through the heterodimerization domain, and is primed for activation. EGF-like repeats 8-13 have been identified through color shading, arrows indicate the minimal EGF-like repeats required for Notch activation; repeats 11 and 12 (further discussed in the 'Signaling Mechanism' section). In this figure, the Notch protein and its domains have been scaled accordingly for relative size.

Differences Between the Notch Receptors

Historically, the majority of original structural work was through research on the *D. melanogaster* and *C. elegans* Notch receptor, and fortunately, due to the high conservation of this pathway, most of the identified domains are equivalently found in the vertebrate Notch receptors. Within the vertebrate Notch family, however, there are some noteworthy differences. There are four members of the mammalian Notch family, aptly named Notch1 through 4, which all play roles in development though with varying degrees of importance and overlapping functions. For example, Notch1 and Notch2 knockout mice are embryonically lethal, whereas mice without Notch3 and Notch4 were viable and fertile (whole-animal and tissue-level, conditional Notch knockouts are reviewed in Hozumi, (2020) [65]).

At a structural level, the four Notch proteins are mostly homologous, though with several distinct differences. First, the EGF-like repeats are variable among the Notch proteins: there are 36 repeats in Notch1/2, 34 in Notch3, and 29 in Notch4 [66,67], though they all still contain EGF11 and 12 which are crucial for receptor-ligand interaction (discussed in the 'Signaling Mechanism' section, also in Fleming, (1998) [68]). This variability in the number of repeats, combined with the substantial amino acid differences between their respective EGF-like repeats [69], may allow the Notch receptors to have preferential ligands and other extracellular interactions.

Second, the presence and functionality of the TAD domain is disputed for the Notch receptors. As for the presence of the TAD domain, none of the other Notch proteins have a C-terminus that strictly resembles the TAD found in Notch1, though the equivalent region in Notch2 does behave somewhat similarly [52]. In contrast, a Notch1-esque TAD is

nonexistent in Notch3 and 4, though the C-terminal region past the ankyrin domain in Notch3 does interact with some zinc finger-mediated transcription factors, resulting in its trans-activation [28].

Finally, there are mixed reports about if the Notch4 protein is even capable of canonical Notch signaling, despite having all the necessary domains for minimal activity. In all cases, a constitutively active Notch4 intracellular domain could induce transcriptional signal, so the question lies in if the extracellular domain can bind to a ligand and induce the cascade of cleavages to release the N4ICD. This question is commonly addressed through co-culture experiments, where one cell type has the Notch4 receptor and is grown alongside another cell type presenting a Notch ligand. Paradoxically, some co-cultures with cells presenting the Notch ligands Delta-like 4 or Jagged1 weren't capable of activating Notch4 [70,71], whereas other co-cultures, using the same ligands, did observe Notch4 activation [72,73]. Therefore, despite having the same proteins present, the collective results here are conflicting. This can likely be contributed to the usage of different cell lines or different overall methodologies, but all told, it's still unknown if or under what contexts, Notch4 if capable of canonical Notch signaling.

Signaling Mechanism

All Notch proteins signal through the same activation format. As summarized in Figure 1.3, Notch proteins are found on the cell surface, primed for activation, awaiting interactions with a ligand displayed by a physically interacting, neighbor cell. These interactions induce a cascade of proteolytic cleavages within the Notch protein that results in the release of the intracellular domain. As a co-transcription factor, the NICD

translocates to the nucleus to induce transcription of target genes. The following section will further explore each step of this signaling mechanism.

After the initial protein cleavage event by Furin, the heterodimerized Notch protein awaits at the cell membrane in an autoinhibited state. In this state, the S2 cleavage site is physically protected by the NRR, where if absent or non-functional, the S2 site is readily available for cleavage and results in a constitutively active Notch receptor [16,40,41,74,75]. Instead, typical Notch activation is through EGF-mediated interactions with the DSL (Delta, Serrate, LAG-2) family of ligands (Delta-like 1, 3, 4 (DLL1,3,4), and Jagged1, 2 (JAG1,2) in humans). These ligands (excluding DLL3, see Chapman et al., (2011); Ladi et al., (2005) [76,77]) are present on neighboring cells' surfaces and interact with the EGF-like repeats within the Notch extracellular domain. These interactions are mediated through two ubiquitous domains found within the DSL ligands: an N-terminal C2 phospholipid recognition domain (also called an MNNL domain) [78,79], followed by a DSL domain [80]. These structural components and interactions are thoroughly reviewed in Handford et al., (2018) [81].

Among the many EGF-like repeats within Notch, substantial mutational analysis initially uncovered that the repeats 11 and 12 were critical for signaling [13], though these repeats alone were not enough for complete ligand-mediated activation [15]. The scope of necessary EGF repeats has expanded since then, where an assortment of other studies implicate repeats 8-13 and beyond to mediate ligand-receptor affinity and preferences [82–88]. Nevertheless, in an antiparallel fashion, the glycosylated Notch EGF repeats 11 and 12 are the minimum required for ligand-receptor interactions. In Figure 1.2 and 1.3, these repeats have been differentially shaded (8-13) and further identified through arrows (11-

12). The engagement between the Notch receptor's repeats 11 and 12 and a potential ligand is through the C2 and DSL domains of a partnered DSL ligand [89] and is sufficient to induce the next step in the activation pathway: ligand-induced proteolysis.

Upon Notch-ligand engagement, the signal sending cell endocytoses the DSL ligand through Clathrin-mediated processes [90,91]. The mechanism or triggering behind this event is not well understood, though evidence suggests that ligand endocytosis is not random or consistently occurring, but instead depends on a Notch extracellular domain interaction [92]. Regardless, this endocytosis transfers a mechanical force through the heterodimerized Notch receptor, inducing an unfolding event within the NRR [91–95]. Previously compared to a mushroom cap protecting its stem, the LNR domains cover and protect the S2 cleavage site found within the HD domain [43]. Through the endocytotic force, the LNR domains unfold and open the S2 site for cleavage by members of the ADAM (a disintegrin and metalloprotease) protease family [96–98].

The primary ADAM member utilized for ligand-induced proteolysis is ADAM10, though some evidence suggests that ADAM17 is also capable of ligand-independent cleavage of Notch [99–103]. As membrane-bound proteases, they can be classified as sheddases where, as in the case of Notch, they cleave the extracellular portion of proteins from the cell surface. The extracellular Notch fragment, still bound to the DSL ligand, is then completely endocytosed into the signal sending cell and targeted for degradation [92]. The other portion, the membrane-spanning and intracellular domain, is further cleaved at the S3 and S4 sites.

These sites are found within the transmembrane spanning region and are cleaved by the γ-secretase complex, also an integral membrane protein (reviewed in Jorissen & De

Strooper, (2010) [104]). Among other structural components, its catalytic subunits are Presenilin 1 or 2, and these are necessary for the complex to cut Notch and cause the release of the intracellular domain [105,106]. Protein cleavage through γ-secretase is prevented in the presence of a large extracellular domain [107], and therefore, this final cleavage step is regulated by the action of the ADAM proteases. The two cleavage sites are cut sequentially (S3 then S4), and the S3 site ends up dictating the new N-terminus of the NICD [44,46,108]. Canonically, the new N-terminus amino acid is Valine 1744 (for mouse N1ICD, human N1ICD is V1754) but the exact cleavage site can be variable. An alternative, though uncommon, cascade of NICD processing and signaling involves an endocytosis-mediated mechanism, and this subfield is still in development [44,109–112]. Post cleavage, the Notch intracellular domain, through its internal nuclear localization signals, is then translocated and imported into the nucleus through the canonical importin-α/β1 transport pathway [113,114]. Here, the functional roles of the Notch signaling pathway take place.

Transcriptional Activation Complex

Within the nucleus is the transcription factor RBPJ, where it interacts with its cognate DNA binding sites within gene enhancers and promoters. This protein has three functional domains: an N-terminal and C-terminal Rel-homology region (RHR-N or -C), and a beta-trefoil domain (BTD) between them [51,115]. The RHR-N and BTD interact with the DNA's major and minor groove, respectively, resulting in its transcription factor nature [51,115,116]. Importantly, the BTD and RHR-C include the sites for protein-protein interactions, including the interaction with the RAM domain of the NICD, along with a suite of interactions with corepressors [115,117,118]. Notably, RBPJ's default state is one of repression, where the interacting co-repressors differ based on specific cell types or tissues

and the state of development of those cells (thoroughly reviewed in Oswald & Kovall, (2018); Contreras-Cornejo et al., (2016); Borggrefe & Oswald, (2009); [119–121]).

An active Notch signaling pathway works to displace the co-repressors bound to RBPJ and instead recruit its own co-activators to drive transcription of target genes. For a bit of history, the first observations of an RBPJ-Notch interaction was well over twenty years ago [122], and was quickly verified in both vertebrate and invertebrate systems [18,20,123,124]. This signaling system has distinct biological functions, dependent on interactions between RBPJ and Notch, and was observed to occur between each of the four mammalian Notch proteins [21,48].

The transition from corepression to coactivation starts with binding of the NICD RAM domain to RBPJ, which displaces any interacting co-repressors [125]. This protein-protein interaction results in a new binding interface created between RBPJ and the ankyrin domain of Notch, where a member of the MAML family is recruited and binds, creating a ternary complex (RBPJ/NICD/MAML, annotated in Figures 1.3 and 1.4) [25,26,51,117,126–129]. The MAML protein can be considered the catalyst for Notch-regulated transcription, as it recruits an assortment of transcriptional machinery (reviewed in Kitagawa, (2015) [130]). First, MAML1 has been shown to recruit p300/CBP, PCAF, and GCN5 which are all histone acetyltransferases and promote nucleosome acetylation [55,56,61,121,131,132]. Second, MAML1 induces the recruitment of RNA polymerase II for gene transcription. Beyond acetylating DNA, p300/CBP also acetylates MAML1 which creates docking sites for the protein PEAK1 related, kinase-activating pseudokinase 1 (also commonly called NACK and Pragmin). Through currently unknown mechanisms, NACK recruits RNA polymerase II, leading to transcription initiation [133,134].

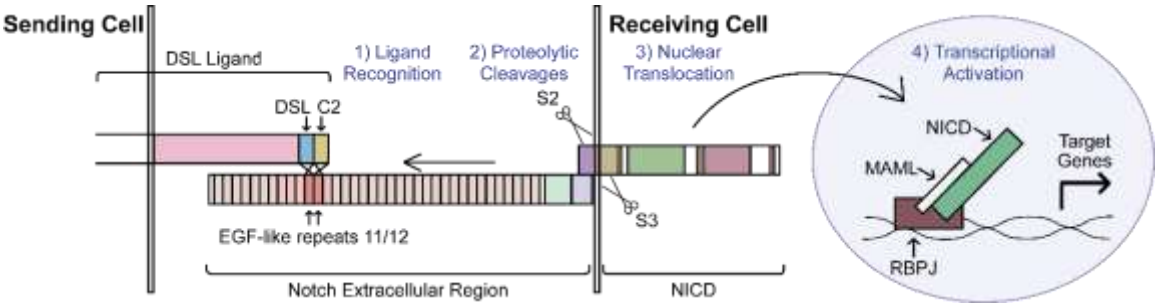

Figure 1.3: Activation of the Notch Signaling Pathway

The activation of the Notch signaling pathway can be summarized into four essential steps, detailed in the above sections. 1) A signal sending cell presents a ligand from the DSL family which interacts with a Notch receptor on the signal-receiving cell's surface. Ligand-receptor recognition, mediated primarily through the ligand's DSL and C2 domains interacting with the receptor's EGF-like repeats 11 and 12, induces endocytosis of the DSL ligand. This places a mechanical pulling force on the attached Notch receptor, inducing an unfolding event of the NRR. 2) This unfolding event allows a series of proteolytic cleavage events; first at the S2 site by an ADAM metalloprotease and then at the S3 site by the γ-secretase complex. 3) These two cleavage events release the transcriptionally active intracellular domain which is free to translocate to the nucleus through the utilization of its nuclear localization signals. 4) Within the nucleus, NICD assembles into a ternary complex with RBPJ and a member of the MAML family. This complex recruits further transcriptional machinery, primarily through interactions with MAML, and eventually drives transcription of Notch target genes.

Signal Inhibition and Protein Degradation

The canonical route for Notch degradation is through the utilization of the Notch PEST domain, though cells utilize several other signaling pathways to turnover and finetune the amount of Notch signal (thoroughly reviewed in Francesca A. Carrieri & Dale,

(2017) [135]). As for PEST-mediated degradation, this route begins immediately after the initiation of gene transcription through the ternary Notch complex. To start, members of the MAML family, all while within the ternary complex, recruit an assortment of kinases that phosphorylate the NICD [131]. This includes the Cyclin C/Cyclin-dependent kinase complex (CycC:CDK1, 2, or 8) which bind directly to MAML and phosphorylate serines and threonines within the NICD TAD and PEST domains [136,137]. The serine/threonine kinases Glycogen synthase kinase-3α/β (GSK-3α or β) are similarly involved phosphorylating amino acids within the PEST domain, but their method of recruitment and regulation is less understood [138–140]. These modified amino acids within the PEST domain form a phosphodegron motif which acts as a specific substrate binding region for the F-box/WD repeat-containing protein 7 (FBXW7), a member of the Skp, Cullin, F-box containing complex (SCF complex), and together act as an E3 ubiquitin ligase [59,60,141–147]. After ubiquitination, the transcriptional signal is halted, the transcription factor complex falls apart, and the NICD is recycled in the proteasome through canonical mechanisms.

While the final proteasome degradation is the same, the route there can change based on alternative mechanisms of Notch signaling or slight protein modifications based on cellular contexts. For some mechanistic examples, there are phosphodegrons found within the RAM and ankyrin domains, regulated through a yet to be identified E3 ligase [148] and through the E3 ligase Itch (also named AIP4) [149,150]. In both of these cases, Notch is signaled for degradation while still in a non-activated state, either before interactions with RBPJ [148] or even at the cell membrane before ligand activation [151–153]. As far as regulation based on cellular context goes, some examples include integrin-linked kinase or the Src family kinases which phosphorylate select serine/threonines or tyrosines,

respectively, found within the Notch ankyrin domain. Their amino acid targets indirectly affect Notch stability through the inactivation or recruitment of other kinases or complex proteins [154–157]. Altogether, these degradation mechanisms allow for the rapid and precise responses to changes in Notch signaling to meet the needs of the cell.

Notch Intracellular Domain Dimerization

Promoter Structure

Canonical Notch target genes, such as those within the hairy and enhancer of split family (Hes1-7) and the Hairy/enhancer-of-split related with YRPW motif protein family (Hey1, 2, L), transition the Notch signal and act as transcriptional repressors (reviewed in Davis & Turner, (2001); Fischer & Gessler, (2007) [158,159]). Among a variety of other promoter elements that all regulate gene transcription, these Notch-target genes generally contain multiple RBPJ recognition sequences. This sequence motif, 5'-CGTGGGAA-3', has not dramatically changed since it was first identified [17], though we now understand that not every base has equivalent nucleotide-RBPJ interactions [35,160,161]. The core RBPJ recognition sequence is 5'-YGTGRGAA-3', where 'Y' is a pyrimidine base (C or T) and 'R' is a purine base (A or G). [4]

Screening for this consensus motif within the Hes family-equivalent *Drosophila* promoters (*Enhancer of split* complex genes, such as *E(spl)m4*, *8*, *γ*) identified two important trends. First, these promoters are controlled by multiple RBPJ binding sites (Su(H) protein in *Drosophila*) spread throughout, both in the proximal promoter and distal enhancers. Second, and significantly relevant to this dissertation, a select number of these sites were in a 'paired' arrangement, abbreviated as an SPS (Su(H) paired site) [19]. An SPS was originally characterized as two RBPJ binding sites in the forward (sense) and reverse

(antisense) orientation, separated by a defined number of nucleotides (16 bp) that was conserved between the *Drosophila E(spl)m4*, *m8*, *mγ* and mouse *Hes1* genes (this separating space has been termed as 'spacer' or 'gap' distances). Herein, it was first hypothesized that the SPS permits synergistic interactions between two Notch ternary complexes [19]. This SPS motif was later identified in more members of the E(spl) complex genes and its necessity for gene transcription was further explored. Interestingly, its presence was required for some *Drosophila* developmental aspects but not in others [24].

Cave et al. (2005) [27] further defined the SPS architecture to only include the forward and reverse site orientations. Manipulation of these sites into other arrangements, such as forward-forward or into a single RBPJ binding site, severely ablated any transcriptional activation from the promoter element [27]. Using a *Drosophila* cell culture model, Cave et al. also observed further synergism with another promoter element, a so-called 'A site,' where proneural basic Helix-Loop-Helix (bHLH) activator proteins bind. Only when in combination with the bHLH activator proteins Achaete and Daughterless was the *Drosophila* NICD able to robustly activate the *E(spl)m8* promoter, which contains both an SPS and A site motif. On a synthetic promoter within mammalian cells, this combination (SPS + A) resulted in substantial promoter activation only when transfected with both NICD and the proneural bHLH activator protein MASH1, and displayed poor activation when only one of these transcription factors was present [27]. However, this specific promoter arrangement has not been further identified or explored in any native mammalian Notch target genes, suggesting that the SPS + A code may be a *Drosophila*-specific mechanism.

The first comprehensive mammalian promoter analysis was by Ong et al. (2006) [28], where the authors explored the promoter activation potential of each Notch family member

(Notch1-4) on a suite of native, mutated, and synthetic promoters in a variety of mammalian cell lines [28]. As hinted at in a previous study [162], they found that the four NICDs have substantially different activation strengths, even on the same promoter. In general, Notch1 is the strongest activator, and Notch3 and Notch4 compete for the 'weakest NICD' title. Their relative activities, therefore, likely depend both on their amino acid compositions and various regulatory interactions dependent on cellular contexts. Since the four mammalian Notches equivalently interact with the same RBPJ protein [161,162], their variable activation strengths may be attributed to either structural differences within their ankyrin or C-terminal domains, or within *cis*-regulatory elements found within different promoters and cell types.

To address these two possibilities, Ong et al. performed substantial promoter mutagenesis on Notch-target genes to find the minimum promoter elements required for Notch-induced transcription. Strikingly, they found that the SPS within *Hes1* (with an additional TATA box) is the minimal promoter element necessary for robust Notch-induced activation. Further, this minimal SPS-induced promoter had variable activation by the different Notch proteins (N1 > N2/4 > N3), all while within the same cell type. This indicates that the different strengths seen in full-length promoters can be primarily attributed to the amino acid composition of the individual Notch proteins, not *cis*-interacting promoter elements [28].

The latter half of their manuscript sought to determine the minimum requirements and signaling potential of sequence-paired sites. In summary, their work confirmed the characteristics identified by the original landmark studies [19,24], where SPSs are composed of two RBPJ binding sites oriented head-to-head, with precisely 16-nucleotides between

them [28]. Further, they demonstrated that they can artificially create a canonical SPS from a monomeric RBPJ-site within *Hes5,* which dramatically increased its transcriptional potential, and any non-canonical formats performed poorly. This agrees with results from Cave et al., who also found the orientation and spacing between these two RBPJ-sites was crucial for activation; any deviation from the canonical motif nulls the transcriptional response. While the promoter mutagenesis performed by Ong et al. indicates the inflexible nature and importance of an intact SPS motif, the mechanistic details behind its NICD-induced activation were again left unanswered.

Notch Dimerization: The First Observations

Just a year after the Ong et al. (2006) paper was published, the question regarding the mechanism behind Su(H) paired sites was addressed. The Blacklow laboratory utilized a Notch ternary complex crystal structure (PDB ID: 2F8X) they had previously solved to model two Notch transcriptional activation complexes (NTC) on DNA [29,126]. This original crystal structure includes partial proteins of RBPJ, MAML1, and N1ICD, as well a segment of the Hes1 promoter including a single, canonical, RBPJ binding site. When observing their ternary complex crystal, as well as a crystal structure of the Notch1 ankyrin domain solved by another independent group [163], they noticed points of contact between the convex surfaces of adjacent NICD ankyrin domains. These contact points led to two important observations: 1) interacting complexes orient in a head-to-head conformation (two NICDs facing each other, as they would be oriented on an SPS) and 2) when connected through the ankyrin domains, the resulting distance between the two NTCs is roughly equivalent to the distance between the two RBPJ binding sites of an SPS. Further, the amino acids implicated in dimerization are conserved both across Notch homologs and within a range

of species [29]. These few observations led the Blacklow laboratory to hypothesize the possibility of NICD dimerization, explore any transcriptional implications of this process, and practically started the field of Notch intracellular domain dimerization. Culminating their work, Figure 1.4 represents the structure, orientation, and interacting amino acids used for NICD dimerization.

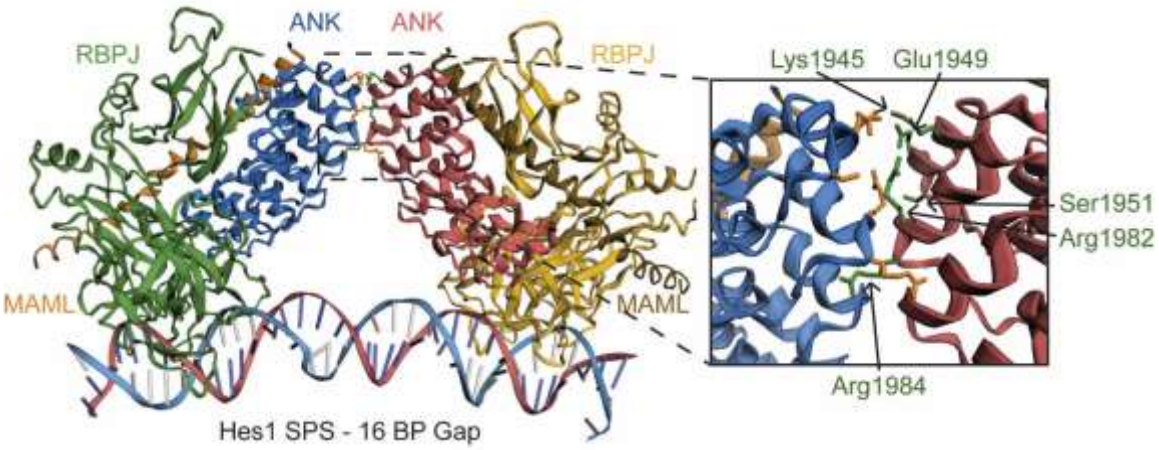

Figure 1.4: Crystal Structure of a Dimerized Notch Ternary Complex

A dimerized NICD ternary complex assembles on the head-to-head RBPJ binding sites within a sequence-paired site. This structure is assembled on the human Hes1 SPS, and is composed of human RBPJ, a fragment of MAML1, and the ankyrin domain of Notch1. The ternary complex proteins are labeled respective to their colors within the figure. The inset box indicates the conserved dimerization interface and the panel to the right is an expanded view of this region. Interacting amino acids are identified (green) and their corresponding amino acids in the reciprocal protein can be found in orange. This crystal structure was solved by Arnett et al., (2010) [30], submitted to the RCSB Protein Data Bank (ID: 3NBN), and further visualized in the EzMol software wizard developed by Reynolds et al., (2018) [164].

Dimerization as a Transcriptional Activator

By modeling two NTC cores on an SPS (hereafter an abbreviation for 'sequence-paired site,' as it changed with the literature), Nam et al. (2007) [29] observed three electrostatic points of contact between the two dimerizing ankyrin domains. The first includes hydrogen bonds between the guanidino group of R1984 (amino acids and positions represent those found within human Notch1) and three backbone carbonyl oxygen atoms within the partner ankyrin domain. The second interaction includes salt bridges between E1949 and K1945 of the two ankyrin domains, and the third includes hydrogen bonds between R1982, S1951, and a backbone carbonyl oxygen atom [29].

While these contacts were sufficient for ankyrin-dependent dimerization, Nam et al. were curious if dimerization was necessary for transcriptional activation through a gene's SPS. This was tested through mutational analysis of the dimerizing amino acids and they found that, upon null-mutations (primarily of R1984, R→A), transcriptional activation of a Hes1 luciferase reporter was abrogated [29]. Similarly, through the utilization of electrophoretic mobility shift assays (EMSA) on the Hes1 SPS, wild-type proteins were capable of cooperatively loading onto the promoter segment, whereas dimerizing-mutants abrogated any complex assembly. To further characterize SPS limitations through EMSA analysis, Nam et al. both expanded and shortened the gap distance between the two RBPJ binding sites. They observed that cooperative loading is slightly flexible, allowing for 15-19 bp gap distances (a wild-type gap is 16 nucleotides). To push complex assembly to its limits, additional mutations of the SPS, such as through site inversions or large nucleotide insertions between the sites, also disrupted any cooperative complex loading, as seen in similar previous studies [27,28]. Altogether, this landmark study discovered Notch

intracellular domain dimerization, associated it with the known mechanisms of sequence-paired sites, and characterized some of its limitations [29]. Further, Nam et al. found that this is a physiologically relevant subset of Notch signaling, where dimerization almost completely controls transcriptional activation of the SPS-inclusive gene, *Hes1*.

In a follow-up study [30], the Blacklow laboratory sought to address a problem with their previous dimerization model: when two NTCs were modeled on an SPS with an ideal B-form DNA conformation, the dimerization interface was almost 50 Å apart. They preface that for native dimerization to occur, then the two NTCs, the gap distance DNA, or both would have to go through substantial conformational change. To address this issue, Arnett et al. (2010) [30] solved the crystal structure of the entire dimeric complex, using partial proteins of RBPJ, Notch1, and MAML1, and a 37-bp DNA segment containing the *Hes1* SPS (PDB ID: 3NBN), visualized in Figure 1.4. As indicated in their original models, the crystal structure resolved with the same contacts between the two NTC's ankyrin domains and had little overall conformational change of the individual NTCs. Instead, the DNA went through substantial bending and untwisting to accommodate the dimerized complexes. Importantly, this suggests that, while the ideal gap distance between two NTCs is 16 nucleotides [29], alternatively spaced gap distances may accommodate dimeric complex assembly as well. This was previously explored by Nam et al., but was through mutational analysis of the *Hes1* SPS, not natural gene targets.

In this follow-up study, Arnett et al. identified alternative sequence-paired sites in genes with a 16-nucleotide (*Hes4*, *FJX1*), a 15-nucleotide (*SYT14*), and a 17-nucleotide gap distance (*CUL1*), all of which demonstrated NTC dimerization through EMSA analysis. Further, to examine the effects of dimerization on canonical Notch-target genes

without standard sequence-paired sites, they used luciferase reporter assays driven by promoter sections of *HeyL*, *Hey2*, and *Hes5*. As anticipated, *HeyL* and *Hey2* activated equivalently with wild-type or dimerization deficient NICDs, but surprisingly, activation of the Hes5 promoter required dimer formation.

These observations split Notch-responsive promoters into two categories; those without dimerization dependence (*HeyL, Hey2*) and those that depended on dimerization for robust activation (*Hes1, Hes5*). However, while *Hes1* contains a canonical SPS, *Hes5* contains several RBPJ binding sites but none in the canonical SPS conformation. To explore this conundrum, Arnett et al. performed mutation analysis of RBPJ sites within the promoter to find the cause of dimer dependence. Through further EMSAs, luciferase assays, and various mutant promoters, they identified a 'cryptic' partner site, 16 nucleotides away from one of the canonical RBPJ binding sites within *Hes5* [30]. This observation adds a critical aspect to the scope of Notch dimerization: sequence-paired sites may contain subpar/cryptic secondary RBPJ binding motifs that alone would not normally bind RBPJ. The presence and activation of a cryptic sequence-paired site results in an important point of concern that will be a theme throughout the rest of this dissertation: screening and identifying genes activated through non-standard sequence-paired sites will prove exceedingly difficult. Altogether, Nam et al. (2007) [29] and Arnett et al. (2010) [30] identified Notch dimerization as a novel method of transcriptional activation and resulted in the categorization of Notch target genes based on their utilization of Notch dimerization. However, these two studies only observed the activation of two dimerization-dependent genes (*Hes1* and *Hes5*), and all work performed was *in vitro*, so the field was wide-open to find further physiological relevance.

Physiological Relevance of Notch Dimerization

A classical model to study Notch activity is through the normal specification and maturation of T cells, as well as in the disease state; T-cell acute lymphoblastic leukemia (T-ALL). For a brief and simplified overview, the differentiation of T cells starts with hematopoietic stem cells found within the bone marrow. Upon cell division, they create multipotent progenitor cells which, through extensive cell signaling, are directed down one of two paths: to become myeloid or lymphoid progenitor cells. Myeloid progenitor cells are eventually specified to become erythrocytes, megakaryocytes, mast cells, and myeloblasts, where the myeloblasts are unipotent stem cells and further differentiate into the granulocyte series. The lymphoid progenitor cells can differentiate into natural killer cells or a precursor cell which further differentiate into T or B lymphocytes. Most of the differentiation steps during hematopoiesis occur in the bone marrow and some in the blood stream, but of note, T cell maturation is unique in that it occurs in the thymus.

Among the large array of cytokines, surface proteins, transcription factors, and other signaling molecules involved in hematopoiesis, among them, the Notch signaling pathway is best known for its role in T cell development. Simply summarized, active Notch signaling transitions the lymphocyte precursor into T cells and is further involved in their maturation in the thymus, whereas inhibited or inactive Notch signaling in the bone marrow results in a B cell lineage. These lineage decisions are normally regulated due to the presence or absence of Notch ligands on bone marrow stromal cells and thymic epithelial cells. However, when Notch-activating mutations occur within the lymphoid progenitor cell line, this commonly results in T cell leukemia. T-ALL is a result from constitutively activating mutations within Notch, commonly within the HD or PEST domains. Mutations

within the heterodimerization domain result in ligand-independent Notch signaling, whereas PEST mutations stabilize the activated Notch intracellular domain. Lesser-activating mutations within Notch are unable to induce T-ALL by themselves, though in combination with other oncogenic hits, can result in an accelerated development of leukemia. While the above summary should provide sufficient basal-level information about hematopoiesis and the normal and abnormal development of T cells for the rest of this dissertation, please refer to the following reviews for more in-depth material: Koch & Radtke, (2011); Radtke et al., (2010); McCarter et al., (2018) [165–167].

The first source of physiological relevance for Notch dimerization was through the Pear laboratory a few years after the first report of NICD dimerization. Using a mix of *in vivo* and *in vitro* techniques, Liu et al. (2010) [31] discovered that not all Notch-dependent processes in T cell development require Notch dimerization. This indicates that Notch dimerization is not some all-encompassing mechanism, but instead regulates the transcription of specific genes and processes. For example, both wild-type and dimerizing mutants (Notch1, R1984A) were equally potent in inducing T-cell development from a multipotent lymphoid progenitor. In contrast, the induction and development of T-ALL in mice through the expression of a constitutively active NICD in hematopoietic stem cells only occurred with wild-type NICDs; R1984A mutants remained leukemia-free. This effect was similarly observed *in vitro* in two T-ALL cell lines, where wild-type NICD induced cell growth and R1984A mutants did not [31].

Liu et al. hypothesized that this is due to the NICD R1984A mutant's failure to induce the expression of critical target genes essential for leukemogenesis. This question led to the identification of the other dimer-dependent genes beyond the original *Hes1* and

Hes5. While the NICD induction of *Hey1* and *CD25* was equivalent between wild-type and mutant proteins (dimer-independent genes), the dimer mutant failed to activate *Hes1* (as seen previously, [29]), *c-Myc* (a proto-oncogene encoding a transcription factor), and *pTα* (a gene encoding a transmembrane protein which is involved in early T-cell development), classifying them all as dimer-dependent genes. These genes were explored further throughout the manuscript, utilizing various reporter and cellular assays, combined with the mutagenesis of proteins and promoters. Together, these experiments indicated that these were novel, dimer-dependent genes and that NICD dimerization was necessary for T cell maturation and leukemic cell growth [31].

The conclusion that *pTα* is a dimer-dependent gene led them to an unexpected observation: just like *Hes5* [30], the promoter of *pTα* did not have a canonical SPS. While the previously identified RBPJ binding site within the pTα promoter has a near-optimal consensus sequence [35,168], there was no standard consensus site found in the antisense strand, 15-17 bases away, as in a canonical SPS. To explore the possibility and mechanism of dimerization on the pTα promoter, Liu et al. performed EMSA analysis with the RBPJ-containing fragment, including the area around it. As its dimerization-dependence suggested, they identified a cryptic RBPJ binding site 16 nucleotides away from the high-affinity site. Interestingly, this secondary site only demonstrated the assembly of an NTC if the high-affinity site was intact; it alone would not load an NTC. Further, while Liu et al. did not initially identify the SPS regulating *c-Myc*, in a follow-up study the Pear laboratory identified a cryptic SPS, with a 15-nucleotide gap, within *c-Myc*'s distal enhancer [169]. These cryptic sequence-paired sites will be further explored in the upcoming manuscripts and in the remaining chapters of this dissertation. Altogether, the Pear

laboratory was the first, and to date, the only group to demonstrate an *in vivo* physiological relevance for Notch dimerization. Through the utilization of models for T cell and leukemic maturation, Liu et al. observed that Notch dimerization is not a ubiquitously used process within downstream Notch target genes. As Arnett et al. also concluded, this signaling mechanism appears to function on a specific subset of Notch transcriptional targets. However, led by the examples of *Hes5*, *pTα*, and *c-Myc*, the discovery of cryptic sequence-paired sites may make this group unpredictably large.

Identification of Sequence-Paired Sites

Following the identification, characterization, and physiological relevance of the first sequence-paired sites [29–31], the search was on to identify further SPS-driven, Notch target genes. The identification of a single RBPJ binding site is relatively easy through the recent advances in sequencing technologies and bioinformatics. Through chromatin immunoprecipitation with parallel DNA sequencing (ChIP-seq), researchers can immunoprecipitate DNA-associated proteins (such as RBPJ), purify the DNA fragments, perform high-throughput sequencing, and through bioinformatics, identify and characterize DNA binding sites of interest.

This process has been performed several times previously to identify Notch-associated genes, though previous efforts did not attempt to identify any paired RBPJ binding sites [170,171]. While not the primary emphasis of the manuscript, Castel et al. (2013) [33] were the first researchers to attempt to identify RBPJ motifs in tandem. By performing ChIP-seq on a single RBPJ-immunoprecipitation, they were able to use bioinformatic screening approaches to find nearby motifs (motifs found with the GimmeMotifs matrix, [172]). Their analysis only found a small pool of tandem RBPJ motifs (26 of 158 high-

confidence RBPJ sites), but when present, sites were most often in the head-to-head conformation and 11- to 21-base pairs apart [33]. Of note, most of their identified SPS-inclusive genes did not contain the ideal 16-nucleotide spacer [29] and instead generally had a shorter gap distance. Further complicating these findings, the RBPJ motifs were not often found in the gene's proximal promoters, but instead found at distal enhancer sites. As this subset of Notch signaling was not the emphasis of the manuscript, the authors did not explore this thread any further.

SPS-inclusive promoters and enhancers were further studied by a complementary approach to ChIP-seq, termed Split DNA adenine methyltransferase Identification (SpDamID, [34,173]). In this experimental approach, an *E. coli* DNA adenine methyltransferase (Dam) is split into two halves and fused to proteins of interest (such as RBPJ and Notch). When their host proteins interact, the two Dam halves can come back together into a functional whole protein, resulting in the methylation of nearby adenines within the DNA sequence 5'-GATC-3'. This creates a recognition site for the restriction enzyme DpnI ($GA^{m}TC$), which allows isolated genomic DNA to be restriction enzyme-treated (digested), put through adaptor ligation, and finally amplified through ligation-mediated PCR. This amplified library pool can then be used as templates for further gene-specific PCR reactions or used in genome-wide arrays like microarray hybridization or high throughput sequencing [34].

While primarily a methods paper, Hass et al. (2015) [34] did validate their approach through basic analysis of Notch dimerization. SpDamID is capable of finding RBPJ sequence-paired sites by fusing the two Dam halves onto two NICDs and comparing the library pool between wild-type and dimerization interface-mutated proteins. Similar to

Castel et al., Hass et al. sequenced their dimer-positive library pool, identified the strongest RBPJ motif, and screened the surrounding nucleotides looking for a paired RBPJ site (motifs found with the HOMER toolkit, [174]). Their work identified two dimerization-dependent sites within the *NRARP* enhancer (gene encodes the Notch Regulated Ankyrin Repeat Protein, which acts as a negative feedback regulator of NICD signaling), both of which contained a canonical and cryptic RBPJ binding site. Further, SpDamID and its motif screening identified an assortment of RBPJ binding motif sequences found within SPSs, both canonical and cryptic, but the authors failed to connect these sequences to any gene's promoters or enhancers.

The most recent attempt at identifying SPS-regulated genes was by the Aster laboratory, who also used ChIP-seq and a host of bioinformatic tools to analyze their datasets [35]. First, however, they sought to further characterize the dimeric complex's sequence requirements to use these guidelines when sorting through their future ChIP data sets. To address this question, they developed a fluorescence resonance energy transfer (FRET)-based assay to quantitatively measure NTC dimerization on a host of DNA sequences. In their system, two maleimide-derived fluorophores are used and attached to NTC components through specific cysteine mutations within the ankyrin domain of NICD. In a FRET assay, one of the fluorophores is excited by an outside source and, if spatially close (<10 nm, as in their NICD dimerization arrangement), will transfer its energy to an acceptor fluorophore (creating a donor-acceptor pair), which then itself excites and emits detectable light at an alternative wavelength. In the absence of NICD dimerization, as in the case of ankyrin interface mutants or non-cooperating sequence-paired sites, the

fluorophores are no longer paired resulting in the excitation and emission of just the donor fluorophore.

Utilization of their FRET-based assay clarified two requirements for NICD dimerization on sequence-paired sites. First, as previously explored through EMSAs [29,30], cooperative assembly (and therefore FRET signal) only occurs on DNAs containing spacer distances of 15 to 17 base pairs. Second, they explored the NTC dimerization on DNA with consensus or a variety of nonconsensus RBPJ binding sites. They observed that when these nonconsensus (cryptic) sites were paired as palindromic sequences (the same site at the forward and reverse locations), they failed to support dimerization. In contrast, when a nonconsensus site is paired with a consensus site (as in the case of *Hes5* or *pTα*, detailed previously [30,31]), this arrangement facilitates dimerization [35]. Since a wide variety of nonconsensus sequences were observed to facilitate dimerization, these previous and current observations indicate that screening for Notch-driven sequence-paired sites is an exceedingly tall order.

To identify further sequence-paired sites, Severson et al. (2017) [35] reanalyzed ChIP-seq data they had previously acquired from a T-ALL cell line, CUTLL1 [175,176]. Their original ChIP-seq analysis identified dynamic RBPJ/Notch binding sites which are spatially associated with Notch responsive genes, and nondynamic RBPJ binding sites, which appeared insensitive to the status of Notch signaling (on or off). The nondynamic sites were purged from their dataset which was then further analyzed for sequences likely to support NTC dimerization, through both canonical and cryptic SPSs. They found that of 996 dynamic and high-confidence RBPJ/Notch binding sites, 197 (~20%) of those contained high-confidence SPSs. Interestingly, while the 16-nucleotide spacer provided the

best structure for NTC cooperation, there was a roughly equivalent number of sites with 15- to 17- base pair spacers (15 bp, n = 78; 16 bp, n = 60; 17 bp, n = 60, note these don't add up to 197 and the authors did not clarify this discrepancy). Finally, as was the case with monomeric RBPJ sites [175], most SPSs (86%) were found within distal gene enhancers.

With the number of SPS-inclusive genes in CUTLL1 cells in mind, Severson et al. sought to identify the contribution of NTC dimerization towards gene expression in T-ALL (using CUTLL1 cells). They performed RNA-seq on cells transduced with either wild-type or ankyrin mutated (R1984A) N1ICD, and of the 281 genes activated by wild-type N1ICD, 93 of those were not activated by the dimerization-deficient protein. At face value, this data indicates that about a third of Notch-induced transcription relies on NICD dimerization. However, a portion of these 281 genes could just be downstream targets of Notch effector proteins, and not actual targets of NICDs themselves, resulting in the possibility of false positives. To narrow the focus of this analysis to genes that are directly regulated by Notch signaling through RBPJ sites in their promoters or enhancers, they referred to the CTCF-bounded chromatin domains model of spatial DNA arrangement.

In this model of genome organization, the genome can be split into functional chromatin domains, divided by insulator DNA elements. These elements prevent inappropriate interactions between neighboring regions of the genome and effectively act as blockades for the effects of enhancers. The DNA binding protein CCCTC-binding factor (CTCF) is a well-characterized insulator-binding protein and plays crucial roles for the insulator's barrier function [177–180]. Severson et al.'s previous ChIP-seq work [175] suggested that dynamic RBPJ binding sites within enhancers are most likely to control genes within

their same CTCF block, even if those RBPJ sites are closer in sequence to the start site of another gene that's within a different CTCF block.

Utilizing this model to rescreen their RNA-seq dataset for direct Notch target genes, they found that of 107 high-probability, direct Notch-target genes in a T-ALL cell line, 38 of those are NTC dimerization dependent. A list of these genes are available in their online supplementary data [35] and includes known dimer-dependent genes like *Hes1*, *Hes4*, *Hes5*, and *NRARP*, though distinctly, the identified site within the *Hes5* enhancer was not the cryptic SPS identified by Arnett et al. Further, this screen does not identify the previously discussed *pTα*, *c-Myc*, *FJX1*, *SYT14*, or *CUL1* genes. While the Severson et al. dimerization-dependent gene list is likely accurate, these discrepancies suggest that this is not a complete story. The absence of *FJX1*, *SYT14*, and *CUL1* from the dimerization-dependent list may be slightly ignored: their SPS sites were only explored *in vitro* through EMSA analysis and may not be even transcribed in T-ALL cell lines [30]. However, their bioinformatic screen not identifying the cryptic SPSs within *pTα*, *c-Myc*, and *Hes5* can't be so easily dismissed. *pTα* (also named *PTCRA*) and *c-Myc* contain a bona fide cryptic sequence-paired site within their enhancers, were significantly controlled by NTC dimerization and were observed in another T-ALL cell line, T6E cells [31,169,181,182]. The cryptic SPS control of the *Hes5* promoter was thoroughly explored as well, though its activation was tested in an alternative cell line. The absence of these three genes on this list may be attributed to some differences in cell line genomics (despite *pTα* and *c-Myc* being explored in the same disease model), their promoters and enhancers may contain a variety of monomeric and SPS sites which could confound these screen results, or most

troubling, cryptic sequence-paired sites may not be sufficiently identified through Severson et al.'s bioinformatic approach.

In summary, Severson et al. developed a technique to quantitate and compare NTC dimer formation on alternative sequence-paired sites and transitioned these findings into a search for both canonical and cryptic SPSs from ChIP-seq data sets. They identified a variety of dimer-responsive elements active in T-ALL cell lines, and are the first group to connect these elements, most often within enhancers, to their effector genes. However, just how exhaustive their screens are, remains to be seen. Their bioinformatic tools are likely proficient at identifying both monomeric and canonical sequence-paired sites involved in T-ALL development. That said, exemplified by the absence of the cryptic SPS genes *pTα*, *c-Myc*, and *Hes5* from their list, their approach is not perfect and may need remodeling. Altogether, bioinformatic tools and techniques have been developed to identify a wide variety of RBPJ/Notch binding sites within the genome. While using ChIP-based approaches to identify single RBPJ binding sites has been well studied and developed, taking those same data sets and reanalyzing for paired-sites is still in its infancy. Hass et al. and Severson et al. both offer tools and approaches to screen and identify active sequence-paired sites, and these techniques should be transferrable to other Notch-regulated models, such as within vascular development.

An Alternative Dimerization Model

Beyond the ankyrin-mediated dimerization model, there exists one other case of Notch dimerization. In a report from 2002, back from before the first crystal structures for the Notch ternary complex were solved, the Capobianco lab isolated stable Notch nuclear complexes from Notch-induced neoplasmic cells and confirmed its protein components

(RBPJ/NICD/MAML), among other unidentified members [183]. They also made note of another NICD complex, smaller than the ternary complex and with substoichiometric amounts of MAML and RBPJ, found within the cytoplasm. In a follow-up report nearly a decade later, the Capobianco lab identified it as a Notch dimer and a precursor to the complete ternary complex [32].

Using recombinant proteins from various host sources (bacterial/insect/mammalian cells), performing both *in vitro* and within cell line experiments, the authors were able to recreate and identify their previous cytoplasmic Notch complex. They found that the complex starts with a simple homodimer between two N1ICDs; no other proteins were necessary for this interaction. Distinctly, this interaction was ankyrin-domain independent. This homodimer instead utilizes sections just outside of the NICD RAM and TAD domains, where the RAM-interacting portion binds to a section near the TAD domain of the partner protein, resulting in an antiparallel arrangement between the bound proteins. For clarity, I'll refer to this arrangement in the rest of this dissertation as the 'antiparallel model' since the Capobianco lab only referred to it as an NICD multimer. Vasquez-Del Carpio et al. (2011) [32] found that this initial antiparallel complex then starts the stepwise assembly of the nuclear ternary complex.

Through a strenuous series of mutations and domain deletions, Vasquez-Del Carpio et al. suggested a model for the assembly of the Notch transcriptional activation complex. First, antiparallel Notch homodimers form in the cytoplasm and then recruit and complex with Ski-interacting protein (Skip), a transcriptional coactivator, through the NICD ankyrin domain. Skip was originally implicated in the Notch signaling pathway through its binding to DNA-bound RBPJ, where the SMRT/HDAC corepressor complex and active NICDs

compete for Skip/RBPJ binding [184]. This model was later refined to include Skip's role in transcriptional activation and recruitment of other transcriptional machinery, though the exact mechanism was not elucidated [137,185]. Vasquez-Del Carpio et al. observed that, in the complex with an NICD homodimer, Skip and NICDs create a docking site for MAML1, forming a preactivated complex. At some point, which is not clarified in the manuscript, the complex must translocate to the nucleus as the next step is to interact with RBPJ. Beyond the canonical contacts with the NICD's RAM domain, RBPJ has also been described as interacting with the NICD's ankyrin domain (briefly reviewed and studied in Wilson & Kovall, (2006); Nam et al., (2006) [117,126]). The NTC complex finally forms by an RBPJ-mediated displacement of Skip from the NICD ankyrin domain, where RBPJ competes for the same contact region [32]. They also hypothesize that the Skip/RBPJ exchange removes the corepressor complexes from RBPJ, though this mechanism was not further explored. Similarly, the preactivation complex interacting with RBPJ was thought to displace the partner NICD in the antiparallel model, which was then free to restart this stepwise assembly, though its fate was not investigated.

There are a few important clarifications between the antiparallel and ankyrin-mediated NICD dimerization models that need to be mentioned. First and foremost, as it currently stands, the antiparallel model does not have any direct implications in dimer-dependent signaling. This model posits that dimerization is completely through the RAM and TAD domains; the ankyrin domain and any mutations (R1984A) did not alter their observed dimerization [32]. Instead, the antiparallel model may have broader impacts on all Notch signaling targets: in their work, NICDs that could not complete the first antiparallel assembly step (Notch homodimerization) were incapable of activating downstream Notch

reporter assays [32]. Second, their reporter assays were only studied with synthetic, dimer-independent promoters. All NICD domain mutations utilized were only applied on head-to-tail RBPJ binding site constructs, and therefore their observed downstream application may not apply to dimer-dependent Notch signaling. This is of particular interest since the mechanism behind the loss of the dimerized NICD partner and its fate was not explored; what if the lost protein could be instead integrated into a secondary RBPJ binding site within a sequence-paired site? Third, the antiparallel model may only apply to Notch1 signaling. In contrast to the highly conserved ankyrin-mediated dimerization interface, these sections of the RAM and TAD domains are not well conserved across the four mammalian Notch proteins. Further, while the other Notch proteins (Notch2-4) were only minimally studied in the ankyrin-mediated model [29], Vasquez-Del Carpio et al. did not look for dimerization within the other Notch proteins, opting to just study Notch1.

In summary, antiparallel NICD dimerization through sites near the RAM and TAD domains appears to be an important first step for NTC assembly and transcriptional activation. Importantly, the two Notch dimerization models are not mutually exclusive. While Vasquez-Del Carpio et al. hypothesized that the second NICD leaves the completed NTC complex, it's also possible that it gets integrated into a secondary complex or doesn't leave at all. To be explored in-depth in the next section, all of the previously discussed manuscripts concerning the ankyrin-mediated dimerization interface have never explored the alternative binding sites found within the antiparallel model. Unfortunately, the dimerization crystal structure solved by the Blacklow laboratory [30] did not include these RAM and TAD sites within their purified NICD. While this was likely due to the size restrictions of X-ray crystallography or perhaps just because of the expression constructs

they had on-hand, regardless, it's still completely unknown if or how the RAM and TAD domains interact in full-length, ankyrin-dimerized, NICDs.

Outstanding Questions

While the field of Notch intracellular domain dimerization has moved steadily forward since it was first described in 2007, the vanguard has left behind concerning gaps in knowledge and open questions in its wake. Many of these gaps can be attributed to two assumptions made in the first dimerization manuscript which have not been addressed in any of the field's research since. The Blacklow laboratory assumed that 1) the other members of the Notch family dimerize the same way as Notch1, and 2) the ankyrin domain is the only site that mediates NICD dimerization. These assumptions, combined with various other observations and experimental weaknesses, led us to ask three outstanding questions which will be addressed and explored within Chapters 2 and 3 of this dissertation. The ensuing questions will be followed by a brief explanation, our research objective, and then concluded by a more thorough explanation and justification.

<u>Question 1: Are all members of the Notch family capable of homodimerization? Would this extend to heterodimerization?</u>

In their original dimerization manuscript [29], the Blacklow laboratory identified several points of contact between two Notch1 ICD ankyrin domains by using two mirrored NTC complexes on the Hes1 SPS. Mutation of these N1ICD residues prevents Notch-driven activation of SPS-inclusive genes (*Hes1*), resulting in a new category of Notch target genes; those that are dimer-dependent. They further note that these contact points are conserved across the Notch family members, indicating that dimerization is likely an evolutionarily conserved function. However, their manuscript and all follow-up studies

since then have lacked evidence demonstrating that this dimerization mechanism is consistent throughout the four mammalian Notch receptors.

Objective 1: To explore which NICD dimerization iterations occur within a protein over-expression, cell culture model.

The single piece of support for dimerization outside Notch1 is through an EMSA of 1-1, 2-2, 3-3, and 4-4 homodimers [29]. While this experiment did demonstrate that two NTCs were loading on the Hes1 SPS, two important controls were missing before we can claim that they dimerize. Beyond N1ICD, the authors did not perform any mutagenesis on the other Notch family members. Without this negative control for dimerization, we shouldn't assume that the other Notch family members contain an identical dimerization interface, or even dimerize at all. While the contact amino acids involved are conserved, there are no crystal structures of the ankyrin domains for Notch2-4 to refer to for structural comparisons. Further, there are other variations within the ankyrin domain (including the interface), RAM domain, and massive differences in the C-terminal region which could all change the small window necessary for ankyrin-ankyrin cooperativity. The second control that was left unaddressed is at the transcriptional level. While Nam et al. demonstrated that N1ICD dimerization mutants cannot activate a Hes1 reporter assay, they did not check if the other suspected Notch family homodimers are in this same category. We know that all NICDs can activate this type of promoter element [28], so even if this activation is through dimerization, we should not assume that it plays an equivalent role for each Notch protein.

The Blacklow laboratory further proposed that since each Notch protein could dimerize, and the interface is conserved among them, then it's feasible that NICD heterodimers could form too. This possibility would depend on cellular contexts, requiring

expression and activation of multiple Notch proteins in the same cell at the same time. This situation occurs in a variety of cell types and within Notch models, such as in T-ALL development [186–188] or within vascular biology [70,189,190]. Regardless, even with the existence of these model systems, the hetero- or homodimerization of NICDs outside of Notch1 has not been explored to date.

Question 2: How do the RAM and C-terminal domains affect NICD dimerization? Does the antiparallel model interact with the ankyrin-mediated dimerization model, or are they independent systems?

When analyzing the Notch crystal structures discussed previously [30,126], it's important to keep in mind that these complexes were built using partial proteins. These NTC crystals are composed of the canonical SPS from *Hes1*, most of an RBPJ protein, a small fragment of MAML1, and just the ankyrin domain of Notch1. While these protein sections are sufficient for complex assembly, and the identified ankyrin-ankyrin contacts have transcriptional implications in a dimerization-dependent system, it's presumptuous to assume that this partial model correctly represents a dimerized transcriptional complex for all Notch family members.

Objective 2: To explore the roles the RAM and C-terminal domains may have in NICD dimerization, particularly emphasizing if these less-conserved regions alter the dimerization abilities of the different Notch proteins.

These crystal structures are potentially poor representatives of a dimerized system because of the missing domains of Notch1. In a canonical system, the RAM domain drives the initial recruitment of an NICD to RBPJ through its BTD domain, and then the NICD ankyrin domain docks with the other domains of RBPJ, RHR-N and -C, which is

hypothesized to be a reversible process. In combination with the RHR domains of RBPJ and the ankyrin domain of NICD, a segment of MAML1 nestles into a newly formed groove derived from both proteins, which is thought to 'lock' the complex together [126]. Since the RAM domain is missing in the dimerized NTC crystals, it's difficult to say for sure exactly how the ankyrin domain will arrange onto RBPJ and therefore interact with a partner complex. This isn't the most troubling observation, however, since Notch variants lacking the RAM domain can still activate transcription, indicating that a ternary complex can still form independently of the RAM domain [53,183]. An even more concerning possibility, however, can be derived from an observation Arnett et al. made of their dimerized NTC crystal. They note that for the ankyrin-ankyrin contacts to come together, the DNA had to go through substantial bending and untwisting [30]. Again, this observation was made from a dimerized NTC complex built without the NICD RAM domain. If this domain was intact, would an increased number of contacts between NICD and RBPJ result in more or less flexibility of the larger complex? If that's the case, would a change in flexibility alter the ideal number of bases between an SPS?

These questions are partially addressed, albeit indirectly, in these pioneer manuscripts. While the Blacklow laboratory used just the ankyrin domain for their crystals, they opted to use the RAM and ankyrin domain (RAMANK) for their *in vitro* EMSA experiments. Beyond supporting canonical dimerization, these EMSAs demonstrate that cooperating NTCs can also form on cryptic SPSs [30,31,169], an observation that will become pertinent later in this dissertation. Ultimately, these experiments produce the same guidelines for dimerization that the crystal structure does and indicates the RAM domain likely has a neutral effect on cooperative assembly. Distinctively, however, neither the

crystal structures nor EMSAs include the NICD's substantially large and highly divergent C-terminal region.

Containing at least two well-accepted domains (TAD/PEST) and littered with less characterized regions, Notch's C-terminus is the least studied part of the Notch protein and is the most variable between the four family members. While each Notch protein contains a PEST domain, earmarked by its roles in protein degradation, the presence and composition of a TAD domain is variable among the Notch family members. Besides necessary assisting roles in transcriptional activation, any structural roles or interactions of the CTD domains within the NTC complex are unknown. Further, the Notch2 TAD deviates heavily from the Notch1 TAD (about 45% overall identity, [191]), while Notch3 and 4 are not considered to contain a TAD at all, and instead, their truncated C-termini are entirely uncharacterized (except for their PEST domain).

These C-terminal uncharacterized regions and the RAM domain contain the alternative dimerization sites used in the anti-parallel dimerization model proposed by the Capobianco laboratory. While the N-terminal location would be present within the Blacklow laboratory's EMSAs, the antiparallel model has the N-terminal site strictly interacting with a region just N-terminus of the TAD, which is lacking in their *in vitro* experiments. While the Capobianco lab hypothesized that the antiparallel dimerized NICDs resolve into monomers on DNA, this theory was only derived from their utilization of reporter constructs with monomeric RBPJ binding sites.

This situation culminates in an interesting possibility and relates back to our original question: perhaps on sequence-paired sites, the N- and C-termini remain associated within their cooperating NTCs. Retaining these interactions would require physical access

to these regions all while assembled within a dimerized NTC, and unfortunately, the substantial crystal structures needed for this conformational information have yet to be resolved. However, while this possibility has not been specifically addressed, we may be able to glean insight from other Notch crystal structures. There are two crystal structures of a Notch ternary complex which include the RAM domain within the purified protein. The first was of the RAMANK domain of the *C. elegans* Notch protein (Lin-12) (PDB ID: 2FO1, [117]), and the second was of human Notch1 RAMANK (PDB ID: 6PY8, [192]). Importantly, both protein crystals resolved the same way: while the specific RBPJ-RAM interactions were structured and resolved, the region containing the proposed N-terminal dimerization region did not have electron density, indicating a disordered, presumably unstructured region. Since this region is within an open interface within the NTC and not already used in an internal interaction, it's a possibility that the N-terminal dimerization site is capable of protein-protein interactions within a dimerized complex.

Structural information regarding the other component of the antiparallel interaction, the C-terminal site, isn't as convenient. There are no crystal structures of the Notch C-terminus, within an assembled ternary complex or even by itself, so trying to predict if this region interacts with the N-terminus would likely be overambitious. Still, a variety of reports have demonstrated its importance for NICD-induced gene transcription of known dimerization-dependent genes [52,54,55]. Further, an *in vitro* analysis was performed which compared NTC complex assembly efficiency between wild-type N1ICD and one that's missing the TAD domain, including the suspected C-terminus dimerization site. Nuclear lysates were collected and allowed to assemble on an oligonucleotide of the Hes1 SPS and demonstrated that the presence of the TAD is important for the proper assembly of a ternary

complex [54]. The authors predicted that the simplest explanation for this behavior is that the TAD participates in intermolecular contacts to stabilize the complex, or perhaps other cofactors interact with the TAD and promote ternary complex assembly [54]. Importantly, either of these two possibilities could be fulfilled by N-/C-terminal interactions as in the antiparallel model.

In combination with hindsight, this evidence suggests that not including the RAM and C-terminal domains in the original characterization assays was a potential misstep. While it appears that in a reduced system (crystallization, EMSAs) the NICD ankyrin domain is sufficient for dimerization, in an *in vivo* system, dimerization may be much more involved. Further, these additional interactions may explain how dimerization results in its profound transcriptional activation or how cooperative loading works at cryptic sequence-paired sites. These possibilities remain to be explored and these findings may drastically affect the model on how NICD dimerization functions across the Notch family.

Question 3: What are the limitations to dimerization on sequence-paired sites? By differing in size and presence or absence of domains, do the other Notch family members have alternative preferences?

The intracellular domain dimerization of Notch1 appears to adhere to strict requirements, where cooperative loading only occurs when the gap distance between RBPJ binding sites is 15-17 base pairs [29,30,35]. While the optimally spaced gap distance appears to be 16 base pairs for Notch1 ICD, Severson et al. found that there was roughly equivalent SPS representation between the three possibilities (15-17 nucleotides), where the 15-nucleotide gap was the most common arrangement [35]. Further, a ChIP-seq screen for sequence-paired sites by Castel et al. identified 22 genes with paired RBPJ motifs with

gaps that range from 11-21 base pairs [33], though the dimerization dependence of these genes was not explored in that manuscript nor elsewhere. Altogether, this argues that the presence of non-optimal and noncanonical sequence-paired sites exist and they may be more abundant than initially thought.

Objective 3: To examine these alternative SPS gap distances and identify if the Notch family members have preferential target arrangements.

Beyond minor variations in the SPS gap distances, the initial characterization studies may have forgotten an important property of their sequence-paired site DNA oligonucleotides: in its standard form, DNA is in a double helix with orientation and spatial implications. The crystal structure and FRET assays dictate that a 16-nucleotide spacer allows for the lowest degree of untwisting and bending of the DNA between the two NTCs so that they are optimally facing each other. Since DNA requires about 10 nucleotides to complete a full rotation, consider how the secondary site rotates around the DNA as the SPS gap distance increases or decreases. They originally tested up to ± 5 bp (11-21 bp), meaning that the secondary NTC site, despite still being in the same orientation, would slowly rotate around the DNA as the gap distance changes. Therefore, in their experiments, it's logical that the contacts would break as the size increases (substantial decreases would lead to spatial overlaps too) and no cooperative assembly was observed at their most extreme distances tested.

It's possible, however, that the NTC complexes could rejoin once more as the NTC rotates around the DNA even further. We hypothesized that an additional five nucleotides would be required to complete a full rotation around the DNA to make the two NTC complexes on the same side of the DNA again. This new gap distance, a total of 26

nucleotides, may allow for long-distance cooperative assembly and therefore dimerization-induced signaling. This logic could be taken to extremes and be applied to previously recognized monomeric sites, but as the DNA gap distance increases, so does the spatial distance, which requires even further kinking or looping of the DNA. Thus far, the potential of these larger gap distances tolerating cooperative assembly has been left unaddressed; both through *in vitro* analysis and bioinformatic screening for sequence-paired sites.

With these possibilities in mind, one question that arises is: What's the limit of SPS gap lengths that are constructive for cooperative assembly and result in dimerization-induced signaling? Considering that the original characterization studies just used partial proteins and these experiments were performed *in vitro*, we should question if the original guidelines transfer to more *in vivo* models. Perhaps some cellular conditions would allow these smaller or larger gap-distanced sites to act as locations for dimerization, or it's a possibility that the alternative-distanced SPSs Castel et al. identified were just false-positives. If they do exist and function as sites for dimerization, one intriguing prospect is through its utilization of other members of the Notch family. If all Notch family members can homodimerize, their slightly different RAM and ankyrin domains, and perhaps their substantially different C-termini, may dictate alternative idyllic gap distances.

This mechanism would have substantial impacts on Notch signaling. As it stands, all active NICDs (Notch1-4) bind to the same RBPJ protein which interacts with the same consensus site to drive gene transcription [161]. At this most rudimentary level of understanding, it implies that all Notch proteins result in the same signaling outcomes. This is not the case, however, thanks to a wide variety of NICD differences and modifications, protein recruitment and cooperativity, and various cellular contexts. Another possible

mechanism for Notch-family control and specification is if they deviate in their preferred SPS gap distances, introducing a method for gene-specific Notch targeting. In a hypothetical situation, for example, if Notch4 homodimers prefer a 14-nucleotide gap distance whereas the other Notch family members prefer alternative distances, then only Notch4 would be able transcriptionally activate *Mdm1*, a gene with a suspected 14-nucleotide SPS detected in the screen by Castel et al. This kind of specification would prove beneficial in the Notch signaling system, where cells generally express multiple Notch receptor family members and their ligand-induced activation is generally non-specific [193–197]. Consequently, an SPS-specific Notch targeting system would grant cells an additional layer of control over their Notch functions. Therefore, the possibility of alternative preferences beyond those set by Notch1 is worth investigating.

Dissertation Summary and Future Directions

The following chapters of this dissertation represent two manuscripts which sought to address the aforementioned concerns and questions. Our overarching goal was to take these questions and answer them outside of an *in vitro* context, attempting to get as close to endogenous interactions as possible, given the tools and methodologies available to our laboratory. While the work performed here is not within a perfect *in vivo* context, it should act as a steppingstone for further Notch dimerization research in our lab and provide direction for the field's future.

Chapter 2 – Analysis of Notch Family Dimerization

Chapter 2 identifies that all Notch homodimer and heterodimer iterations (1-2, 1-3, 2-2, 2-3, etc.) can exist within cells, though they were at varying abundances. Further, NICD dimerization with an N4ICD partner led to, by far, the most abundant interactions.

Herein, we also implicated a dimerization-responsive region within the Notch protein's C-terminal region, in contrast to the NICD's N-terminus which acted equivalently. Our methodology used here was primarily co-immunoprecipitations of overexpressed, peptide tagged NICDs, which is a step towards *in vivo* work that has rarely been taken in the Notch dimer field. However, this technique cannot discriminate between the two dimerization models (ankyrin versus anti-parallel), thus we are not able to conclude if, when, or where these two dimerization states exist.

Chapter 3 – Dimerization within Transcriptional Systems

Chapter 3 found that all members of the Notch family adhere to the strict dimerization guidelines set by Notch1; the only SPS gap distances that elicited signal were of 15-17 nucleotides. Further, in our minimalistic dimerization reporter assay, a cryptic sequence-paired site (*Hes5*) was unresponsive to dimerization, contrasting the dimerization-dependence seen when using the full-length promoter.

In this chapter, we wanted to specifically examine the transcriptional outcomes of NICD dimerization, and further manipulate and change the sequence-paired sites in the most basic ways to push this signaling system to its limit. When first using the dimer-dependent reporters that previous studies utilized, we noted that these assays were likely too generic for our purpose. They contain large segments of the promoters of dimer-dependent genes, such as *Hes1* and *Hes5*, and any effects of small manipulations of these promoters would be muted behind the roles of other transcription factors and regulatory systems. Thus, in this chapter, we developed a new type of reporter assay to specifically study the roles and limitations of dimerization-mediated transcriptional activation. These novel reporter assays consist of the sequence-paired site found within dimer-dependent

genes with its few surrounding nucleotides, and this minimalized system is sufficient to drive transcription of a luciferase gene, thus resulting in a minimalistic luciferase reporter assay.

These reporter assays demonstrated that while canonical sequence-paired sites (*Hes1*) are sufficient for dimerization and further transcriptional activation, the same cannot be said for cryptic sequence-paired sites (*Hes5*). Distinctly, while previous reports suggest that a cryptic SPS oligonucleotide can cooperatively load NTCs *in vitro* [30,31,169], our report suggests that this minimalized segment either does not assemble complexes within cells or does assemble but is insufficient for robust transcriptional activation. We were then able to take these functioning SPS-luciferase reporters and manipulate their gap distances to observe any differential preferences of the Notch family members. Contrary to our original hypothesis, each Notch family member followed the requirements set by Notch1 in the original landmark studies; only SPSs with a gap of 15-17 nucleotides were capable of dimerization-induced activation. Therefore, the alternative gap distances identified by Castel et al. and any other larger gap distances (>21 bp) are likely just coincidentally similar to traditional SPSs and are not activated through canonical NICD dimerization.

Future Directions

The work described here has filled-in some potentially troubling holes the vanguard left behind during their initial surge of research activity and has further solidified the foundation for future work to build upon. However, as with all sciences, the recovery of some holes has uncovered the possibility of others. The mystery surrounding cryptic SPS activation, the troubles of identifying genes controlled through SPSs, and further

identification of Notch dimer-dependent models are all worthwhile avenues of future research.

Given the apparent abundance of cryptic SPS-driven genes, future work should aim to identify what dictates their transcriptional activity compared to canonical SPSs. We and others have shown that the complete Hes5 reporter is dimer-dependent, yet when its cryptic SPS was isolated out in our studies, this minimalized reporter lost its dimer-dependence. We propose two possible explanations that would need further validation. First, it's a possibility that while cryptic SPSs can load two NTC complexes in a purified, high stoichiometry system (EMSAs), this may not occur in a natural cell state without the aid of *cis*-regulatory elements or other co-transcription factors. Alternatively, like in others' EMSAs, our Hes5(SPS) luciferase reporter may be loading cooperating complexes but is lacking another promoter element that transitions dimerization into transcriptional output. Both explanations lead to a single experimental resolution: expand the Hes5(SPS) into the surrounding natural promoter area in an attempt to find a *cis*-regulating element. This element could then be screened for and identified in other known cryptic SPS genes to find some shared co-transcription factor regulating Notch dimerization.

In addition to screening for other *cis*-elements, perhaps more importantly, the Notch dimerization field needs to improve their methodology of finding genes regulated through sequence-paired sites. The current standard of performing ChIP-seq after a single round of purification and screening those targets for secondary RBPJ binding sites has left much to be desired. Our previous discussions on studies which utilized ChIP-seq screening pointed out that the screens used either have holes too specific which miss many cryptic sequence-paired sites or have holes too wide which identify genes that contain alternatively spaced

SPSs or ones with RBPJ motifs in the wrong orientation. Further, this dissertation demonstrates that any alternatively spaced SPSs are not constructive for dimerization, and thus should be purged from future ChIP-seq attempts. One resolution to this problem, which we have shown is experimentally feasible, is to perform ChIP-seq on targets that went through two rounds of purification. Instead of immunoprecipitating the standard RBPJ, future attempts should target differentially tagged NICDs (or heterodimers) for double selection and then perform ChIP-seq on this more specific pool. While a more stringent approach, it should identify active SPS motifs specifically regulated through dimerization.

Along with identifying further SPS-driven genes, it's necessary to do this within the context of multiple Notch-regulated cell systems. With expanded knowledge that all Notch proteins are capable of dimerization, it's pertinent to see how this can be applied to Notch models for development and disease. While a good starting point has been the role of Notch dimerization in the development of T cell acute lymphoblastic leukemia, this is still a cancer model of constitutively active Notch signaling. Future work should expand into other Notch models such as within neurogenesis [198] or the vasculature [199,200], with a particular interest in systems that utilize multiple Notch receptors to further explore the potential of Notch heterodimerization.

With further identification of dimerization-induced Notch target genes, this system could provide an interesting opportunity for Notch therapeutics. One potential therapeutic approach for leukemia and other cancers, for example, is through treatment with γ-secretase inhibitors. These inhibitors prevent Notch S3/S4 proteolysis through interactions with the γ-secretase complex, thereby stopping Notch signaling. However, these inhibitors

have been disappointing in clinical trials because of dose-limiting and on-target toxicities [167,201]. Notch dimerization presents a new target for therapeutic intervention; the dimerization interface. As previously proposed by both the Blacklow and Pear laboratories, specifically targeting the dimerization interface with a small molecule inhibitor, abrogating just a single facet of Notch signaling, may have more favorable toxicity profiles than other pan-Notch inhibitors. Efficacy of this method of inhibition and the development of these dimerization-inhibitors remains to be explored.

CHAPTER TWO

Homodimerization and Heterodimerization of Notch NICD domains

Jacob J. Crow[1], Chloe J. Munroe[2], Hannah Theriault[3], Travis M. Wood[2] & Allan R. Albig[1,2]

[1] Biomolecular Sciences Ph.D. Program. Boise State University. Boise, ID 83725, USA

[2] Department of Biological Sciences. Boise State University. Boise, ID 83725, USA

[3] Department of Chemistry. Boise State University. Boise, ID. 83725, USA.

Abstract

Notch signaling is universally conserved in metazoans where it is important for a wide variety of both normal and abnormal physiology. All four mammalian Notch receptors are activated by interactions with Notch ligands present on adjacent cells in the cellular microenvironment and trigger the release of Notch intracellular domains (NICDs) that translocate to the nucleus and stimulate transcription from Notch sensitive promoters. All NICDs contain highly conserved ankyrin domains which are important for NICD homodimerization and are flanked by more divergent N- and C-termini. Due to the highly conserved nature of Notch ankyrin domains, we hypothesized that NICDs may also engage in heterodimerization. Using a co-immunoprecipitation approach, we show that all NICDs engage in both homodimeric and heterodimeric interactions. The Notch4 ICD (N4ICD) demonstrated the greatest capacity for dimerization. Interestingly, ankyrin domains were not necessary for co-immunoprecipitation. Instead, a 50-amino acid segment immediately C-terminus of the Notch4 ankyrin domain was necessary and sufficient for strong dimerization. Finally, chromatin-IP confirmed that at least a fraction of heterodimers formed on DNA. Collectively, these results confirm that NICDs can engage in heterodimeric complexes with other NICDs and suggest a mechanism by which Notch signaling may be diversified through NICD heterodimeric interactions.

Introduction

The Notch signal transduction system is an ancient cell-cell communication mechanism that is conserved in essentially all multicellular animals [1,3]. Under normal conditions, Notch serves a wide variety of functions such as development, vascular biology, and immune function [202]. In contrast, dysregulation of Notch is linked to a variety

of diseases [202]. A clearer understanding of Notch signaling will provide new insights into the diverse processes governed by Notch.

There are four individual Notch receptors (Notch 1-4) present in mammalian genomes. Notch1 and Notch2 are highly similar molecules while Notch3 is significantly different, and Notch4 is the most divergent compared to the other Notches [203]. All Notch receptors are thought to be activated by the same mechanism involving juxtracrine interactions between adjacent cells when a Notch ligand on one cell is presented to a Notch receptor on a neighboring cell. Following ligand-receptor interaction, endocytosis of the Notch ligand provides ~4-12 pN of force [204] which physically separates the Notch receptor's extracellular domain at the S1 cleavage site thus priming the molecule for subsequent cleavage at the S2, then S3 cleavage sites (reviewed in Kadesch, (2004) [205]). The solubilized cytoplasmic S3 fragments (Notch intracellular domain, NICD) of all Notch receptors then translocate to the nucleus and participate in a tripartite co-transcriptional complex with the DNA binding protein and the transcriptional activator MAML [18,26]. interacts with an 8 bp-optimized sequence (*i.e.* TP-1 elements) on the DNA [17], and these sequences can be arranged as monomers, or in head-to-tail (HT), tail-to-tail (TT), or head-to-head (HH) orientations also known as sequence-paired sites (SPS).

Experimental evidence from EMSA and crystallography studies have shown that NICD tripartite complexes can form HH homodimers on SPS sites and that HH dimerization is important for transcriptional activation of SPS sites [19,24,28–30]. NICD dimerization is thought to occur between the ankyrin domains of interacting NICD molecules and both EMSA and crystallographic studies have confirmed the importance of ankyrin domains in NICD dimerization and transcription from sequence paired sites [29,30].

The importance of NICD dimerization through ankyrin interactions is illustrated by the observations of Liu et al, who found that NICD dimerization is required for Notch induced leukemogenesis and T-cell development [31]. Sequences in the more divergent N- and C-termini of Notch receptors have also been implicated in NICD homo-dimerization although this is less well understood [32]. Given the high degree of conservation within the ankyrin domains of all four mammalian Notch receptors, a long-outstanding question is whether or not different NICD molecules can engage in both homodimeric as well as heterodimeric complexes.

The goal of this investigation was to test the hypothesis that the N1-4ICD molecules can engage in heterodimeric interactions. Using an immunoprecipitation approach, we were able to confirm that all NICDs interact in both homo- and heterodimeric complexes. Moreover, we found that the N4ICD was unique in that it demonstrated the strongest homo- and heterodimeric interactions. Interestingly, ankyrin domains were not important for the unique behavior of Notch4. Instead, we determined that a region of the Notch4 C-terminus, directly downstream of the ankyrin domain, was responsible for mediating strong interactions with other NICDs.

Materials and Methods

Cell Culture

HEK293T cells were cultured in Dulbecco's Modified Eagle's medium (DMEM) supplemented with 10% equafetal (Atlas Biologicals) and 1x penicillin-streptomycin solution. Cells were grown in 10 cm plates and passaged at 80-90% confluence.

Plasmids and Plasmid Mutagenesis

The FLAG-NICD constructs were all gifts from Raphael Kopan [28] and acquired from Addgene. N1ICD (Addgene #20183), N2ICD (#20184), N3ICD (#20185), and N4ICD (#20186) all have an N-terminal 3xFLAG tag and code for the transcriptionally active, intracellular domain of the mouse Notch proteins. The NICD coding regions were then subcloned into pKH3 (#12555), a gift from Ian Macara [206] to add a C-terminal 3xHA tag as well as into pcDNA3.1/MYC-His (Invitrogen) to add a C-terminal MYC-His tag. The C-terminally truncated N1ICD-MYC construct was given to us by Raphael Kopan [23] (#41730) and encodes for the mouse N1ICD from V1744 to S2184.

The mouse Notch ankyrin domain mutants were created by aligning the human and mouse N1ICD to find the equivalent arginine involved in N1ICD dimerization [29,63]. Afterward, the mouse NICDs were aligned to find the equivalent arginines across the mouse Notches. N1ICD (R1974A), N2ICD (R1934A), N3ICD (R1896A), and N4ICD (R1685A) mutants were all created through site-directed mutagenesis in each tagged-variation of the NICD (FLAG/HA/MYC).

The N1ICD-N4ICD domain-swapped proteins were created through Gibson assembly using the FLAG-tagged variants. The equivalent mouse ankyrin domain was found using the previously outlined human Notches [191] and centered our swaps around these sites. Therefore, we have three NICD regions to swap between each other; the N-terminus region (N1: V1744-D1863, N4: V1463-D1571), the ankyrin domain (N1: V1864-S2111, N4: V1572-A1826), and the C-terminus region (N1: P2112-K2531, N4: H1827-N1964).

The N4ICD C-terminus truncations were created through Gibson assembly. The N4ICD C-terminus consists of 138 amino acids (everything C-terminus of the ankyrin domain), which we truncated into nearly equal portions. The first truncation was of 13 amino acids (-13 V1463-H1951) and from there we cut off 25 amino acids at a time (-38 -A1926, -63 -R1901, -88 -C1876, -113 -G1851, and -138 -A1826).

For the transcriptional reporter assays, *Hes5*-Luc (#41724) was a gift from Ryoichiro Kageyama and Raphael Kopan. This luciferase reporter contains portions of the mouse Hes5 promoter and includes several RBPJ binding sites to report the activity of Notch signaling. The Hes4-luc reporter (-139 to -9) was cloned by PCR amplification of the ChIP isolated Hes4 DNA shown in figure 2.8. This PCR fragment was cloned into pGL3-basic (Promega) with 5'Kpn1 and 3'SacI sites. The CMV-β-gal plasmid was originally from Clonetech.

All primers used for vector cloning and NICD mutagenesis can be found in Supplementary Table 2.1.

Immunoprecipitations

Cells were plated into 6-well plates at a density of 300,000 cells/well. The following day, cells were transfected with polyethylenimine (PEI, Polysciences) at a ratio of 5 μg PEI for every 1 μg plasmid DNA. Since the various NICD molecules are expressed at different levels in cells, we transfected varying amounts of NICD expression construct to standardize protein concentrations in CO-IPs as follows (750ng N1ICD, 500ng N2ICD, 500ng N3ICD, 250ng N4ICD). Forty-eight hours after transfection, cell lysates were prepared for immunoprecipitations and performed as previously described [157].

Western Blotting

Prepared protein lysates and CO-IP samples were separated through SDS-PAGE on polyacrylamide gels. Samples were then blotted onto nitrocellulose membranes and blocked in TBS-T (140 mM NaCl, 25 mM Tris-HCl, pH 7.4, 0.1% Tween-20) with 5% bovine serum albumin. Membranes were incubated with primary antibody (1:500; MYC, 1:1000; FLAG, 1:2000; HA) overnight on a rotator at 4^{o}C. Following incubation, membranes were washed 3 x 10 minutes in TBS-T and then incubated with a secondary antibody solution, composed of horseradish peroxidase-conjugated secondary antibodies at a concentration of 1:10,000. Membranes were then washed again 3 x 10 minutes in TBS-T and proteins were detected through enhanced chemiluminescence.

Antibodies

For western blotting, primary antibodies against FLAG(DYKDDDDK)-tag (D6W5B) were purchased from Cell Signaling Technology, while antibodies against HA(YPYDVPDYA)-tag (Y-11, sc-805) and MYC(EQKLISEEDL)-tag (9E10, sc-40) were purchased from Santa Cruz Biotechnology. Secondary antibodies were purchased from GE Healthcare Life Sciences and consisted of α-mouse (NA931V) or α-rabbit (NA934V) horseradish peroxidase-conjugated antibodies. The anti-FLAG antibody resin used for CoIP was from Genscript.

Luciferase Assays

Cells were plated in 24-well plates at 50,000 cells/well. The following day, cells were transfected with PEI at a ratio of 5 μg PEI for every 1 μg DNA. Cells were transfected with 100 ng/well Hes5-luciferase and 10 ng/well of the various NICD constructs. To normalize data for transfection efficiency and potential cell growth/death, we co-

transfected with 10 ng/well of a CMV-β-Galactosidase construct. Cells were lysed 48 hours post-transfection in 1x firefly luciferase lysis buffer (Biotium). Lysates were analyzed following the manufacturer's protocol (Firefly Luciferase Assay Kit, Biotium) using a Promega© Glomax Multi Detection System luminometer. Luciferase activity was normalized to β-Galactosidase activity (Promega) and values were reported as a fold change to control. To minimize transfection variations and output noise, all conditions were performed in triplicate for each independent experiment.

RT-PCR Analysis

A variety of cell lines were grown to collect their mRNA and analyze their Notch expression profiles. Cells were plated in 10 cm dishes and grown until 80% confluence. To collect the cells and their mRNAs, they were washed with 1xPBS and lysed with RiboZol RNA Extraction Reagent (Amresco). mRNA was collected and purified following the manufacturer's recommended protocol. Equivalent amounts of RNA was reverse transcribed with iScript (Bio-Rad) following the manufacturer's protocol and diluted for PCR analysis. Primers used to target human Notch mRNAs are listed in Supplementary Table 2.1. Primers targeting 18S rRNA was used as an internal control to check cDNA quality.

Chromatin IP

Chromatin immunoprecipitation (ChIP) analyses were performed as previously described [207], with minor modifications including omission of SDS from the dilution, high-salt wash, and elution buffers, and omission of spermidine from the micrococcal nuclear buffer. 293T cells were transfected with two differentially tagged NICDs and then 48 hours later were fixed by formaldehyde-induced crosslinking and the nuclear fraction was

isolated and collected. Micrococcal nuclease (NEB) was used to cut the chromatin into 300-1,500 base pair fragments, the nucleus briefly sonicated to lyse the fraction, and the DNA collected. To specifically isolate the dimerized complexes bound to DNA, they were placed through two rounds of selection, targeting both partners within the Notch dimer. The first round of selection was performed with anti-FLAG G1 affinity resin (GenScript), samples thoroughly washed, and complexes eluted with 3xFLAG-peptide (ApexBio). Those complexes were placed through a second round of selection, probing for an HA-tagged NICD partner, with biotinylated HA antibodies (Bioss). These targets were precipitated out of solution with streptavidin magnetic beads (NEB), thoroughly washed again, and the DNA was isolated out of the complexes with Proteinase K (Amresco) and reverse crosslinking. DNA was cleaned and purified with a PCR purification kit and samples were analyzed for Notch-dimer targets using Hes1 or Hes4 primers as indicated in supplementary tables.

Results

NICD dimerization in mammalian cells

Previous work revealed the canonical crystal structure of the mammalian Notch transcriptional complex containing fragments of RBPJ, MAML1, and the N1ICD ankyrin domains in a head-to-head dimerized state [29,30]. Nam et al., [29] further defined key residues in the Notch1 NICD (N1ICD) ankyrin domain critical for dimerization of N1ICD molecules and determined that these residues are highly conserved in Notch 2-4 (N2ICD, N3ICD, N4ICD). This data suggested that all Notch NICD domains may engage in head-to-head dimerization interactions. Furthermore, given the overall sequence similarity of the Notch ankyrin domains and the conservation of these key amino acids required for

dimerization, it was hypothesized that NICD domains may also be able to engage in heterodimeric interactions, although this has not been investigated.

To test this hypothesis, we first established a cellular co-immunoprecipitation (CO-IP) assay to monitor NICD homodimerization. To differentiate between two dimerizing versions of the same molecule, we generated various plasmids encoding FLAG-, MYC, or HA-tagged versions of mouse NICD molecules. 293T cells were transiently co-transfected with cDNAs encoding one FLAG-tagged and a second MYC- or HA-tagged pair of NICD molecules. Anti-FLAG co-immunoprecipitation was used to isolate FLAG-tagged NICDs, then immunoblotting with anti-MYC or anti-HA antibodies was used to detect MYC- or HA-tagged Co-IP NICD partners, depending on combination.

To validate this co-immunoprecipitation system, we first sought to detect homodimerization of N1ICD molecules, which had previously been observed to dimerize by EMSA [30]. We co-transfected 293T cells with a FLAG-tagged full-length N1ICD (1FL) and a truncated MYC-tagged N1ICD (1T) similar to the N1ICD previously used in EMSA experiments to study the interaction between N1ICD proteins (*i.e.* 347 amino acids of the N1ICD C-terminus including the PEST domain deleted). As shown in figure 2.1A, MYC-tagged truncated N1ICD readily precipitated with full-length N1ICD. Importantly, precipitation of MYC-tagged N1ICD was dependent on the presence of FLAG-tagged N1ICD thus demonstrating specificity of the CO-IP approach. Having successfully observed N1ICD homodimerization, we next sought to monitor homodimerization of the other NICD molecules (Fig 2.1B). Interestingly, while we again observed homodimerization between full-length and truncated N1ICD, homodimerization of two full-length N1ICD molecules was only inconsistently observed. For example, results

shown in figure 2.1B do not demonstrate homodimerization between full-length N1ICD molecules while data shown in figure 2.2A does illustrate a successful co-immunoprecipitation of full-length N1ICD molecules. This inconsistency of homodimerization between full-length N1ICD molecules continued for unknown reasons throughout the project. In contrast, experimentation with FLAG- and MYC-tagged full-length N2ICD and N3ICD determined that the N2 and N3ICDs engaged in what appeared to be fairly weak, but consistent, homodimerization (Fig. 2.1 deep exposure). Finally, and in stark contrast, N4ICD homodimerization was consistently observed and appeared to be significantly more robust compared to N1-3ICD homodimerization despite having equivalent protein concentration in whole-cell lysates. Thus, these results demonstrated that all NICD molecules are capable of homodimerization, although the strength of homodimeric interactions did not appear to be equivalent for all dimer complexes.

Heterodimerization of NICD proteins

Due to the overall amino acid similarity of Notch proteins, especially in the ankyrin domains, and the shared ability of the Notch proteins to form homodimers, we hypothesized that NICD molecules may also be able to engage in heterodimeric complexes. To address this possibility, we used the same co-transfection model as described above but transfected cells with all permutations of epitope tagged N1, 2, 3, and 4ICD molecules. As shown in figure 2.2a, full-length FLAG-N1ICD engaged in homodimeric interactions with full-length HA-tagged N1ICD and heterodimeric interactions with the HA-tagged N2, N3, and N4ICD molecules. Interestingly, N1ICD co-immunoprecipitated with N2, N3, and N4ICD better than with N1ICD suggesting that N1ICD preferentially engaged in heterodimeric interactions. Moreover, N1ICD most strongly precipitated with N4CID.

N2ICD also formed homodimers and heterodimers with each of the other NICDs and again, the N2ICD-N4ICD interaction appeared to be the most robust (Fig. 2.2B). N3ICD formed heterodimers with each of the other NICDs (Fig 2.2C) although dimerization with N1ICD and N2ICD appeared to be weak (Fig 2.2C dark) and as before, the interaction between N3ICD and N4ICD appeared to be the strongest (Fig. 2.2C light). Finally, N4ICD demonstrated strong heterodimerization with the other NICDs, but again, N4ICD homodimerization appeared to be the most robust (Fig. 2.2D). Importantly, co-precipitation of N4CID-HA was dependent on N4ICD-FLAG co-transfection thus again illustrating the specificity of the co-immunoprecipitation system.

Collectively, this series of Co-IP experiments demonstrated that all Notch heterodimer combinations appear to be capable of formation. Moreover, these results also showed that Notch NICDs do not appear to equally engage in dimerization and that N4ICD consistently displayed the most robust homodimerization and heterodimerization compared to the other NICD molecules.

N4ICD homodimers and N4/N1 heterodimers outcompete N1ICD homodimers

Our results support the hypothesis that all NICD domains can engage in both homo- and heterodimer interactions. In cells that express multiple Notch proteins, it is therefore possible that NICD heterodimerization may present an opportunity for diversification of Notch signaling outputs through alternative dimerization similar to what has been described for other transcriptional systems [208]. To assess the expression of multiple Notch receptors in single cell lines, and thus the possibility of NICD heterodimerization, we screened several cell lines for co-expression of Notch receptors. Reverse-Transcription PCR (RT-PCR) was used to monitor mRNA expression of each Notch protein. As shown

in figure 2.3A, each of the cell lines examined expressed at least two Notch receptors, while several expressed three or even all four Notch receptors. Consistent with previous results [67], Notch4 expression was limited to the endothelial cell lines (*i.e.* HUVEC and HMEC).

Based on our observation that the majority of cell lines express more than one Notch protein and our results showing that N4ICD demonstrates the strongest potential for dimerization in our system, we next sought to determine if N4ICD would dominate dimer formation even when expressed in tandem with N1ICD. To accomplish this, we performed an experiment wherein HA-tagged N1ICD and N4ICD were allowed to simultaneously compete for binding and co-immunoprecipitation with a single FLAG-tagged "bait" protein (Fig 2.3B). FLAG-N1ICD or FLAG-N4ICD were co-transfected individually with both HA-tagged N1ICD and HA-tagged N4ICD, and immunoprecipitated with anti-FLAG antibodies as before. Despite nearly equivalent expression of HA-tagged N1ICD and N4ICD in whole cell lysate, we observed that N1ICD preferred forming heterodimers with N4ICD rather than engage in homodimer interactions, although N1ICD-N1ICD homodimers were also detected. In contrast, we found that N4ICD preferentially engaged in homodimer formation and we were unable to detect N4ICD-N1ICD heterodimers when N4ICD was used as bait, possibly as a result of the stronger interaction between N4ICD molecules.

Ankyrin domains are not required for NICD dimerization

The Notch ankyrin domains have been shown to interact in a head-to-head orientation that is important for NICD dimerization [29,30]. Given our results, we sought to determine if the NICD ankyrin domains were important for NICD dimerization in our immunoprecipitation assay. Arg1984 within the human N1ICD ankyrin domain was

previously identified as important for NICD dimerization and transcriptional responses from promoters with paired RBPJ binding sites such as the Hes5 promoter [29,30]. Using sequence alignments, we found equivalent arginine residues in the mouse Notch1 and Notch4 NICDs (Arg1974 and Arg1685 respectively) and performed site-directed mutagenesis to change these arginines to alanine residues. To confirm that these mutations decreased transcriptional activity from paired RBPJ sites, we monitored luciferase expression downstream from the Hes5 promoter that was previously used by Arnett et al., [30] to monitor NICD transcriptional activity. This element contains paired RBPJ sites in a "head-to-head" orientation that are important for efficient transcription from this promoter. As shown in figure 2.4A, ankyrin mutant N1ICD demonstrated much weaker transcriptional activity compared to wild-type N1ICD. Moreover, ankyrin mutant N4ICD was also less efficient at driving Hes5 promoter activity, although the inherently low transcriptional activity of wild-type N4ICD made this effect less obvious compared to N1ICD.

Having confirmed the importance of the N1ICD and N4ICD ankyrin domains for driving transcription from paired RBPJ binding sites, we next sought to determine if ankyrin domains are required for NICD co-immunoprecipitation. To accomplish this, we again used our co-immunoprecipitation assay to compare the ability of wild-type and ankyrin mutant N1 and N4ICD to co-precipitate in 293T cells (Fig 2.4B). Due to the inconsistencies observing full-length N1ICD homodimers previously stated, the C-terminally truncated N1ICD construct was again employed for this experiment. Despite the importance of ankyrin domains for transcriptional activity, even when the ankyrin domains of both NICD partners were mutated we were unable to detect significant changes in N1

or N4ICD homodimerization. Interestingly, however, when we compared the ability of HA-tagged N4ICD to CO-IP with various FLAG-tagged N1ICD truncations, we found that N4ICD was able to CO-IP with a C-terminal deletion fragment of N1ICD (RAM/Ank) and the isolated N1ICD ankyrin domain (Figure 2.4C). Finally, since the effect of the R1685A mutation on N4ICD transcriptional activity was relatively weak, we further characterized the role of the N4ICD ankyrin domain in N4ICD dimerization. We found that N4ICD homodimerization was not affected by a complete deletion of the N4ICD ankyrin domain (Figure 2.4D). Taken as a whole, these results confirm that NICD ankyrin domains are important for NICD transcriptional activity and also suggest that NICD ankyrin domains may contribute to NICD dimerization but are not required for NICD dimerization as detected by CO-IP.

Dimerization is controlled by NICD C-terminal domain

Analysis of N1ICD by both crystallography and EMSA has shown that N1ICD homodimerization and transcriptional activity of homodimers appears to be dependent on interactions between opposing ankyrin domains. Our results confirm that ankyrin domains are important for NICD transcriptional activity but also suggest that NICD ankyrin domains are dispensable for co-immunoprecipitation of NICD dimers. Therefore, it was important to determine which domains of NICD molecules are important not only for the dimerization of NICDs but also for dictating the differential strengths of NICD homo- and heterodimerization that we had observed. To accomplish this, we took advantage of the differential dimerization of the N1ICD and N4ICD dimers. We constructed chimeric proteins that swapped the N-termini, ankyrin domains, and C-termini between N1ICD and N4ICD (Fig 2.5A) and compared the ability of these constructs to co-immunoprecipitate.

We found that the N1ICD and N4ICD N-terminus and ankyrin domains could be interchanged without any obvious effect on dimerization (Fig 2.5B and C) suggesting these sequences are interchangeable during dimerization and not important for controlling differential NICD dimerization. In contrast, swapping the N4ICD C-terminus onto N1ICD significantly enhanced dimerization (Fig 2.5B) whereas swapping the N1ICD C-terminus to N4ICD drastically reduced N4ICD dimerization (Fig 2.5C). These results taken together with those presented in figure 2.4 indicate that co-immunoprecipitation is not dependent on interactions between ankyrin domains and that control of differential dimerization resides in the C-terminal sequences. However, based on this experiment we were unable to determine if the enhanced dimerization of N1ICD with the N4ICD C-terminal domain was due to either the simple deletion of the N1ICD C-terminus, the addition of the N4ICD C-terminal domain, or a combination of these changes. Yet, we had previously shown that truncated N1ICD co-immunoprecipitated better than full-length N1ICD suggesting the N1ICD C-terminal domain contains a dimerization inhibition domain. Similarly, we were also unable to conclude if decreased dimerization of N4ICD with N1ICD C-terminal domain was due to the deletion of a dimerization enhancer in the N4ICD C-terminal domain, addition of the N1ICD C-terminal domain, or a combination of these changes.

N4ICD contains a dimerization enhancing domain

Having shown that the N4ICD C-terminal domain was associated with enhanced dimerization potential, our next goal was to dissect the N4ICD C-terminal domain to identify regions important for strong dimerization. To accomplish this, we created a progressive series of FLAG-tagged N4ICD C-terminal deletions (summarized in figure 2.6A) and compared dimerization between full-length and truncated N4ICD. To our

surprise, we failed to observe any effect of N4ICD C-terminal deletion on dimerization between mutant and full-length N4ICD (Fig 2.6B). According to Vasquez et al., [32] NICD domains dimerize through interactions between the N- and C-termini of dimerizing molecules. Based on this, we rationalized that a single full-length C-terminal domain may still be sufficient to promote strong dimerization. To confirm this, we compared dimerization of two truncated N4ICDs or two WT N4ICDs in our co-immunoprecipitation assay. As shown in figure 2.6C, CO-IP between truncated N4ICDs was significantly weaker compared to WT N4ICDs suggesting that an enhancer of dimerization resides in the N4ICD C-terminus. Therefore, we next compared dimerization between C-terminal truncated HA-tagged N4ICD, and the set of FLAG-tagged C-terminal progressive truncations. As shown in figure 2.6D, deletion of the most C-terminal 88 amino acids did not impact dimerization. However, further deletion of the most C-terminal 113 amino acids significantly decreased dimerization while deletion of the entire C-terminal 138 amino acids prevented dimerization entirely.

To determine if the 50 amino acid region between amino acids A1826 and C1876 (*i.e.* the region of interest or ROI) was sufficient by itself to enhance NICD dimerization, we swapped this ROI into the equivalent site of N1CID and again compared co-immunoprecipitation between various NICD molecules. As shown in figure 2.6E, despite the introduction of the N4ICD ROI into N1ICD, we were still unable to consistently observe dimerization between N1ICD molecules. However, dimerization was consistently increased between N4ICD and the modified N1ICD containing the N4ICD ROI. Based on this observation we believe the 50 amino acid region directly C-terminal to the N4ICD ankyrin domain, between amino acids A1826 and C1876, is responsible for efficient

N4ICD dimerization and that efficient dimerization between N4ICDs requires only a single N4ICD C-terminus.

Dimerization of NICD domains does not correlate with transcriptional activity

Our results demonstrated that the N4ICD displays significantly stronger dimerization potential compared to the other NICDs. Optimal activation of some Notch promoters including the Hes5 promoter is dependent on NICD dimerization since the RBPJ binding sites in these promoters are arranged in a head-to-head orientation or SPS site. Given this, we hypothesized that increased dimerization would correlate with increased transcriptional activity from the Hes5 promoter, which we previously confirmed, requires NICD dimerization for optimal transcriptional activation (Fig 2.4). 293T cells were transfected with luciferase reporters driven from the Hes5 promoter and various chimeric proteins developed in figure 2.5. As shown in figure 2.7A, chimeric N1ICD/N4ICD proteins did display somewhat altered transcriptional activity compared to N1ICD, however, the addition of the N4ICD C-terminal decreased transcriptional activity despite increasing the dimerization activity of N1ICD. Conversely, the addition of the N1ICD C-terminal to N4ICD did not significantly change N4ICD transcriptional activity despite decreasing N4CID dimerization potential. Interestingly, swapping the N4ICD ankyrin domain to N1ICD decreased reporter activity while swapping the N1ICD ankyrin domain to N4ICD increased transcriptional activity despite these swaps having no discernable effect on dimerization. Therefore, these results further suggested that dimerization of NICD proteins (as measured by co-immunoprecipitation) does not directly correlate to transcriptional activity.

NICD molecules heterodimerize on DNA

Our results indicated that dimerization between NICD molecules (as measured by Co-IP) did not directly correlate to transcriptional activity. Nonetheless, dimerization between NICD molecules on Notch sensitive promoters has been observed by X-ray crystallography and EMSA analysis. These two observations appeared to be in conflict and therefore suggested that NICDs may exist in multiple dimerization states. One state was detected by co-immunoprecipitation, dependent on NICD C-terminals, but did not apparently correspond to transcriptional activity. The second state was transcriptionally active and dependent on interactions between ankyrin domains but was apparently not detected by Co-IP. These observations raised the important question whether or not the NICD complexes that were being recovered by Co-IP were engaged in heterodimer complexes on DNA or rather were strictly in a non-transcriptional state as suggested by Vasquez et al., [32]. To address this question, we transfected 293T cells with combinations of FLAG-tagged N1ICD or N4ICD coupled with HA-tagged N1ICD or N4ICD binding partners. DNA/protein complexes were crosslinked, fragmented by micrococcal nuclease treatment, and lysates were subjected to a two-step co-immunoprecipitation, first with anti-FLAG resin and second with anti-HA antibodies. Control samples included transfection with FLAG-tagged N1ICD alone and a single anti-FLAG immunoprecipitation step (+control) and negative control that was transfected with HA-tagged NICD and subjected to the two-step Co-IP procedure. In all cases, precipitated DNA was detected by PCR with oligos that were designed to flank the paired head-to-head binding sites within the Hes4 and Hes1 promoters. As shown in figure 2.8A, both Hes1 and Hes4 sequences were detected in the precipitated chromatin of all NICD combinations. Importantly, the ChIP

was specific since Hes4 and Hes1 promoters were not recovered if a FLAG-tagged protein was not included. This result showed that NICD molecules were engaged in heterodimer complexes on DNA. Based on this result, it was logical to compare the effect of N1ICD, N4ICD, or N1ICD + N4ICD transfection on transcriptional activation from the Hes1 and Hes4 promoters. As shown in figure 2.8B, N1ICD activated the Hes1 promoter significantly more than N4ICD, and the combination of N1ICD and N4ICD was heavily biased towards lower activation. Interestingly, this trend was not consistent for the Hes4 promoter. Instead, Hes4 activation was equivalently activated by N1ICD, N4ICD, and the N1ICD/N4ICD combination. Together these results indicated that not only were N1ICD and N4ICD were forming homodimer complexes on DNA but also that N1ICD/N4ICD heterodimers were forming on DNA. Moreover, these results also suggested that N4ICD might be able to regulate N1ICD transcriptional activity on some promoters through heterodimeric interactions.

Discussion

The Notch signaling mechanism is highly conserved in the earliest metazoans and understanding Notch function is likely to be important not just for basic biology, but also for the many diseases with which Notch malfunction has been associated. Previous work found that Notch1 NICD domains dimerize through interaction between NICD ankyrin domains and these findings are supported by both EMSA and X-ray crystallography. However, it has also been shown that NICD dimerization is influenced by interactions between the N- and C-terminals of dimerizing NICD molecules [32]. The results presented in this work expands these findings by showing that 1.) all mammalian Notch NICD domains engage in homodimerization, 2.) that all mammalian Notch NICD domains also

engage in heterodimerization, 3.) that the N4ICD demonstrates robust dimerization potential compared to the other NICDs, and 4.) that the C-terminal domains of Notch1 and Notch4 contain negative and positive regulators of dimerization respectively. Collectively, our findings provide new insight into the molecular underpinnings of Notch signaling and should help understand how Notch function, and malfunction, contributes to cell biology.

The majority of our understanding of Notch dimerization comes from experimentation with partial domains of the three proteins found in the Notch tripartite complex of (*i.e.* N1ICD, MAML, and RBPJ) that were produced in bacterial cells and analyzed by EMSA, X-ray crystallography, or FRET [29,30,35,51]. Overall, the major findings of these studies were to determine the structure of the Notch tripartite complex and to understand how NICD molecules engage in head-to-head dimerization through their ankyrin domains. A limitation of these works, however, was that the partial N1ICD molecules used primarily represented the highly conserved NICD ankyrin domains and lacked the more divergent N- and C-termini. Therefore, it was concluded that N1ICD dimerization is dependent on interactions between NICD ankyrin domains. This conclusion was supported by reporter assays wherein mutation of key ankyrin domain residues significantly reduced transcriptional activation from paired (head-to-head) RBPJ binding sites [30]. Our results partially support this result since we also find that mutation of key residues within the ankyrin domains decrease transcriptional activity from promoters containing paired RBPJ binding sites. However, we also found that these same mutations, which negatively impacted transcriptional activity, did not affect co-immunoprecipitation of NICD molecules, although an isolated N1ICD ankyrin domain was capable, but not required, for co-immunoprecipitation with N4ICD. Therefore, it appears that the previous

conclusion that NICD dimerization is dependent on interactions between ankyrin domains was oversimplified.

A major difference between our experiments and those that observed dimerization through ankyrin domains [29,30,35,51] is that we employed NICD molecules with full-length N- and C-terminal domains whereas the previous studies utilized ankyrin domains lacking N- and C-terminal sequences. In addition, our experiments were performed with whole-cell lysates whereas much of the work cited above has been performed with purified components. Using these full-length NICD constructs, we found that N-terminal sequences in N1ICD and N4ICD appeared to perform equivalent and interchangeable roles in dimerization. In comparison, the N4ICD C-terminal sequence enhanced dimerization whereas the N1ICD C-terminal decreased dimerization. These findings are largely compatible with results presented earlier by Vasquez et al., [32] who also used co-immunoprecipitation to demonstrate that dimerization of N1ICD also engages interactions between the N- and C-terminal domains of N1ICD.

As outlined above, there are conflicting observations regarding the nature of NICD dimerization. We envision two possibilities that may help to unify the existing data. The first possibility is a "two-state model" where NICD molecules can exist in two different states, each with different functions. In the first state, (which may not require DNA) dimerization is driven primarily by interactions between the N- and C-termini of dimerizing NICDs. This first state may exist independently of transcription or even DNA binding and the ankyrin domains would have a negligible effect on dimerization. This is supported by our co-immunoprecipitation experiments showing that N4ICD lacking its ankyrin domain is still capable of dimerization (figure 2.4D). This model is favored (and

initially proposed) by Vasquez et al., [32] who hypothesize that NICD multimers (first state) are required to recruit MAML during assembly of the final NICD transcriptionally active tripartite complex, (*i.e.* the second state). In this second state, NICD molecules together with and MAML dimerize on head-to-head SPS sites in an ankyrin domain-dependent fashion. The role of the N- and C-termini in this second state appears to be secondary to the ankyrin domains although evidence suggests the N- and C-terminals still have a role during transcriptional activity. For example, we found that swapping the N4ICD C-terminal onto N1ICD decreased transcriptional activity from the Hes5 promoter (figure 2.7). Similarly, Blain et al., [209] observed that overexpression of N1ICD with a C-terminal 238 amino acid deletion does not recapitulate normal Notch signaling. This is a point of practical concern since this Notch1 C-terminal truncation construct has been described as "full-length" and used in a number of studies, including the generation of a transgenic mouse model for Notch activation [210]. In addition to this "two-state" model of NICD dimerization, a second possible model of NICD dimerization is that a single dimer state exists that simultaneously engages the N-terminals, ankyrin domains, and C-terminals of dimerizing NICDs. In this model, the ankyrin domains might contribute less to dimerization but more to transcriptional activity while the N- and C-terminals might still be primarily responsible for dimerization perhaps through reciprocal interactions around the central ankyrin domain interactions. However, since the existing NICD structural models use isolated ankyrin domains, this remains a hypothesis and would need to be tested in future experiments.

One of the important results from our work is the confirmation that all NICD domains are capable of homodimerization as previously demonstrated [29]. An important

difference between previous homodimerization studies however is that we monitored homodimerization of full-length NICD molecules in whole-cell lysates compared to purified ankyrin domains in in-vitro EMSA assays. Therefore, our results add an important perspective to the understanding of NICD homodimerization. Taking this a step further, our co-immunoprecipitation studies also discovered that all NICD domains engage in heterodimeric interactions. Moreover, the apparent strength of interaction between NICDs was not equivalent. Instead, we found that N4ICD appeared to most robustly form NICD heterodimers but had an even greater preference for N4ICD homodimerization. The implications of this finding remain unknown; however, several tantalizing possibilities present themselves. First, we and others have shown that many cells express more than one Notch receptor (figure 2.3A). Since the various NICD molecules demonstrate varying transcriptional activity, it is possible that NICDs with lower transcriptional activity such as N3ICD or N4ICD may act as negative regulators for N1ICD or N2ICD by engaging in heterodimeric interactions at sequence paired sites. In particular, since N4ICD seems to promiscuously engage in dimerization and is expressed almost exclusively in endothelial tissues, it is tempting to speculate that N4ICD may serve to regulate Notch1 function in the vascular system. In support of this, we confirmed the presence of N1/N4ICD heterodimers on the Hes1 and Hes4 promoters by ChIP analysis and found that N1ICD transcriptional activity on the Hes1 and Hes4 luciferase reporters was reduced by co-transfection with N4ICD (Figure 2.8). Care must be taken to interpret this result however since the overall reporter activity probably represents a sum of N1ICD homodimers, N4ICD homodimers, and N1/N4ICD heterodimers.

In conclusion, our results suggest that there remain many important questions about the basic mechanism of Notch signaling. Major outstanding questions that remain include the formation and function of the NICD dimerization complex(s), the extent to which NICD heterodimerization influences Notch signaling output, and if Notch homodimerization or heterodimerization can be regulated by cell signaling. Answering these questions should shed light on Notch signaling and help to understand how this ubiquitous signaling mechanism regulates cell biology.

Acknowledgments

This work was supported by funding from the National Institute of General Medical Sciences to A. Albig (2R15GM102852-02) and from grants NIH/NIGMS P20GM103408 and P20 GM109095. Author contributions were as follows: A. Albig and J. Crow conceived and designed the experiments. A. Albig, J.Crow, C. Munroe, H. Theriault, and T. Wood performed the experiments. A. Albig and J. Crow prepared the final manuscript.

Conflicts of Interest

The authors declare no conflicts of interest.

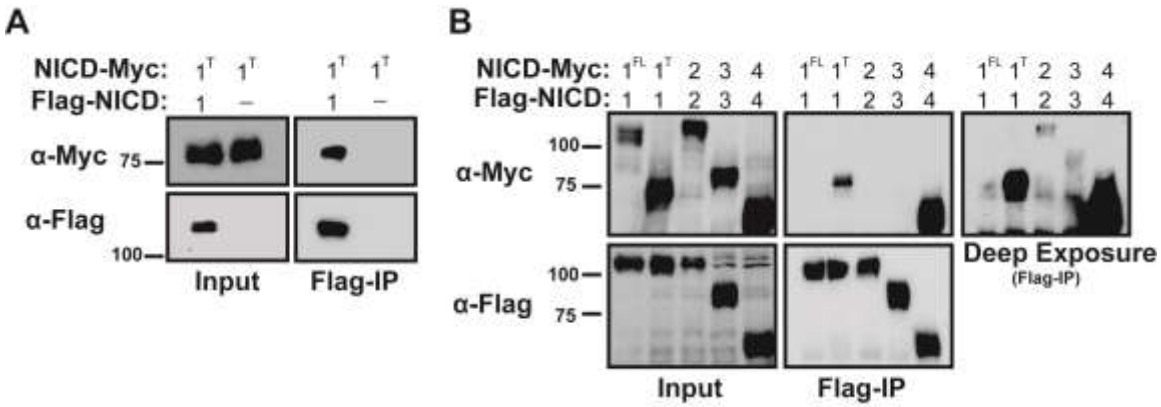

Figure 2.1: Detection of Notch intracellular domain homodimer complexes within a cell culture model

(A) HEK293T cells were co-transfected with cDNAs encoding FLAG-tagged full-length N1ICD and MYC-tagged truncated N1ICD (1T). Whole-cell lysates were immunoprecipitated with anti-FLAG antibodies and western blotted with anti-MYC and anti-FLAG antibodies. Input represents 10% of whole-cell lysate used in immunoprecipitation. Shown is a representative image of a single experiment that was performed four independent times. (B) FLAG- and MYC-tagged N1-4ICDs were transfected into 293T cells, homodimer complexes were detected by immunoprecipitation (IP) with an anti-FLAG antibody and western blotting with anti-MYC antibodies. A longer anti-MYC western blot exposure (deep exposure) was required to visualize N2 and N3ICD homodimers. Shown is a representative image of a single experiment that was performed four independent times.

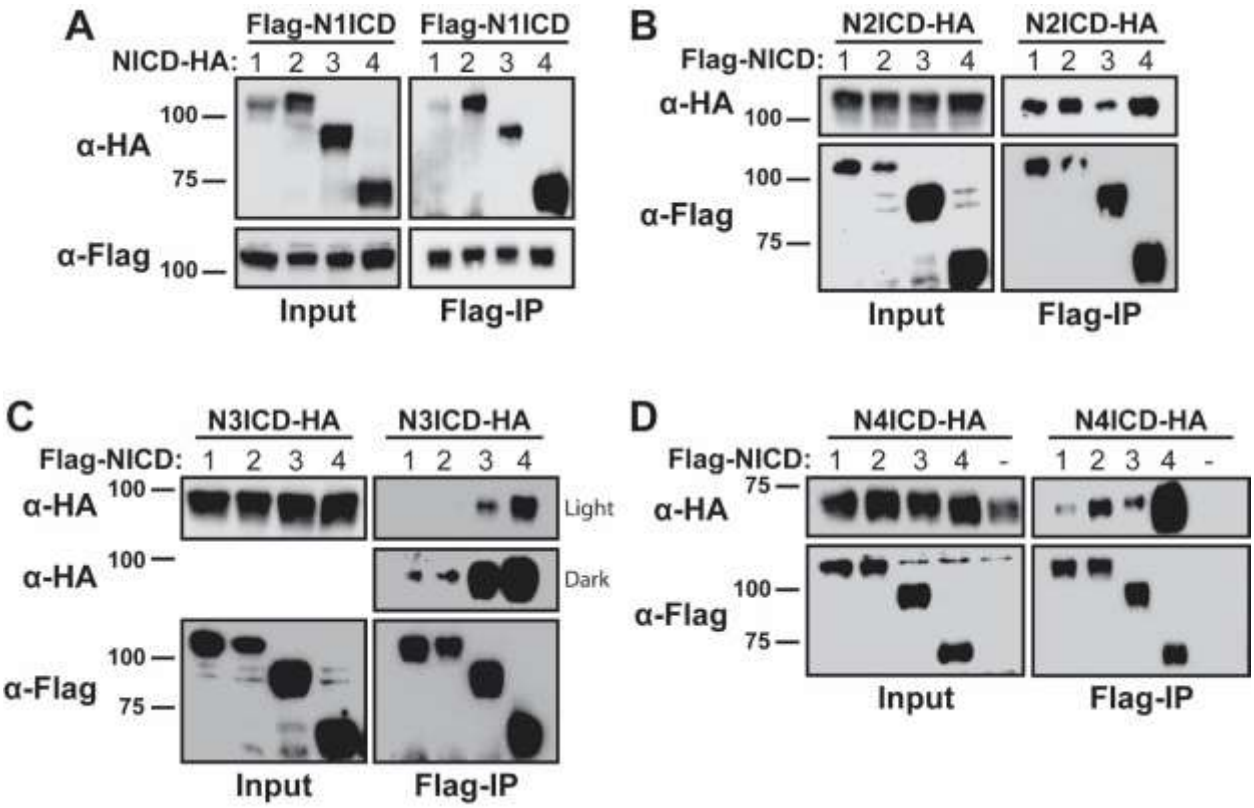

Figure 2.2: Detection of Notch intracellular domain homo- and heterodimer complexes

293T cells were transfected with FLAG- and HA- tagged species of various NICDs and dimerization was detected by co-immunoprecipitation with anti-FLAG antibodies and western blotting with anti-HA antibodies. In all panels, Input represents 10% of whole-cell lysates before CO-IP. The heterodimerization possibilities are represented with (A) N1ICD, (B) N2ICD, (C) N3ICD, and (D) N4ICD. To prevent confounding results from residual unstripped antibodies, lysates were run twice on two different membranes for cleaner western blot analysis. Panel D also includes a negative FLAG-tagged NICD lane (-), controlling for non-specific interactions between HA-tagged protein on anti-FLAG antibody resins.

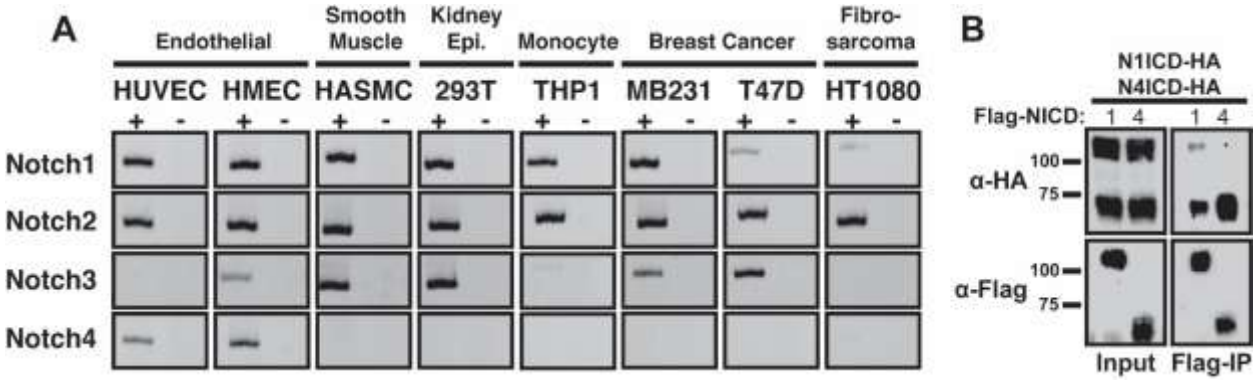

Figure 2.3: N4ICD outcompetes N1ICD

(A) RT-PCR was used to monitor expression of Notch proteins in cell lines from various tissues. +/- denotes +RT experimental samples and -RT control samples. Image shown represents data from two independent repetitions. (B) HA-tagged N1ICD and N4ICD were simultaneously co-transfected with either FLAG-tagged N1ICD or N4ICD. Dimerization was detected by precipitation with anti-FLAG antibodies and western blotting with anti-HA antibodies. Input represents 10% of whole cell lysate used in the immunoprecipitation. The image depicts a representative example of a single experiment that was performed three times.

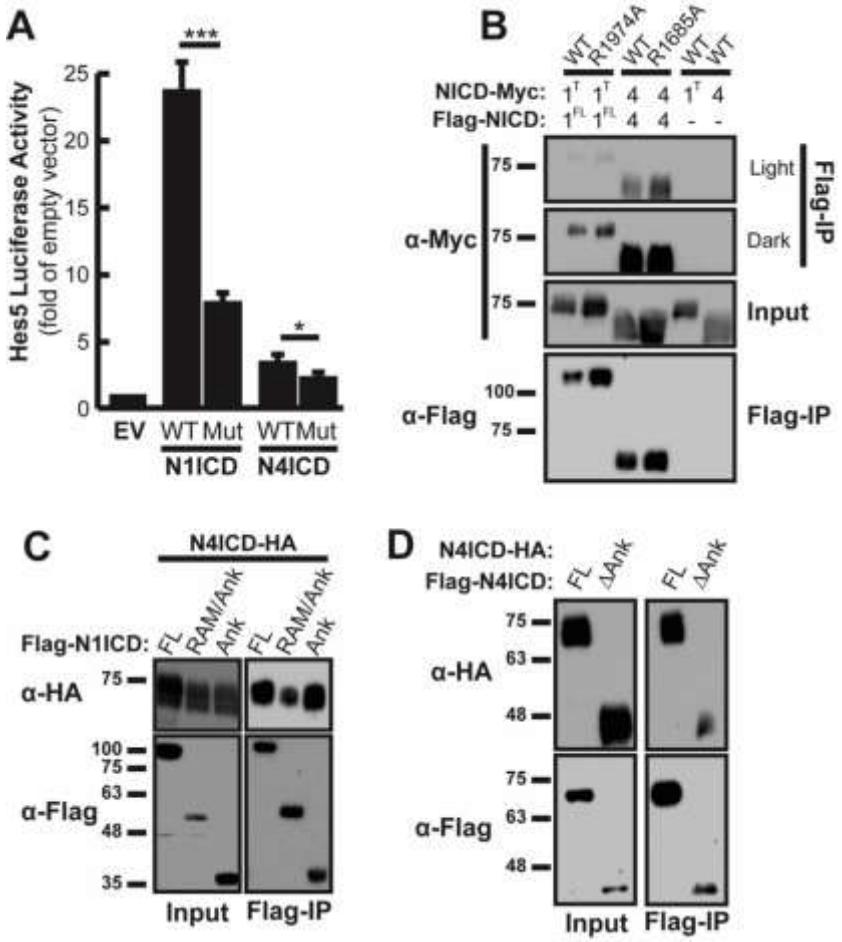

Figure 2.4: Ankyrin domains are not required for NICD dimerization

293T cells were co-transfected with Hes5-promoter luciferase reporter and wild-type (WT) or corresponding ankyrin domain mutant (Mut) NICDs. Reporter activation is compared to its basal activity in cells, which received an equivalent amount of empty overexpression vector (EV). Shown are the average +/- SE of six experiments. Transfection efficiency was normalized by co-transfection with CMV-β-gal reporter plasmids and measuring β-gal activity. Statistical significance was determined through a student's two-tailed *t* test, where *** is $p < 0.001$, and * is $p < 0.05$. (B) 293T cells were transfected with pairs of cDNAs encoding FLAG- and MYC-tagged WT NICD domains or mutant FLAG- and MYC-tagged mutant ankyrin NICD domains. Anti-FLAG

antibodies were used to isolate FLAG-tagged proteins and western blotting with anti-MYC antibodies was used to detect interacting NICD domains. Shown is a representative image of a single experiment that was performed four independent times. To account for dimerization intensities, the figure includes a light and dark exposure of the co-immunoprecipitated MYC-partners. (C) 293T cells were transfected with HA-tagged N4ICD and various FLAG-tagged N1ICD constructs including the full-length (FL) N1ICD, N1ICD lacking the C-terminus (RAM/Ank), and the isolated N1ICD ankyrin domain (Ank). Anti-FLAG antibodies were used to detect interacting HA-tagged molecules. Shown is a representative image of a single experiment that was performed three times. (D) 293T cells were transfected with full-length HA-tagged N4ICD and either full-length or ankyrin deletion mutant (ΔAnk) FLAG-tagged N4ICD. CO-IP and western analysis was performed as above. In all panels, Input represents 10% of whole cell lysate from each sample as a control for protein expression.

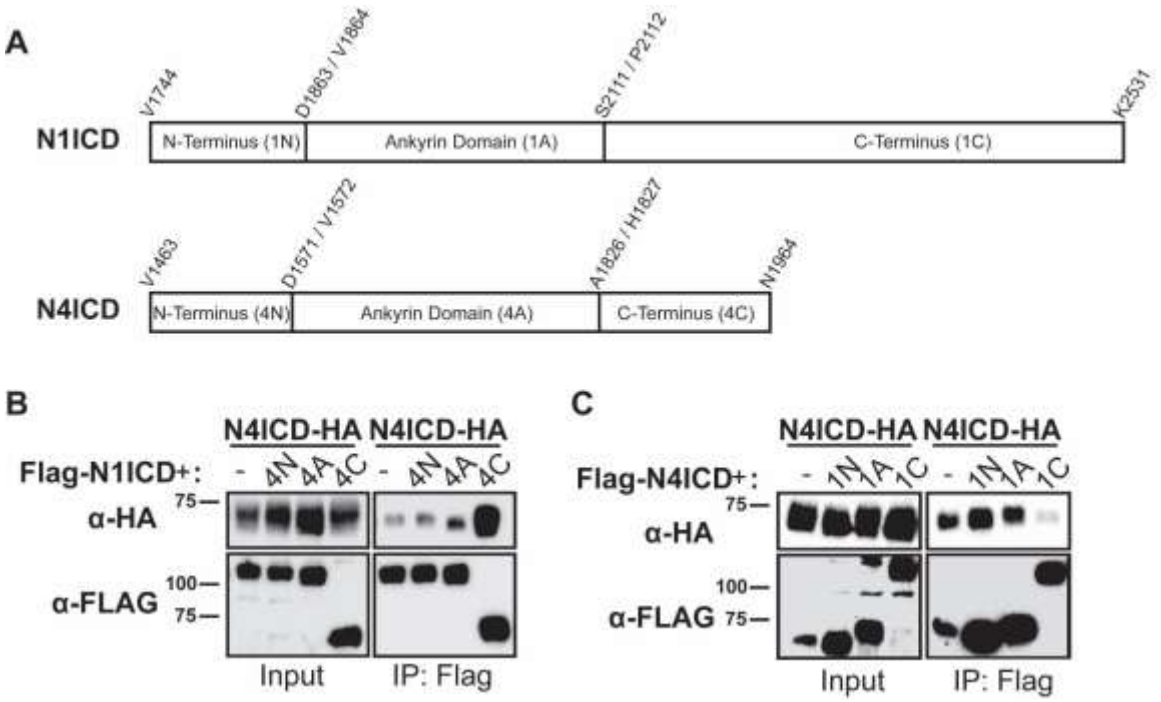

Figure 2.5: NICD C-termini regulate dimerization

(A) Chimeric proteins were made by swapping the N-terminals (N), Ankyrin domains (A), and C-terminals (C) between wild-type N1ICD and N4ICD. Amino acids demarking domain positions on N1ICD and N4ICD are indicated. (B) CO-IP between WT HA-tagged N4ICD and chimeric FLAG-tagged N1ICD. (C) CO-IP between WT HA-tagged N4ICD and chimeric FLAG-tagged N4ICD. In B and C, Input represents 10% of whole cell lysate as a loading control. Shown are representative images of an experiment that was performed three independent times.

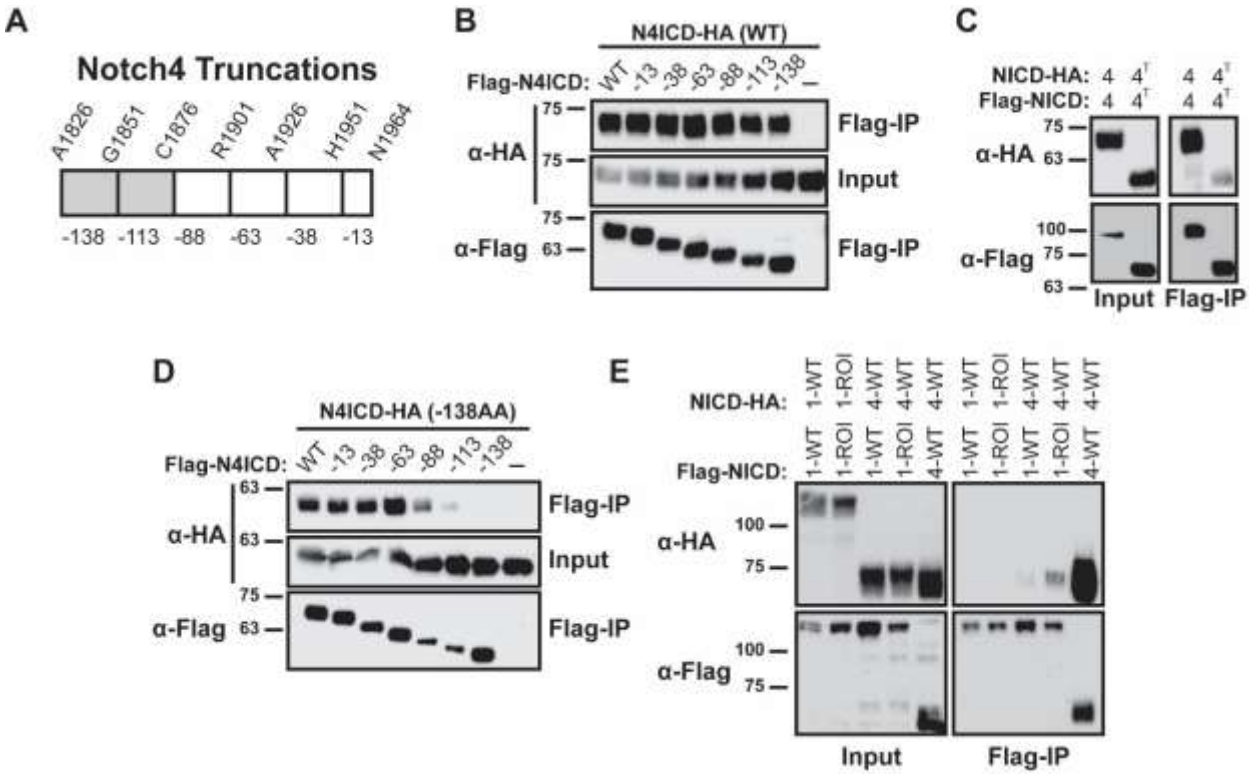

Figure 2.6: Identification of dimerization enhancer domain in Notch4

(A) N4ICD was progressively truncated beginning from the C-terminal. Shaded, is the region of interest (ROI) of N4ICD linked to enhanced dimerization potential. (B) Various FLAG-tagged N4ICD truncations were co-transfected with full-length HA-tagged N4ICD and co-immunoprecipitated. (C) Deletion of the N4ICD C-terminal prevents efficient dimerization. The C-terminal 138 amino acids were deleted from FLAG- and HA-tagged N4ICD then full-length (4) or truncated (4T) cDNAs were transfected into 293T for immunoprecipitation analysis. (D) Paired sets of progressive N4ICD C-terminal deletions were monitored for dimerization by immunoprecipitation. (E) Amino acids A1826 to C1876 corresponding to the N4ICD ROI, were swapped into the corresponding region downstream of the N1ICD ankyrin domain then co-transfected with various combinations of N1ICD or N4ICD. Co-immunoprecipitation was used to monitor

interactions. All panels depict representative images of experiments that were performed at least three independent times.

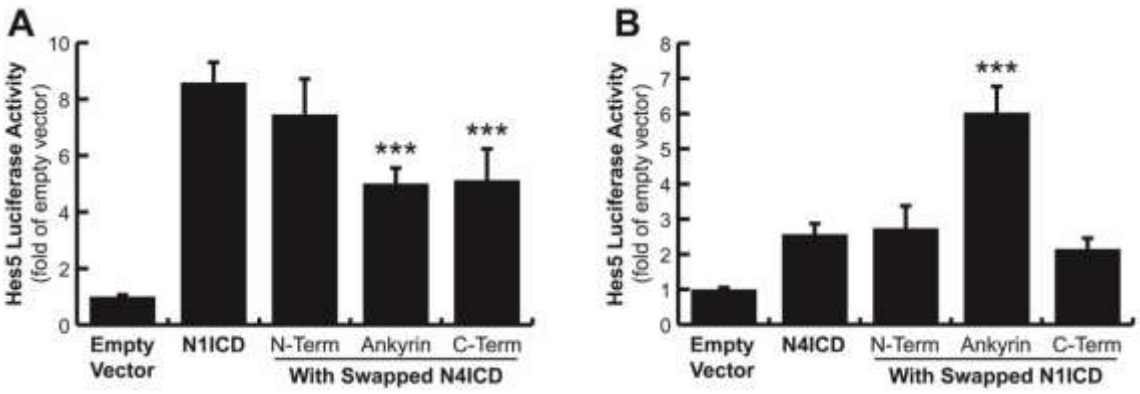

Figure 2.7: Transcriptional activity of N1ICD / N4ICD chimeric proteins

(A and B) 293T cells were transfected with the Hes5-luciferase reporter construct and various chimeric proteins. Shown is the average +/- SE of six independent experiments. *** indicates $p<.01$, student's t-test.

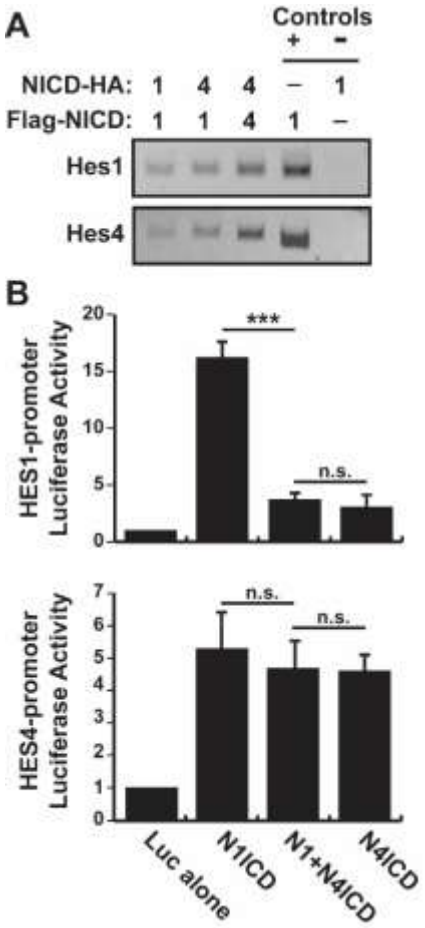

Figure 2.8: Detection of NICD homodimer and heterodimer complex on DNA

(A) 293T cells were transfected with combinations of FLAG-tagged N1ICD or N4ICD and FLAG- or HA-tagged binding NICD partners. ChIP was performed by two-step CO-IP with anti-FLAG then anti-HA antibodies. A positive control reaction was transfected with FLAG-tagged N1ICD alone and subjected to anti-FLAG CO-IP. A negative control reaction was transfected with HA-tagged N1ICD and subjected to anti-FLAG and anti-HA CO-IP. Hes1 and Hes4 promoter sequences were detected by PCR with antibodies flanking the head-to-head binding sites in each promoter. Shown is a representative image of a single experiment that was performed three independent times with similar results. (B) 293T cells were transfected with Hes1 (top) or Hes4 (bottom) promoter

luciferase reporters and equivalent amounts of either empty CMV control vector, N1ICD, N4ICD, N1 and N4ICD. Shown are the average +/- SE of six independent experiments.

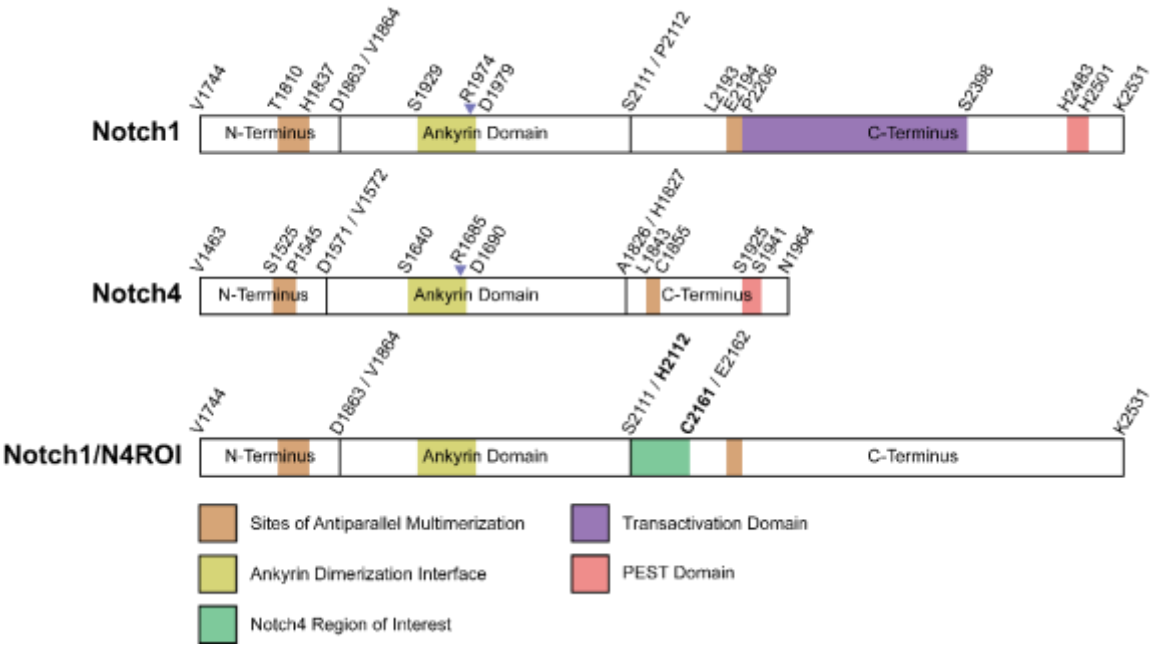

Figure S2.1: Diagram of important landmarks in N1ICD and N4ICD

Indicated in each figure are the 1.) sites of antiparallel multimerization as defined by Vasquez et al., [32] 2.) ankyrin dimerization interface with key amino acids indicated based on sequence alignment between human and mouse NICDs as described by Nam et al., [29]. 3.) The region of N4ICD C-terminal we define as important for enhanced dimerization, 4.) the transactivation domain (TAD) present in N1ICD but not N4ICD, and 5.) the PEST domain present in both N1ICD and N4ICD.

Supplementary Table 2.1 Primers Utilized Throughout the Manuscript

The following constructs were cloned with a restriction enzyme mediated approach:

Plasmid Number	Desired Construct/ Primer Function	Dir.	Sequence (5'→3')
285 N1ICD-MYC	Transfer N1ICD into pcDNA3.1-MycHis B	FWD (KPN1)	TTATTAGGTACCACCATGGTGCTGCTGTCCCGC
		REV (XBA1)	TTATTATCTAGAGCTTTAAATGCCTCTGGAATGTGG
286 N2ICD-MYC	Transfer N2ICD into pcDNA3.1-MycHis B	FWD (KPN1)	GGCGGCGGTACCACCATGATGGCCAAGCGGAAGCG
		REV (XBA1)	GGCGGCTCTAGATGCATACACCTGCATGTTGCTGTG
287 N3ICD-MYC	Transfer N3ICD into pcDNA3.1-MycHis B	FWD (KPN1)	GGCGGCGGTACCACCATGATGGTTGCCAGGCGAAGC
		REV (XBA1)	GGCGGCTCTAGAGGCCATCACCTGCCTCTTG
288 N4ICD-MYC	Transfer N4ICD into pcDNA3.1-MycHis B	FWD (KPN1)	GGCGGCGGTACCACCATGGTCCTCCAGCTCATTCGG
		REV (XBA1)	GGCGGCTCTAGAGCGTTCAGATTTCTTACAACCGAGTTTAAGGG
296 N1ICD-HA	Transfer N1ICD into pKH3	FWD (SAL1)	TTATTAGTCGACACCATGGTGCTGCTGTCCCGC
		REV (XBA1)	TTATTATCTAGATTTAAATGCCTCTGGAATGTGG
297 N2ICD-HA	Transfer N2ICD into pKH3	FWD (SAL1)	GGCGGCGTCGACACCATGATGGCCAAGCGGAAGCG
		REV (XBA1)	GGCGGCTCTAGATGCATACACCTGCATGTTGCTGTG
298 N3ICD-HA	Transfer N3ICD into pKH3	FWD (SAL1)	GGCGGCGTCGACACCATGATGGTTGCCAGGCGAAGC
		REV (XBA1)	GGCGGCTCTAGAGGCCATCACCTGCCTCTTG
299 N4ICD-HA	Transfer N4ICD into pKH3	FWD (SAL1)	GGCGGCGTCGACACCATGGTCCTCCAGCTCATTCGG
		REV (XBA1)	GGCGGCTCTAGAGTTCAGATTTCTTACAACCGAGTTTAAGGG
391 Hes4-Luciferase	Clone Hes4 promoter to pGL3-Basic	FWD (KPN1)	GGCCGGGGTACCCGAGGCGTGACTGACA
		REV (SAC1)	GGCCGGGAGCTCCAGGCCGTTTCCCTATTTAAG

The following constructs were cloned with the desired mutation inserted within partially overlapping primers:

Plasmid # Plasmid name	Desired Construct/ Primer Function	Dir.	Sequence (5'→3')
281 N1ICD-FLAG (R1974A)	Mutagenesis of N1ICD ankyrin domain (R1974A)	FWD	CCGGAACGCCGCCACAGATCTGGATGCCCGAATGC
355 N1ICD-MYC (R1974A)			
289 N1ICD-MYC (R1974A) (ΔS2184)		REV	GTGGCGGCGTTCCGGAGCAGGATCTGGAAGACACC
358 N1ICD-HA (R1974A)			
282 N2ICD-FLAG (R1934A)	Mutagenesis of N2ICD ankyrin R1934A	FWD	CCGCAACGCCGTAACCGATCTGGATGCCAGAATGA
356 N2ICD-MYC (R1934A)			
359 N2ICD-HA (R1934A)		REV	GTTACGGCGTTGCGGATCAGAATCTGAAAGACACCTTGGGC
283 N3ICD-FLAG (R1896A)	Mutagenesis of N3ICD ankyrin R1896A	FWD	CAGGAACGCCTCCACTGACCTGGATGCCCGAATGG
357 N3ICD-Myc (R1896A)			
360 N3ICD-HA (R1896A)		REV	GTGGAGGCGTTCCTGATGAGAATCTGGAAGACACCCTGGG
284 N4ICD-Flag (R1685A)	Mutagenesis of N4ICD ankyrin R1685A	FWD	CCAGCGCCCAGACTACGGTGGACG
290 N4ICD-Myc (R1896A)		REV	GTCTGGGCGCTGGCCAATAGGAGCT
361 N4ICD-HA (R1896A)			

The following constructs were cloned with Gibson Assembly:

Plasmid # Plasmid name	Construct	Gibson Component	Dir.	Sequence (5'→3')
382 N1ICD-ANK-FLAG	N1ICD ankyrin Alone Creation (Flag Vector)	Flag Vector Linearization	FWD	TAAGGATCCCGGGTGGCATC
			REV	TCTAGAGTCGACCTGCAGG
385 N1ICD-ANK-FLAG (R1974A)		N1 ankyrin Isolation	FWD	GCCTGCAGGTCGACTCTAGAGTCAATGTTCGAGGACCAGATG
			REV	GATGCCACCCGGGATCCTTAGCTGCGCACCAGGTTGTAC
384 N1ICD-ANK-MYC	N1ICD ankyrin Alone Creation (Myc Vector)	Myc Vector Linearization	FWD	GCTCTAGAGGGCCCGCGG
			REV	CATGGTACCAAGCTTAACTAGCCAGC
386 N1ICD-ANK-MYC (R1974A)		N1 ankyrin Isolation	FWD	TAGTTAAGCTTGGTACCATGGTCAATGTTCGAGGACCAGATG
			REV	AACCGCGGGCCCTCTAGAGCGCTGCGCACCAGGTTGTA
383 N1ICD-ANK-HA	N1ICD ankyrin Alone Creation (HA Vector)	HA Vector Linearization	FWD	TCTAGAATGTACCCATACGATGTTC
			REV	CATGGTGTCGACCTGCAG
		N1 ankyrin Isolation	FWD	TTCTGCAGGTCGACACCATGGTCAATGTTCGAGGACCAGATG
			REV	TCGTATGGGTACATTCTAGAGCTGCGCACCAGGTTGTAC
362 N1ICD/N4 N-terminal-FLAG	N1ICD/N4N-Term Chimera Creation	N1ICD Linearization	FWD	GTCAATGTTCGAGGACCAGATG
			REV	TCTAGAGTCGACCTGCAGGC
		N4 N-Terminus Isolation	FWD	GCCTGCAGGTCGACTCTAGAGTCCTCCAGCTCATTCGG
			REV	TCTGGTCCTCGAACATTGACATCCAGAACCTCCGATTC
363 N1ICD/N4-Ank-FLAG	N1ICD/N4Ank Chimera Creation	N1ICD Linearization	FWD	CCACAGCTGCATGGCACTGCC
			REV	ATCCATGCAGTCAGCATCCACCTCC
		N4 ankyrin Isolation	FWD	TGGATGCTGACTGCATGGATGTGGACACCTGTGGACCTGATGGG
			REV	GCAGTGCCATGCAGCTGTGGCGCACGGGCCTCCTGCGT
364 N1ICD/N4 C-terminal-FLAG	N1ICD/N4C-Term Chimera Creation	N1ICD Linearization	FWD	GGATCCCGGGTGGCATCC
			REV	GCTGCGCACCAGGTTGTAC
		N4 C-Terminus Isolation	FWD	AGTACAACCTGGTGCGCAGCCACGCACGCACCACGCCG
			REV	AGGGATGCCACCCGGGATCCCTAGTTCAGATTTCTTACAACCGAGTTTAAGGGAATCTC

Plasmid # Plasmid name	Construct	Gibson Component	Dir.	Sequence (5'→3')
365 N4ICD/N1 N-terminal-FLAG	N4ICD/N1N-Term Chimera Creation	N4ICD Linearization	FWD	GTGGACACCTGTGGACCTG
			REV	AAGCTTGTCATCGTCATCCTTG
		N1 N-Terminus Isolation	FWD	AGGATGACGATGACAAGCTTGTGCTGCTGTCCCGCAAG
			REV	TCAGGTCCACAGGTGTCCACATCCATGCAGTCAGCATCCAC
366 N4ICD/N1-Ank-FLAG	N4ICD/N1Ank Chimera Creation	N4ICD Linearization	FWD	CACGCACGCACCACGCCG
			REV	ATCCAGAACCTCCGATTCAC
		N1 ankyrin Isolation	FWD	GTGAATCGGAGGTTCTGGATGTCAATGTTCGAGGACCAGATG
			REV	CCCGGCGTGGTGCGTGCGTGGCTGCGCACCAGGTTGTAC
367 N4ICD/N1 C-terminal-FLAG	N4ICD/N1C-Term Chimera Creation	N4ICD Linearization	FWD	GCACCGGAAGCCGTCTAGAGGATCCC
			REV	CGCACGGGCCTCCTGCGT
		N1 C-Terminus Isolation	FWD	CTACGCAGGAGGCCCGTGCGCCACAGCTGCATGGCACTG
			REV	CTCTAGACGGCTTCCGGTGCTTATTTAAATGCCTCTGGAATGTGGGTG
387 N1ICD/N4 ROI-FLAG	N1ICD/N4ROI Chimera Creation	Notch1 Linearization	FWD	GAAGCTAAGGACCTCAAGGC
			REV	GCTGCGCACCAGGTTGTAC
388 N1ICD/N4 ROI-HA		N4 ROI Isolation	FWD	AGTACAACCTGGTGCGCAGCCACGCACGCACCACGCCG
			REV	GCCTTGAGGTCCTTAGCTTCGCAGCGAGCATACACCTTCCCTC

The following constructs were cloned through blunt-end ligations:

Plasmid # Plasmid name	Desired Construct/ Primer Function	Dir.	Sequence (5'→3')
375 N1ICD-RAM/CTD-FLAG	Creation of N1RAM/CTD (Δankyrin Domain)	FWD	CCACAGCTGCATGGCACTGCC
376 N1ICD-RAM/CTD-HA			
377 N1ICD-RAM/CTD-MYC		REV	ATCCATGCAGTCAGCATCCACCTCC
378 N4ICD-RAM/CTD-FLAG	Creation of N4RAM/CTD (Δankyrin Domain)	FWD	CACGCACGCACCACGCCG
379 N4ICD-RAM/CTD-HA		REV	ATCCAGAACCTCCGATTCAC
380 N1ICD-RAM/ANK-FLAG (ΔCTD)	Creation of N1RAM/Ank (ΔC-Terminus Domain) (Flag Vector)	FWD	TAAGGATCCCGGGTGGCATC
		REV	GCTGCGCACCAGGTTGTAC
381 N1ICD-RAM/ANK-MYC (ΔCTD)	Creation of N1RAM/Ank (ΔC-Terminus Domain) (Myc Vector)	FWD	GCTCTAGAGGGCCCGCGG
		REV	GCTGCGCACCAGGTTGTAC
	N4ICD C-Terminus Truncations	FWD	TAGGCACCGGAAGCCGTCTAGAGGATCC
368 N4ICD V1463-H1951 (-13) -FLAG		REV	GGCTTCCGGTGCCTAGTGAACTGGAAGACCCCAGG
369 N4ICD V1463-A1926 (-38) -FLAG		REV	GGCTTCCGGTGCCTACGCACTGCAGGCGGAG
370 N4ICD V1463-R1901 (-63) -FLAG		REV	GGCTTCCGGTGCCTAGCGTCGTCCACGGGAG
371 N4ICD V1463-C1876 (-88) -FLAG		REV	GGCTTCCGGTGCCTAGCAGCGAGCATACACCTTCC
372 N4ICD V1463-C1851 (-113) - FLAG		REV	GGCTTCCGGTGCCTACCCGCGCGGGCG
373 N4ICD V1463-A1826 (-138) -FLAG		REV	GGCTTCCGGTGCCTACGCACGGGCCTCCTG
374 N4ICD V1463-A1826 (-138) – HA	N4ICD C-Terminus Truncations (HA Vector)	FWD	TCTAGAATGTACCCATACGATGTTCCAG
		REV	TCGTATGGGTACATTCTAGACGCACGGGCCTCCTG

Primers used for Chromatin Immunoprecipitation Analysis:

Human Hes1 Promoter Primer for Notch-Dimer Driven ChIP	FWD	TCCTCCCATTGGCTGAAA
	REV	GGCCTCTATATATATCTGGGACTG
Human Hes4 Promoter Primer for Notch-Dimer Driven ChIP	FWD	CGAGGCGTGACTGACA
	REV	CAGGCCGTTTCCCTATTTAAG

Primers used for RT-PCR Analysis of the Notch Expression Profiles:

Notch1	FWD	AGGTCAATGAGTGCAACAGCAACC
	REV	TCAATACACGTGCCCTGGTTCAGA
Notch2	FWD	AATGGTGGCACATGTGTTGATGGG
	REV	ACATAGGCACTGGGACTCTGCTTT
Notch3	FWD	GATGGCATGGATGTCAATGTGCGT
	REV	AGCGGTTTCGGATGAGAATCTGGA
Notch4	FWD	ACTCCTGTGCCACTTGGAAGACAT
	REV	AGAGGCACTCATTGTGATCAGCCT
18S	FWD	CAGCCACCCGAGATTGAGCA
	REV	TAGTAGCGACGGGCGGTGTG

CHAPTER THREE

Notch family members follow stringent requirements for intracellular domain dimerization at sequence-paired sites

Jacob J. Crow[1] and Allan R. Albig[1,2]

[1] Biomolecular Sciences Ph.D. Program. Boise State University. Boise, ID 83725, USA

[2] Department of Biological Sciences. Boise State University. Boise, ID 83725, USA

Abstract

Notch signaling is essential for multicellular life, regulating core functions such as cellular identity, differentiation, and fate. These processes require highly sensitive systems to avoid going awry, and one such regulatory mechanism is through Notch intracellular domain dimerization. Select Notch target genes contain sequence-paired sites (SPS); motifs in which two Notch transcriptional activation complexes can bind and interact through Notch's ankyrin domain, resulting in enhanced transcriptional activation. This mechanism has been mostly studied through Notch1, and to date, the abilities of the other Notch family members have been left unexplored. Through the utilization of minimalized, SPS-driven luciferase assays, we were able to test the functional capacity of Notch dimers. Here we show that the Notch 2 and 3 NICDs also exhibit dimerization-induced signaling, following the same stringent requirements as seen with Notch1. Furthermore, our data suggested that Notch4 may also exhibit dimerization-induced signaling, although the amino acids required for Notch4 NICD dimerization appear to be different than those required for Notch 1, 2, and 3 NICD dimerization. Interestingly, we identified a mechanical difference between canonical and cryptic SPSs, leading to differences in their dimerization-induced regulation. Finally, we profiled the Notch family members' SPS gap distance preferences and found that they all prefer a 16-nucleotide gap, with little room for variation. In summary, this work highlights the potent and highly specific nature of Notch dimerization and refines the scope of this regulatory function.

Introduction

Notch signaling is a cornerstone of multicellularity and dictates cellular fate and identity. Notch signaling is heavily influenced by microenvironmental cues [3], including

adjacent “sending cells” which present any of five Notch ligands to up to four Notch receptors expressed on so called “receiving cells”. Ligand bound and activated Notch receptors undergo a series of proteolytic cleavages which release an active intracellular domain (NICD) [22,23,211]. This transcriptionally active fragment translocates to the nucleus to act as a co-transcription factor. Common Notch signaling targets are transcription factors themselves, which have their own broader implications and cascades, culminating in a system which requires a fine-tuned, highly sensitive signaling network. Disruption of Notch signaling, both through over- and under-activation, leads to a variety of developmental abnormalities and cancers [4]. Understanding mechanisms behind this precise level of internal control may pave the way for treatments of many of its resulting disorders.

The mammalian Notch signaling system consists of four mostly homologous receptors (Notch1-4) which are all activated through this manner. Each NICD molecule can be readily split into three sections; the N-terminus which contains the RBPJ associated module (RAM) domain, the central ankyrin domain, and a variable C-terminus which houses the Pro-Glu-Ser-Thr (PEST) domain used in protein turnover and in some Notch proteins, a transactivation domain (TAD). Through the RAM domain, all Notch proteins bind to the same transcription factor, recombination signal binding protein for immunoglobulin kappa J region (RBPJ, also commonly called CSL, CBF-1/Suppressor of Hairless/Lag-1) [212]. Upon NICD binding to RBPJ, a new NICD/RBPJ interface is formed which recruits another co-activator, a member of the Mastermind-like (MAML) family [25]. This new tri-protein complex recruits a cascade of other transcriptional machinery to drive transcription of its target genes [121]. While each Notch protein contains the conserved RAM

and ankyrin domains, their transcriptional activation profiles are not identical and are largely dependent on context within promoter elements [28].

The DNA target sites which the Notch transcriptional activation complex (NTC) binds to have been the subject of thorough analysis. The consensus binding site was originally defined as a "TP1 element" with the sequence 5' CGTGGGAAAAT 3' that recruits RBPJ to Notch responsive promoters [213,214]. TP1 elements are found in a variety of configurations within promoters. Perhaps most importantly, TP1 elements orientated in a head-to-head directionality and separated by 16 base pairs (bp), also known as sequence-paired sites (SPS), enable cooperative binding of two NICD molecules [19,24]. This cooperation results in better repression in the absence of NICD, and enhanced activation in its presence [27,28]. Upon modeling of two N1ICD transcriptional cores on a SPS, it was proposed that complex dimerization occurs through the N1ICD ankyrin domain [29] and this was further supported through crystallization of the interface [30]. Importantly, theses SPS-driven promoters appear to be dimer-dependent. When dimerization was interrupted, N1ICD's transcriptional potential was substantially reduced on promoters containing SPSs [29,30] and could no longer induce T-cell acute lymphoblastic leukemia [31]. Together, sequence-paired sites and Notch dimerization appear to be potent regulators of Notch signaling and warrant a closer investigation into their mechanics.

In the search for new Notch responsive genes, ChIP-Seq approaches have recently been adopted to identify new SPS sites based on DNA interaction with RBPJ. While the NTC-dimer crystal structure dictates a 16-nucleotide spacer region, ChIP-Seq analysis by Castel, et al. identified a variety of potential SPS-driven genes with spacer regions from 11 to 21 base pairs [33]. These possible targets are opposed by *in vitro* analysis which observed

a more limited spacer region of 15 to 17 base pairs [29,35]. This discrepancy in spacer length is further complicated due to ChIP-Seq approaches that experimentally identified individual RBPJ binding sites then computationally screened for nearby secondary sites [33,35,175]. Screening for secondary sites however is not straightforward since loading of a NTC onto a high-affinity site directly enables cooperativity on cryptic, low affinity sites which may not even resemble traditional RBPJ binding sequences [30,31,35]. While the transcriptional outcomes seem to be clear, the mechanisms dictating this SPS-response within promoters and enhancers are not clearly understood.

While dimerization-induced signaling of Notch1 has been previously explored, the ability, specifications, and limitations for the other members of the Notch family remain unknown. To compare dimer-dependent signaling of the various NICDs, we generated luciferase reporter constructs driven by either isolated sequence-paired sites from known dimer-dependent promoters or an artificial/optimized SPS site. We observed that all NICDs activate these promoters with varying efficiency. We also observed that Notch1, 2, and 3 functions through dimerization dependent mechanisms, while Notch4 appeared dimer independent. Finally, we compared the optimal gap length within SPS sites and found that all NICD molecules prefer promoters with 16bp between RBPJ binding sites, with little room for deviation. These results should help us to understand how the various NICD molecules interact in cells and potentially diversify Notch signaling outputs in cells that express multiple Notch proteins.

Materials and Methods

Cell Culture

HEK293T cells were cultured in Dulbecco's Modified Eagle's Medium (DMEM) (Mediatech, Inc.) supplemented with 10% EquaFetal Bovine Serum (FBS) (Atlas Biologicals) and 1x penicillin-streptomycin solution (Mediatech, Inc.). Cells were grown in 10 cm culture plates and subcultured at 70-80% confluency.

Expression and Reporter Plasmids

Protein expression constructs were obtained through the following: FLAG-N1ICD (AddGene #20183), N2ICD (#20184), N3ICD (#20185), and N4ICD (#20186) were all gifted by Raphael Kopan [28] and acquired through AddGene.org. All constructs code for the intracellular domain of the mouse Notch proteins and have a 3xFLAG peptide tag on the N-terminus. The N1ICD-MYC ΔS2184 construct, also a gift from Raphael Kopan [23] (#41730), includes a substantial C-terminal truncation, encoding mouse N1ICD V1744 to S2184 with a MYC tag located at the C-terminus. The NICD coding regions were subcloned into pKH3 (#12555), a gift from Ian Macara [206] to add a C-terminal 3xHA tag. N1ICD (R1974A), N2ICD (R1934A), N3ICD (R1896A), and N4ICD (R1685A) mutants were all created through site-directed mutagenesis of the NICDs based on sequence alignment to identify amino acids (Figure S3.2) in mouse NICDs homologous to the human N1CID R1984 site previously shown to be essential for NICD dimerization [30]. The empty coding vector pcDNA3.1/MYC-His was obtained from Invitrogen and pCMV-β-Galactosidase was obtained from Clontech/Takara Bio.

Transcriptional reporter constructs were obtained or created as the following: Full-length mouse promoters for *Hes1* (#41723) and *Hes5* (#41724) were a gift from Ryoichiro

Kageyama and Raphael Kopan [215]. 4xTP1 (#41726), a synthetic promoter containing four high-affinity RBPJ binding sites in tandem, was a gift from Raphael Kopan [216]. These promoter sequences were designed and cloned into pGL2-Basic (Promega), a luciferase reporter plasmid, which upon promoter activation drives expression of firefly luciferase.

Construct Creation and Mutagenesis

To create luciferase reporters that activate specifically upon Notch dimerization, we isolated the sequence-paired sites from the native mouse and human *Hes1* and *Hes5* genes and cloned these fragments into the pGL3-Basic vector (Promega) which contains a minimal promoter that is incapable of transcriptional initiation without additional enhancer elements. Our synthetic promoters, the 2xTP1 constructs, were designed using the TP1 response element as originally isolated from the Epstein-Barr virus, which contains two high-affinity binding site for RBPJ [213,214]. TP1's 'complete' RBPJ consensus sequence (5'-CGTGGGAAAAT-3') and a ubiquitous "core" sequence (5'-GTGGGAA-3') were taken from the response element, its secondary site reversed and placed in the complementary strand to result in a head-to-head arrangement, and two nucleotides were inserted into TP1's spacer region to result in a sixteen-base pair, sequence-paired site.

These fragments were synthesized as oligonucleotides (Integrated DNA Technologies, IDT) and were designed to be partially complementary so that when annealed, the ends were left overhanging, matching cuts from the restriction enzymes KpnI and SacI (New England Biolabs, NEB). pGL3-Basic was cut with these two enzymes, dephosphorylated with shrimp alkaline phosphatase (NEB), inserts phosphorylated with T4 Polynucleotide Kinase (NEB), and ligated together with T4 DNA Ligase (NEB).

A variety of sequence-paired site gap distances were created through blunt-end ligation. PCR primers to mutate Hes1, Hes5, and 2xTP1 were designed to align with the desired base excisions or to include base extensions. Base extensions were designed to keep the gap distance nucleotide composition (G/C vs A/T) approximately consistent with the native promoters'. PCR products were phosphorylated, ligated, and reaction template digested with the restriction enzyme DpnI (NEB). A statistical comparison of the modified constructs' basal activity levels did not indicate the addition or subtraction of any other regulatory elements (data not shown).

All constructs were sequenced verified before experimental use. SPS sequence information can be found in Supplementary S3.1 table.

Western Blotting

For western blotting analyses, HEK293T cells were plated into 6-well plates at a density of 300,000 cells/well. The following day, cells were transfected with polyethylenimine MW 25,000 (PEI, Polysciences) at a ratio of 5 μg PEI to 1 μg DNA. Wells were transfected with 1000 ng of plasmid DNA for the various FLAG-NICD constructs, allowed to grow for two days, and cells collected and prepared in 1x SDS-page lysis buffer. Western blotting was performed as described previously [157]. Membranes were incubated with primary antibodies against FLAG tag (Cell Signaling Technology, #14793) or GAPDH (Santa Cruz Biotechnology, sc-25778) and detected through horseradish peroxidase conjugated α-rabbit antibodies (GE Healthcare Life Sciences, NA934V). Experiments were repeated independently three times, where the figure displayed uses the best representative exposures.

Luciferase Assays

For all luciferase assays, HEK293T cells were plated into 24 well plates at a density of 50,000 cells/well where the experimental conditions were treated as triplicates or duplicates. The following day, cells were transfected. When analyzing the full-length promoters, 100 ng of luciferase construct and 10 ng of NICD expression plasmid were used, whereas in experiments of sequence-paired site constructs, 200 ng and 100 ng were used, respectively. In all experimental variations, 10 ng of a β-Galactosidase expression plasmid was used per well to normalize data for transfection efficiency and cell growth/death. To equate amounts of DNA between experimental conditions, the empty coding plasmid pcDNA3.1/MYC-His was utilized. Forty-eight hours post transfection, cells were collected and analyzed as previously described [157]. All samples were treated in triplicates, except for the single-base change experiment, which was in duplicates. Independent experiments were performed at least four times.

Chromatin Immunoprecipitation and PCR Analysis

Chromatin immunoprecipitation (ChIP) analyses were performed as previously described [207], with minor modifications. Briefly, cells were transfected with two differentially tagged NICDs and the 2xTP1(SPS)-Core luciferase construct to act as a dimerization target. Following formaldehyde-induced crosslinking, the nuclear fraction was isolated and collected. Micrococcal nuclease (NEB) was used to cut the chromatin into 300-1,500 base pair fragments, the nucleus briefly sonicated to lyse the fraction, and the DNA collected. To specifically isolate the dimerized complexes bound to DNA, they were placed through two rounds of selection, targeting both partners within the Notch dimer. The first round of selection was performed with anti-FLAG affinity resin (GenScript) and

captured complexes were eluted with 3xFLAG-peptide (ApexBio). Those complexes were further enriched through a second round of selection, probing for a HA-tagged NICD partner, with biotinylated HA antibodies (Bioss). These targets were precipitated out of solution with streptavidin magnetic beads (NEB) and the DNA was isolated out of the complexes with Proteinase K (Amresco) and heat-induced reverse crosslinking. DNA was cleaned and purified with a PCR purification kit and samples were analyzed for Notch-dimer targets. To observe our synthetic luciferase construct, we used primers 5'-CTAGCAAAATAGGCTGTCCC-3', FWD and 5'-CTTTATGTTTTTGGCGTCTTCCA-3', REV. Three independent experiments were performed and the most representative analysis was used in our figure.

Statistical Analysis

Statistical significance was determined through a student's two-tailed *t* test, comparing two-samples with homoscedastic variance. Significance is determined as *** is $p \leq 0.001$, ** is $p \leq 0.01$, and * is $p \leq 0.05$.

Results

Activation of Notch target genes containing sequence-paired sites requires ankyrin-dependent dimerization

Notch target genes often have multiple RBPJ binding sites within their promoter sequences and a fraction of these are orientated in head-to-head, paired sites [33,35]. This arrangement allows for NTC dimerization through NICD ankyrin domains, resulting in potent transcription of SPS containing genes. The canonical Notch target genes *Hes1* and *Hes5* have previously shown to be activated by Notch1 in a dimer-dependent manner [30,35].

Using luciferase reporter assays, we first sought to confirm if other members of the mammalian Notch family also activate *Hes1* and *Hes5* in a dimer-dependent manner.

HEK293T cells were co-transfected with commercially available luciferase reporter plasmids containing large fragments of the Hes1 or Hes5 promoters, and either wild-type or dimerization incompetent Notch1–4 NICD expression plasmids to observe dimerization dependence of these promoters. In agreement with previous work, the full-length Hes1 (Figure 3.1A) and Hes5 (Figure 3.1B) constructs were significantly activated by wild-type N1ICD and transcriptional activation was significantly less for dimer incompetent N1ICD. Likewise, wild-type N2ICD and N3ICD also displayed activation on both promoters but dimer-dependent activation only on the Hes1 promoter. Indeed, mutant N2ICD and N3ICD dimer incompetent constructs demonstrated a similar ability to activate the Hes5 promoter suggesting the N2ICD and N3ICDs were functioning in a dimer-independent manner on the Hes5 promoter. Finally, N4ICD activated the Hes1 promoter to a similar degree as the other NICDs but was significantly weaker on the Hes5 promoter compared to the other NICDs. Moreover, N4ICD failed to demonstrate dimer dependence on either the Hes1 or Hes5 promoters. In agreement with previous observations [29], western blot analysis of the various NICDs demonstrated that the decreased transcriptional activation of the dimer incompetent ankyrin mutant NICD molecules was not associated with decreased protein expression of these mutant NICDs (Figure 3.1C). Moreover, mutation of NICD ankyrin domains did not impinge the basal transcriptional activity of NICD molecules since WT and ankyrin mutant NICDs exhibited nearly identical transcriptional activity on the non-dimerizing 4xTP1 promoter (Figure 3.1D).

Collectively, these results largely supported the previously reported dimer-dependent nature of the Hes1 and Hes5 promoters. However, we also noted several weaknesses with these experiments. In particular, we noticed significant background with modest activation of the Hes1 promoter and reduced dimer dependence for N2-4ICD on the Hes5 promoter. Based on these weaknesses, we more closely examined these promoter sequences (Figure S3.1). We searched for high affinity binding sites that were defined by the RBPJ consensus sequence TGTGGGAA, and low affinity sites that were defined as having up to two nucleotide differences compared to the high-affinity sites. We found a multitude of possible low affinity RBPJ binding sites in addition to the high-affinity SPS sites previously described [28]. Based on this result, we hypothesized that the overall promoter complexity and number of potential low affinity RBPJ binding sites within these promoter sequences might have been responsible for the high background, low relative activation, and dimer independence observed in our experiments. Moreover, beyond Notch signaling, Hes genes are also controlled by a variety of other transcription factor families [217,218], including self-regulation [219,220], suggesting that these relatively large promoter fragments might have been responding to both Notch specific and non-Notch transcriptional activity. Collectively, these observations prompted us to perform further experiments on the Hes1 and Hes5 promoters with the goal of refining these promoters into more specific tools to monitor dimer-dependent NICD activation.

<u>The isolated Hes5 sequence-paired site does not respond to dimerization</u>

Our results in Figure 3.1 show that the Hes5 promoter demonstrated both stronger activation than the Hes1 promoter and N1ICD dimer dependence. We therefore rationalized that isolation of the Hes5 SPS site should yield a promoter element that would

specifically and robustly respond to NICD dimerization. We isolated the mouse and human Hes5 SPS elements containing two head-to-head orientated RBPJ binding sites separated by a 16-nucleotide gap, and the 4 to 5 surrounding nucleotides (Figure 3.2A) as previously described [30] and cloned these sequences into a luciferase reporter vector containing a minimal promoter that was incapable of transcriptional initiation without additional enhance elements. Interestingly, this cloned region includes one canonical RBPJ binding site and a partnered "cryptic site" which doesn't match standard RBPJ binding sequences, but instead was hypothesized to form the partner site for the high-affinity site [30]. In addition, there are two nucleotide differences between the mouse and human genes in this region (Fig 3.2A), one of which is inside the cryptic RBPJ binding site. As shown in Figure 3.2B, we found that both mouse and human isolated Hes5 SPS promoters were indeed responsive to N1ICD, however, neither of these isolated elements appeared to be dependent on NICD dimerization since they were equivalently activated by WT and dimer-incompetent versions of N1ICD. In addition, the isolated Hes5 SPS responded to Notch activation almost exactly the same as to promoters with RBPJ binding sites in a non-dimerizing head-to-tail orientation (*i.e.* 2xTP1(H-T) and 4xTP1(H-T) constructs). Moreover, N1ICD activated the Hes5 SPS construct less than the 2xTP1 construct despite these promoters both containing two RBPJ binding sites. Interestingly, N4ICD was unable to activate transcription from the isolated Hes5 SPS sites despite successfully activating the full length Hes5 promoter in Figure 3.1. In stark contrast to this result, the full-length Hes5 promoter did display dimer dependence to N1ICD (Figure 3.1B). This difference between the full-length and SPS versions of the Hes5 promoter suggested that the Hes5 promoter might have been functioning differently than previously thought. Given the

weakness of the cryptic RBPJ binding site, the presence of several other potential RBPJ binding sites within the full-length promoter, and the dimer dependence of the full-length Hes5 promoter, we hypothesized that the high affinity RBPJ binding site might be making a long-distance interaction with another high-affinity site within the promoter. This possibility would allow cooperation between previously thought independent NTCs within gene promoters and enhancers and perhaps explain the transcriptional differences between full-length and SPS versions of the Hes5 promoter. To test this possibility, we designed a series of Hes5 SPS mutants based on the helical nature of DNA. Since a DNA helix completes approximately one rotation every 10 bp, we hypothesized that an insertion or deletion of five extra base pairs would place the secondary NTC on the opposite side of the DNA, breaking any cooperativity. Further, an addition of an extra five nucleotides may restore cooperativity, despite the NTC being further away, due to a long range NTC dimerization. However, no obvious cooperative binding, or loss thereof, was observed in these constructs (Figure 3.2C).

Collectively, these results indicated that the Hes5 SPS does not function in a dimer-dependent manner in cells and instead behaves as a monomeric RBPJ binding site. Due to this unexpected complication, to further explore SPS capabilities we moved on to the Hes1 promoter, which contains a more canonical SPS site.

The Hes1 SPS acts through traditional NICD dimerization mechanisms

Hes1 is another Notch target gene which demonstrates dimer-dependence. Its promoter contains a single canonical RBPJ binding site and secondary site 16 nucleotides away in the reverse orientation (Figure 3.1A). This secondary site is slightly non-consensus, but only displays a minor decrease in RBPJ affinity compared to the high

affinity consensus site [35,160]. Therefore, we took the same reductionist approach used with *Hes5* and isolated the SPS element out of the Hes1 promoter.

Since the human and mouse sequences in this promoter region are identical, a generic Hes1(SPS) construct was cloned into a minimal promoter luciferase vector to quantitatively monitor its activation by Notch signaling (Figure 3.3A, Top). As before, transfections of this construct into HEK293T cells, along with WT or ankyrin mutated NICDs, allowed us to analyze dimer dependence of the Hes1 SPS element. The Hes1(SPS) construct responded to NICD activation (Fig 3.3A, Bottom) and interestingly, the isolated Hes1 SPS demonstrated approximately 5 times greater sensitivity to N1ICD compared to the full-length Hes1 promoter, most likely due to reduced background of the isolated SPS construct. Both N1ICD and N2ICD ankyrin mutants showed a significant decrease in activation compared to their wild-type counterparts. In comparison, N4ICD was again dimer independent, matching trends observed on the counterpart full-length promoter (Figure 3.1A). Finally, N3ICD only weakly activated the isolated Hes1 SPS. Indeed, compared to the full-length Hes1 promoter, N3ICD showed no increased activity on the isolated Hes1 SPS. Moreover, N3ICD did not demonstrate dimer dependence on the isolated Hes1 SPS but did demonstrate dimer dependence on the full-length Hes1 promoter (Figure 3.1A). This is potentially unsurprising since Notch3 has been shown to synergistically utilize other nearby transcription factors for its own signaling responses [28], which would be lacking in this minimalized promoter.

With a properly responding SPS-driven promoter, we again wanted to determine if long-range interactions were possible between RBPJ binding sites. We again followed the same logic employed when mutating the *Hes5* SPS and we created gap distances in steps

of five nucleotides to take advantage of the periodicity of the DNA helix. We found that the wild-type, 16-nucleodtide gap, was the only distance all NICDs were capable of cooperatively binding and eliciting activation on (Figure 3.3B). This observation further limits the options of dimerization dependent signaling since independent NTC sites within this promoter are unlikely to cooperate over long distances by methods of kinking, looping, or untwisting the gap DNA.

Establishment of a high activity, NICD dimer-specific reporter construct

Having found that the SPS element isolated from the Hes1 promoter functions in a dimer-dependent manner, we next sought to optimize an SPS-driven luciferase construct as a tool to specifically study the transcriptional activity of NICD dimers. To accomplish this, we constructed a synthetic SPS site that contained two high-affinity RBPJ binding sites in a head-to-head configuration separated by 16 bp. We utilized the complete TP1 consensus sequence (5'-CGTGGGAAAAT-3') originally described by Meitinger et al., [213] thus forming the 2xTP1(SPS)-Complete construct. RBPJ shows high affinity towards this site and multiple copies of this RBPJ binding site have previously been arranged in a head-to-tail orientation to measure the activation of Notch signaling [214,221,222]. These sequences however have not previously been orientated in a head-to-head orientation to measure transcriptional activation by dimerized NICD molecules.

As shown in Figure 3.4A, the 2xTP1(SPS)-Complete construct successfully responded to Notch signaling. Unexpectedly however, dimer-incompetent N1ICD mutants increased activation even better than wild-type proteins indicating this promoter was not dimer-dependent. We hypothesized that since the last three nucleotides in the consensus sequence were not necessary for RBPJ-DNA interactions [213], this effectively resulted in a

22 nucleotide gap distance between RBPJ binding sites, and therefore the promoter lost its dimerization dependence. In response to this possibility, we created another SPS construct, this time with a core, essential sequence for RBPJ responsiveness (5'-GTGGGAA-3') [17,213] separated by 16 bp. We named this new construct the 2xTP1(SPS)-Core construct. Cloning of this fragment resulted in a 'T' on the 5' side of each core sequence. This addition coincidentally matches the RBPJ consensus sequence found in Hes1/5, though this position within the consensus is variable [161]. As shown in Figure 3.4B, wild-type N1, N2, and N3ICD all strongly activated this promoter while the corresponding dimer-incompetent ankyrin domain mutants demonstrated significantly reduced transcriptional activity. N4ICD also activated the promoter, but remained dimerization independent, which has persisted across all SPS promoter variations tested. Nonetheless, the 2xTP1(SPS)-Core construct appeared to be an optimized promoter for evaluating dimer-dependent Notch signaling.

To ensure that NICD proteins were in fact forming dimers on the 2xTP1(SPS)-Core construct, we performed a "proof of concept" ChIP analysis of NICD partners binding to the Core promoter (Figure 3.4C). Our goal in this experiment was not to attempt to quantitate binding or cooperative binding, but instead to enable for a more direct visualization of NICD molecules in the head-to-head orientation. To enable this, it was necessary to transfect cells with two differentially tagged NICDs (Flag- or HA- variants of N1 and N4ICD) in unison and perform a two-step IP, first with anti-Flag antibodies and second with anti-HA antibodies. This was required to enable both the isolation of dimerized NICDs and the exclusion of monomeric NICDs. Moreover, this procedure was also required for the identification of potential N1ICD/N4ICD heterodimer pairs since

heterodimers could only be distinguished from homodimers based on the two-step co-IP approach. In addition to the anti-FLAG + anti-HA two-step Co-IP procedure, we also co-transfected cells with the 2xTP1(SPS)-Core construct and detected this construct by PCR of the final precipitate. This was essential for the elimination of false positives since this luciferase construct only has two RBPJ binding sites. In contrast, native Notch target genes such as Hes5 and Hes1 have multiple monomeric RBPJ binding sites in addition to their SPS element (Figure 3.1) that likely could result in the recovery of false positive NICDs bound to non-dimerizing sites. To control for non-specific isolation of DNA by Co-IP, we also performed negative controls consisting of either 2xTP1(SPS)-Core transfected alone, or 2xTP1(SPS)-Core transfected with HA-tagged NICD that were subjected to the two-step Co-IP. A positive control reaction was transfected with 2xTP1(SPS)-Core and Flag-tagged N1ICD but only subjected to one-step IP with anti-Flag antibodies. As shown in Figure 3.4C, PCR with primers extending over the 2xTP1(SPS)-Core promoter sequence successfully detected DNA in the single IP positive control reaction indicating the presence of (at least) monomeric N1ICD bound to DNA. Importantly, DNA was also detected in the N1ICD and N4ICD homodimer samples. Moreover, PCR also detected DNA in the N1ICD/N4ICD sample suggesting that N1ICD + N4ICD heterodimer complexes were also present in transfected cells. Finally, DNA was not detected if no NICD molecules were transfected or if only a single HA-tagged NICD was transfected.

Non-optimal SPS sites select against transcriptional activation by NICD dimers

The results in Figure 3.4A revealed an interesting phenomenon wherein non-dimerizing ankyrin mutant NICDs performed better than their WT counterparts on the 2xTP1(SPS)-Complete construct which had a slightly longer gap than the 16 bp preferred

by NICD molecules. This observation suggested that two RBPJ binding sites gapped slightly more or less than 16 bp within a promoter might actually suppress promoter responsiveness to NICD dimer-dependent Notch signaling and favor NICD dimer-independent Notch signaling, a phenomenon which has not been previously described. To test this hypothesis, we compared WT and ankyrin mutant N1ICD transcriptional activation from the Hes1(SPS) and 2xTP1(SPS)-Core constructs which we modified to contain head-to-head RBPJ binding sites separated by 11, 16, or 21 bp. As shown in Figure 3.5A and 3.5B, WT N1ICD strongly activated reporter transcription on the 16 bp gap promoters and was significantly weaker on the 11 bp and 21 bp gap promoters. Moreover, the ankyrin mutant N1ICD also performed as expected, showing no synergistic activity across the various gap distances. Importantly however, the ankyrin mutant N1ICD slightly outperformed the WT N1ICD on the 11 bp and 21 bp gap promoters (Figure 3.5A and B right panels). This observation suggested that head-to-head orientated RBPJ binding sites with non-optimal gap widths are more likely to be activated by non-dimerizing NICD molecules. Whether or not there is a condition that actively manipulates NICD dimerization is currently unknown.

A restrictive spacer range dictates the signaling capabilities of NICD dimerization

Having established a highly active and NICD dimer-specific promoter, we set out to compare the promoter specificity of the various NICD molecules. To accomplish this, we established a series of 2xTP1(SPS)-Core promoters with modified SPS gap distances ranging from 11 to 21 bp in one bp increments. Combinations of each NICD protein coupled with each spacer variation were then transfected into HEK293T cells and assayed for their transcriptional activity. Our rational for this approach was the previous finding

that ChIP-Seq screening identified SPS-driven genes with various gap distances, from 11-21 base spacers [33]. Our data in Figure 3.3 did not support the idea that gap distances greater or less than 16 bp (in 5 bp increments) can support dimer-dependent transcription on the Hes1 promoter. Nonetheless, we wanted to use our optimized promoter to investigate the possibility that smaller variation in gap distances may be tolerated during NICD dimerization, or that different Notch family members may exhibit slightly different preferences in SPS gap width. As shown in Figure 3.6, all mouse NICDs have a strong preference for the SPS sites with 16 bp gaps, with little room for variation. For N1ICD, there was some flexibility observed with 15 and 17 bp spacers, though anything outside of this range did not demonstrate cooperative signaling (Figure 3.6A). In contrast, N2ICD showed even more specificity, where there was only slight cooperativity at the 15 bp gap, and none observed at 17 (Figure 3.6B). N3ICD showed cooperativity at 16 bases (Figure 3.6C), and N4ICD at 16 and 17 bases (Figure 3.6D), however it's difficult to make a judgement call about their flexibility due to their low activation and their apparent dimerization independent signaling. Also, it's worth noting is that N4ICD preferred a 16 bp gap suggesting that N4ICD was functioning as a dimer which is in conflict with our earlier observations that N4ICD functioned dimer-independently. Moreover, N4ICD demonstrated slight inhibition on promoters with 11 or 14 bp gaps, which was similarly observed in the Hes5 (Figure 3.2C) and Hes1 (Figure 3.3B) SPS promoter constructs. This might indicate that N4ICD proteins generally act as transcription inhibitors on monomeric NTC sites, or perhaps occupy RBPJ binding sites and prevent other NICDs from binding, though we did not explore these possibilities. Further we also observed a slight increase in activation of the 12 or 13 bp gap constructs for all four NICD proteins, which could be

attributed to some form of cooperativity, though we did not explore this thread any further. Finally, as with the Hes5(SPS) and Hes1(SPS), we extended the gap distances of the 2xTP1(SPS)-Core out to 36 nucleotides and again observe little to no long-range cooperativity.

Discussion

Notch signaling is an important cellular communication mechanism that is required for multicellular organisms. Ongoing research continues to reveal how Notch functions and how Notch signaling is integrated into many facets of cell biology. Despite our growing understanding of Notch function, however, there are basic questions about Notch signaling that remains to be addressed. In this study, we sought to address some of these basic questions about Notch signaling that have been overlooked in the quest to dig into the deeper questions of Notch function. In particular, we felt that a head-to-head transcriptional comparison of the full-length Notch NICD molecules on a variety of promoter elements should be performed. Most of what we know about Notch dimerization, including how the proteins interact and on which promoters, comes from studies with Notch1. While the four mammalian Notch proteins are mostly homologous within the N-terminal and ankyrin domains, there are substantial differences within the C-terminal regions. Notably, this domain is absent in much of the field's previous characterization work. Indeed, molecular modeling [29] and crystallization [30] were performed with just the ankyrin domain, and these studies laid the original groundwork for the NTC's spatial conformations, interacting amino acids, and DNA preferences. Similarly, further *in vitro* work with EMSAs and FRET assays supported NTC cooperative loading and SPS gap preferences, though these were performed using N1ICDs with just the N-terminal RAM

and ankyrin domains [29,30,35]. Importantly, the C-terminus has known transcriptional effects [52], regulatory capacity [135], and contains a multimerization site [32]. Therefore, it was important to ensure 1) the presence of these domains don't interrupt dimerization responses in a cellular context, and 2) if the lessons learned by studying Notch1 can be broadly applied to the other mammalian Notch proteins.

To address these concerns, we first revisited full-length, Notch-responsive promoters, which contain canonical sequence-paired sites to drive transcription. While these promoters did require NICD dimerization for full activation and therefore allowed for preliminary conclusions, our data collection suffered from low activation levels (Hes1) or high experimental variability (Hes5). This is a logical byproduct from using full-length promoters since these genes are regulated through mechanisms beyond just Notch signaling and overexpression of constitutively active NICDs would have wide, overarching, signaling outcomes. For example, as in the case of Hes1, this gene is understood to be self-regulated, resulting in its oscillatory nature [223]. For our purposes, this implies that endogenous Hes1 may be activated by NICD overexpression and circles back to our Hes1-luciferase promoter to negatively-regulate it, resulting in its poor overall activation. For reasons like this, we sought to create minimalized promoters to more specifically monitor dimerization-induced signaling.

Since synthetic promoters with tandemly arranged RBPJ sites had been previously used to monitor Notch activity (e.g. 4xCSL-Luc, [216]), we reasoned that the SPS alone should also be sufficient for Notch activation. Therefore, we isolated the known sequence-paired sites out of Hes1 and Hes5 and created the Hes1/5(SPS)-luciferase vectors. Since the reverse sites within Hes1 and 5 do not perfectly match the canonical RBPJ binding site,

we also crafted the synthetic 2xTP1(SPS)-Core promoter to make a "perfect" SPS element. Upon testing we found that the Hes1(SPS) and the 2xTP1(SPS)-Core promoters operated as expected in that they were robustly activated by N1ICD and inefficiently activated by dimer-incompetent NICD ankyrin mutants. Surprisingly however, our results did not indicate that the isolated Hes5 SPS site functions in a dimer-dependent manner, although the full-length Hes5 promoter was dimer-dependent. We return to this point later in this discussion.

Having established two reporters with high activity and specificity for dimerized NICD signaling we were able to specifically ask questions about dimerization of full-length NICD proteins in cells. We found that full-length N1ICD and N2ICD activated sequence-paired sites in a dimerization-dependent mechanism. In contrast, N3ICD's activation of these minimal promoters was poor, which may be partially attributed to its lack of a TAD domain in its C-terminal [52] or usage of other transcription factors for its activation [28]. It also differed in its dimer-dependence; where it was not dimer-dependent on the Hes1(SPS) but was on the 2xTP1(SPS)-Core. This implies there is some difference located within these two minimalized constructs that can affect dimerization outcomes. The primary source of variation can be found within the 16 bp gap between RBPJ binding sites. The original crystallography studies found that the Hes1 gap distance DNA must go through substantial untwisting to bring the ankyrin domains into contact with each other for dimerization [30]. Gap composition of the 2xTP1(SPS)-Core construct has even higher G/C content than Hes1's, so while N1ICD and N2ICD can utilize variable gap compositions, perhaps N3ICD utilizes a more inflexible gap sequence. Whether or not this would enable differential transcriptional activity of Notch remains to be tested. We also found that

N4ICD activated these promoters and our ChIP data indicated that N4ICD formed homo- and heterodimers on DNA. In contrast, however, N4ICD did not appear to have dimer-dependent activation on the Hes1(SPS) or 2xTP1(SPS)-Core constructs despite still displaying a preference for a 16 bp gap between RBPJ binding sites on these promoters. Based on these results, we believe that the single R1685A mutation (which ablates dimerization of the other NICDs) on N4ICD was insufficient to abolish its dimerization activity suggesting that perhaps N4ICD has an alternative dimerization interface. Indeed, crystallography work on human N1ICD homodimers indicated two other amino acids (K1945 and E1949) beyond the R1984 that are involved in ankyrin-mediated dimerization [30]. Interestingly the N4ICD is the only NICD with an "R" located at the K1945 site, suggesting this position may be especially important for N4ICD dimerization (Figure S3.2).

In addition to comparing the activation parameters of the various NICDs on these optimized promoters, we were also curious about the standard 16-nucleotide gap distance established by the N1ICD containing tripartite complex. Two hypotheses presented themselves to us. First, given the contortion of DNA evident in the crystalized N1ICD trimeric complex, we hypothesized that RBPJ sites outside of the optimal 16 bp gap might be utilized through further contortions of DNA between RBPJ binding sites. Second, we further hypothesized that given the variable sequences and sizes of the NICD proteins, different NICDs might have preferences for slightly longer or shorter gap distances between RBPJ binding sites. To test the first hypothesis, we created SPS sites with variable gap distances in 5 bp increments to take advantage of the periodicity of helical DNA. We found that none of these long-range alternative gap distances, for any of the NICDs, had

significantly enhanced signaling above monomeric signaling. This indicated that long-range interactions between NTC complexes are unlikely to occur. Our analysis however only extended to measuring 36 bp gaps and therefore, longer-range interactions between RBPJ binding sites cannot be ruled out. To address the second hypothesis (that different sized NICDs might have subtle differences in SPS preference), we compared NICD activity on SPS sites with 11-21 bp gap distances in one bp increments. Similar to previous results [30,35,51] , we found that all full-length NICDs also prefer a 16 bp gap distance, with little room for variation. Based on this result, we conclude that the C-terminal regions of NICDs do not appear to change the SPS dimensions preferred by NICDs nor impact NICD dimerization. It should also be stated, however, that deletion of the N1ICD C-terminal tail (ΔS2184) which contains the trans-activation domain (TAD) significantly reduced transcriptional activity (Figure S3.3). Minor differences in the NICDs however were observed. For example, N2ICD appeared slightly more restrictive when choosing SPS sites than Notch1, since N2ICD activated 15/16 bp spacers but not the 17 bp gap. This poses an interesting possibility where N1ICD might dimer-dependently activate *CUL1* or *TXN2*, which have SPSs with a 17-nucleotide gap distance [30,33], whereas binding of N2ICD on this promoter would only cause monomeric levels of transcription, though this idea was left untested. While N3ICD and N4ICD had questionable dimerization activities, they did seem to have cooperative binding and higher activity on the 16/17 bp gap SPSs. Making firm conclusions about their preferences is difficult however due to their low overall activity and high variability. Together, these experiments highlight the stringent requirements for dimerization-induced transcription.

Our results have also shed some light on the nature of NICD dimerization. First, there has been some debate as to the order of events leading up to NICD activated transcription. It is currently unclear whether individual NICD molecules first bind to RBPJ/DNA then form dimers, or alternatively if two NICDs first form a dimer, then bind to RBPJ/DNA. In Figure 3.4 and 3.5, we demonstrated that dimer-incompetent N1ICD performed slightly better than WT N1ICD on SPS elements with non-optimal 11 or 21 bp gaps. This suggests that the attempt to dimerize may impede NICD molecules from binding to these sites and might be a clue as to the mechanics of NICD function. Our result indicates that non-optimal SPS elements discourage NICD dimer formation and we believe this is evidence that NICD molecules are pre-forming dimers before binding to RBPJ/DNA. Whether or not this has an actual impact on how promoters with non-optimal SPS sites are utilized by Notch signaling remains to be seen but as shown by Castel et al., [33], several Notch responsive promoters with non-optimal SPS elements have been identified. Another outstanding question about NICD dimerization is whether or not NICD molecules can engage in heterodimerization. Given the conservation of sequence in the ankyrin domains and the importance of ankyrin domains for NICD dimerization it has been hypothesized that NICD heterodimers may exist. While further research on this topic is certainly warranted, our results in Figure 3.6 showing similar SPS element preferences and in Figure 3.4 showing ChIP recovery of N1/N4 complexes suggests that heterodimers between N1ICD and N4ICD can form in transfected 293T cells and therefore possibly under more physiological conditions. Here again, the biological implications of this observation are unknown but given the strong differences in transcriptional activation between N1ICD and N4ICD, we hypothesize that N1/N4ICD heterodimers would have

intermediate activity compared to N1ICD or N4ICD homodimers. Thus, heterodimerization of NICD molecules may offer a new mechanism to regulate outputs from Notch signaling.

Finally, our minimized Hes5(SPS) promoter was not sufficient to elicit dimerization-dependent activation. The Hes5 promoter does not contain a canonical sequence-paired site and instead has been described as 'cryptic' [30], with a standard forward RBPJ binding site but an abnormal reverse site. When arranged as a palindrome in a SPS, this abnormal reverse site does not support dimerization, yet it facilitated dimerization when paired with a strong RBPJ binding site [35]. Work with EMSAs of this cryptic SPS showed that N1ICD homodimers can form, and dimerization-dependent activation through this site was supported through luciferase assays [30], but distinctly, these luciferase assays were still performed with the full-length promoter. In our analyses we isolated out this SPS, which should be sufficient for dimerization, yet this construct did not demonstrate dimerization-dependent activation.

This inconsistency poses two thought-provoking problems. First, and as originally described by Severson et al. [35], if cryptic sequence-paired sites are capable of forming NICD dimers, then searching for SPSs by 'sequence-gazing' becomes far more difficult. For example, previous ChIP work isolated out RBPJ-bound DNA targets, and these sequences were screened for nearby RBPJ binding motifs located in tandem [33]. The issue here lies in the partner sequence, wherein any non-conforming RBPJ sequences would be missed through a simple screening approach. To further identify other cryptic sequence-paired sites, like those in Hes5 or *pTα* [30,31], we propose that a logical course of action is to perform ChIP-Seq on a double-selected pool of DNA, as in our simplified ChIP

experiment. The second problem concerns the activation of Hes5 through its SPS. While it appears that NTC complexes dimerize on this promoter segment *in vitro*, do they still form in living cells and if so, what's the missing link for transcriptional activation? Other than the cryptic RBPJ binding site, the Hes5(SPS) construct is nearly identical to the Hes1(SPS) and 2xTP1(SPS)-Core constructs which respond as expected. Since the full-length Hes5 promoter is apparently dimer-responsive and the other minimalized SPS constructs are sufficient for activation, we predict that there are other promoter elements involved which enable these low-affinity dimers to form and signal in a cellular context. Comparing the promoters and enhancers of multiple, cryptic, SPS genes may identify other sequence motifs in common and identify signaling or regulatory pathways involved.

In conclusion, since much of the work on NICD dimerization has been performed studying C-terminally truncated N1ICD, we felt it was important to 1.) examine full-length NICD molecules to insure the C-terminal domain does not affect NICD promoter preference, and 2.) compare promoter preferences of the other NICD molecules, which have been largely overlooked. In so doing, we confirmed that while the C-terminal domain of the various NICDs has a transcriptional role, this domain does not appear to play a role in promoter preference. In addition, we also found that all the mammalian NICDs have remarkably similar SPS gap length preferences with only minor (+/- one bp) flexibility. Overall, these results both support previous work but also help fill in missing gaps in our understanding of Notch transcriptional activity.

Acknowledgments

This work was supported by funding from the National Institute of General Medical Sciences to A. Albig (2R15GM102852-02 and 1R15GM134501-01) and from grants

NIH/NIGMS P20GM103408 and P20GM109095. Author contributions were as follows: A. Albig and J. Crow conceived and designed the experiments. A. Albig and J.Crow, performed the experiments. A. Albig and J. Crow prepared the final manuscript.

Conflicts of Interest

The authors declare no conflicts of interest.

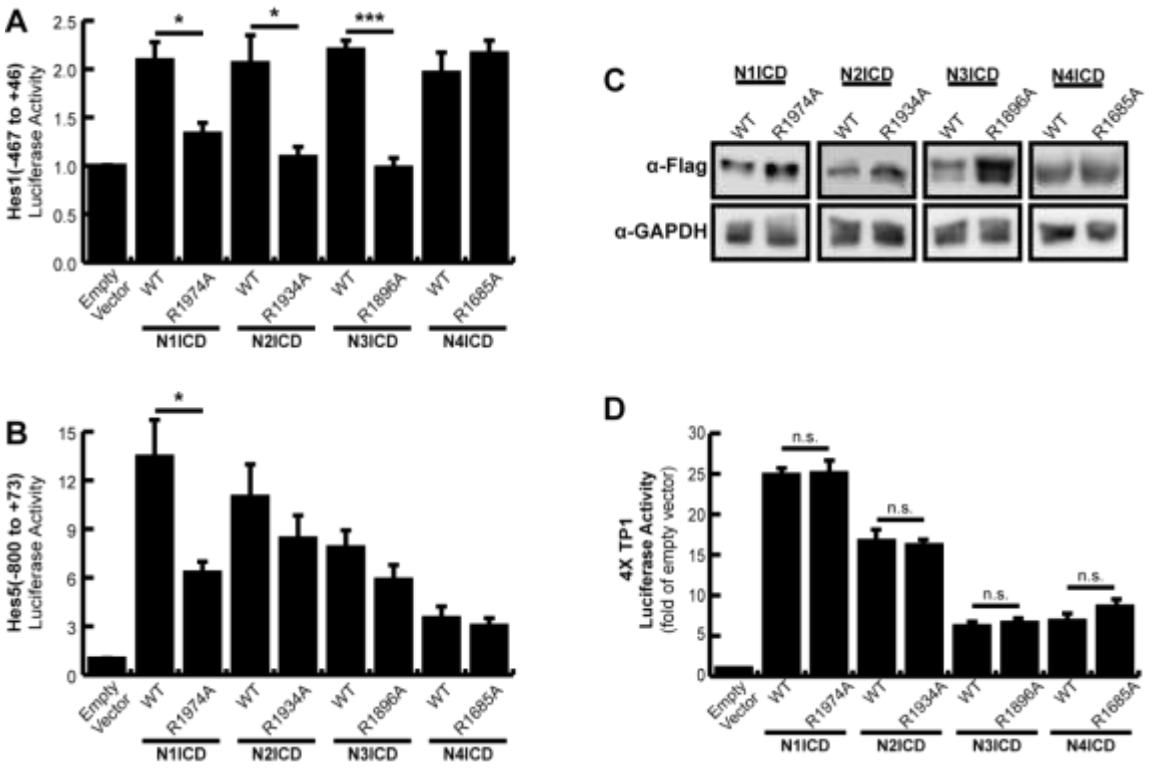

Figure 3.1: Dimerization dependence of full-length Hes1 and Hes5 promoters

HEK293T cells were transfected with portions of the (A) *Hes1* (-467 to +46) (B) *Hes5* (-800 to +73) promoters for luciferase assays to monitor promoter activation. Cells were co-transfected with wild-type (WT) or ankyrin mutated (R→A) NICDs to compare their dimer dependence. Shown are the average +/- SE of 5 independent experiments. * indicates P<.05, **<.01, ***<.001 (student's t-test). (C) Western blots to compare the protein abundancies of WT or dimer incompetent ankyrin mutated NICDs. HEK293T cells were transfected with NICD expression constructs and NICD proteins were detected with anti-Flag antibodies. Endogenous GAPDH was also detected from the same lysates for use as a loading control. The image displayed is a representative blot from an experiment that was replicated three independent times. (D) 293T cells were transfected with the dimer independent 4XTP1 luciferase construct and WT or ankyrin mutated NICDs as above. Shown are the average +/- SE of three independent experiments.

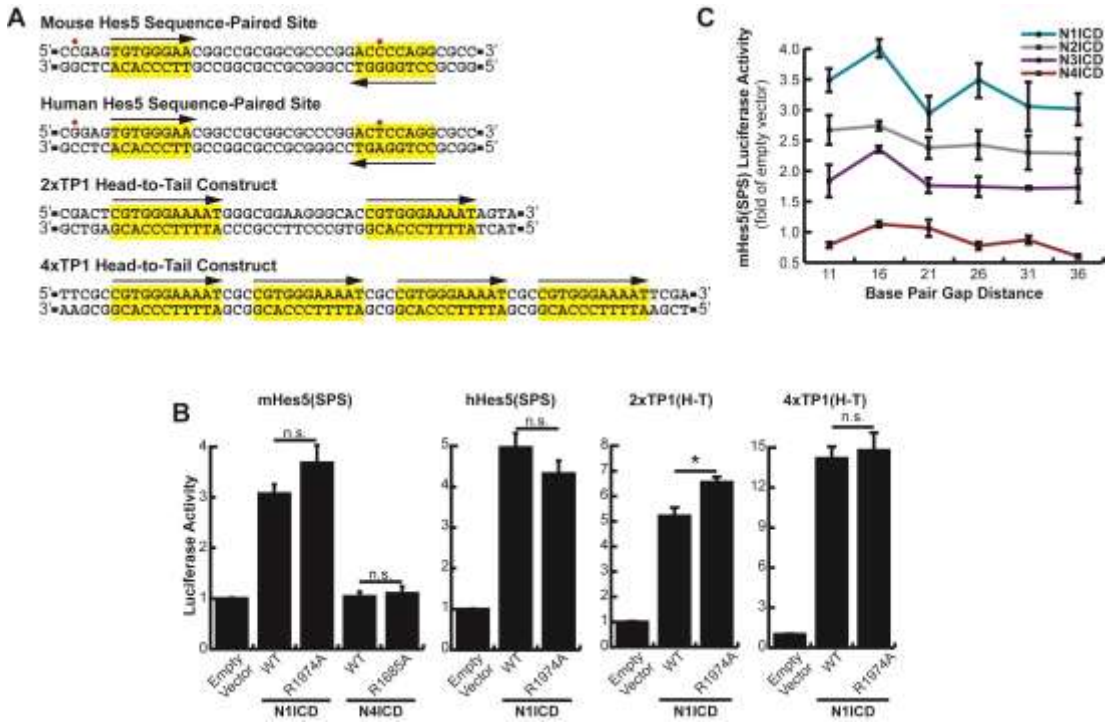

Figure 3.2: Lack of dimerization dependence of the *Hes5* sequence-paired site

(A) Promoter structure of the Hes5, 2xTP1(H-T), and 4xTP1(H-T) luciferase constructs. Red dots indicate nucleotide differences between the human and mouse Hes5 SPS sites. Suspected RBPJ binding sites are highlighted in yellow and arrows depict directionality of RBPJ binding sites. (B) HEK293T cells were transfected with either the mouse (mHes5(SPS)) or human (hHes5(SPS)) sequence-paired site constructs or with the 2xTP1(H-T) or 4xTP1(H-T) head-to-tail constructs and WT or dimer-null versions of NICDs. Shown is the average +/- SE of n = 4 independent experiments. * <0.05, ** <0.01, *** <0.001, student's t-test. (C) HEK293T cells were transfected with various NICDs and Hes5 SPS constructs with 11 – 36 bp spacer regions (5 bp increments), n = 6.

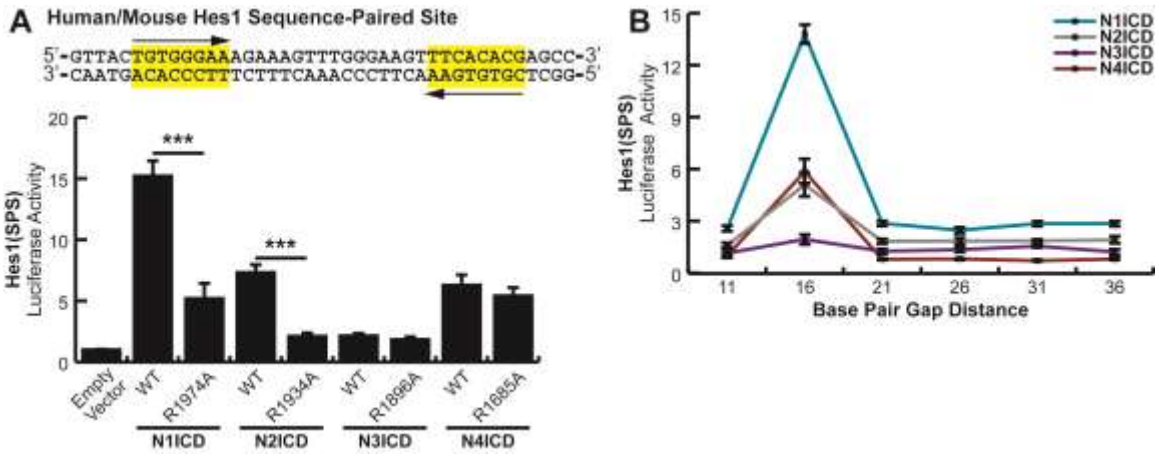

Figure 3.3: Dimer dependence of the *Hes1* sequence-paired site

(A, Top) Sequence information for the human and mouse isolated *Hes1* SPS element. (A, Bottom) HEK293T cells were transfected with the Hes1(SPS) construct and WT or dimer-null versions of NICD proteins. Shown is the average +/- SE of n = 4 independent experiments. Student's t-test was performed to compare the activation between WT and mutant NICDs where * <0.05, ** <0.01, *** <0.001. (B) HEK293T cells were transfected with various NICDs and Hes1(SPS) constructs that had been modified to contain variable gap distances between RBPJ binding sites in 5 bp interments. Shown is the average +/- SE of 4 independent experiments.

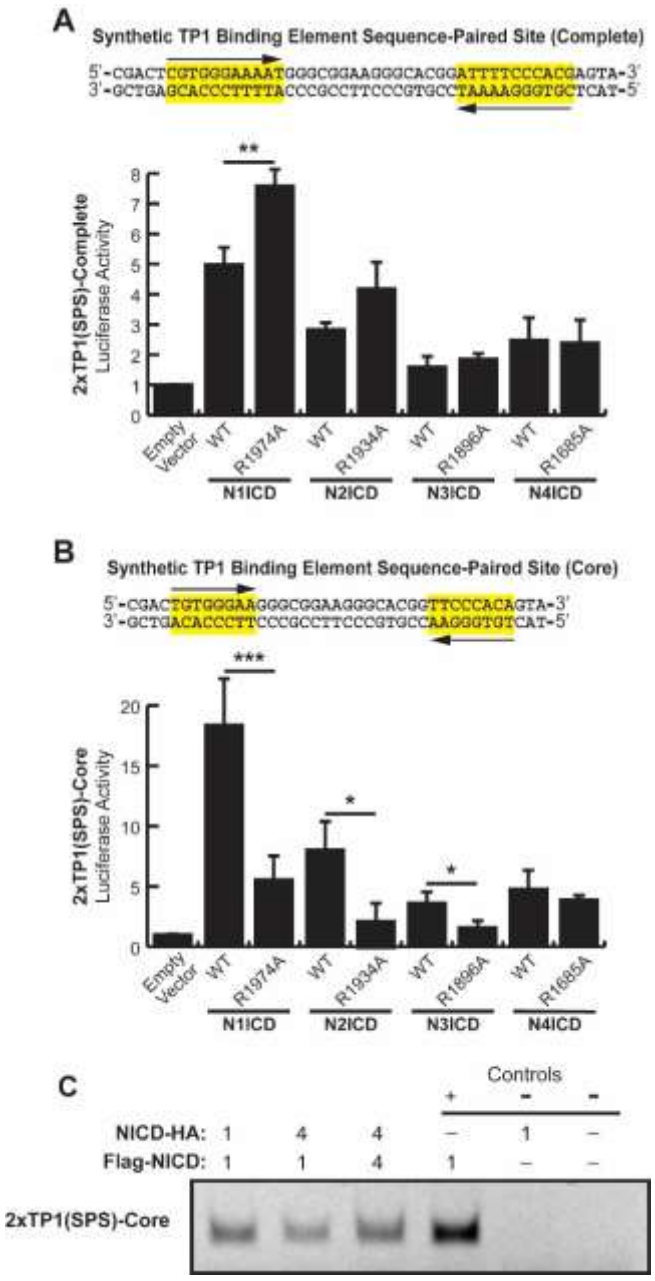

Figure 3.4: An optimized Notch responsive SPS element

(A and B) A synthetic SPS-driven promoter, using the (A) complete TP1 binding element or (B) core TP1 binding element, was transfected into HEK293T cells. These two constructs were activated with either wild-type (WT) or ankyrin mutated (R→A) NICDs to observe their dimer responsiveness. Shown are the average +/- SE of n = 4 independent experiments. Student's t-test was performed to compare the activation

between WT and mutant NICDs where * <0.05, ** <0.01, *** <0.001. (C) ChIP was used to confirm NICD dimer formation on the 2xTP1(SPS)-Core construct. HEK293T cells were transfected with various combinations of plasmids encoding FLAG-tagged NICD and HA-tagged NICD proteins. NICD dimers were detected by immunoprecipitation first with anti-FLAG antibodies then with anti-HA antibodies followed by PCR to detect the co-transfected 2xTP1(SPS)-Core construct. Positive control reaction was subject to a single round of selection with anti-FLAG antibodies. Negative controls were transfected with 2xTP1(SPS)-Core alone or 2xTP1(SPS)-Core and HA-N1ICD then subjected to both anti-FLAG and anti-HA immunoprecipitation. Shown is a representative image of a single experiment that was performed three independent times.

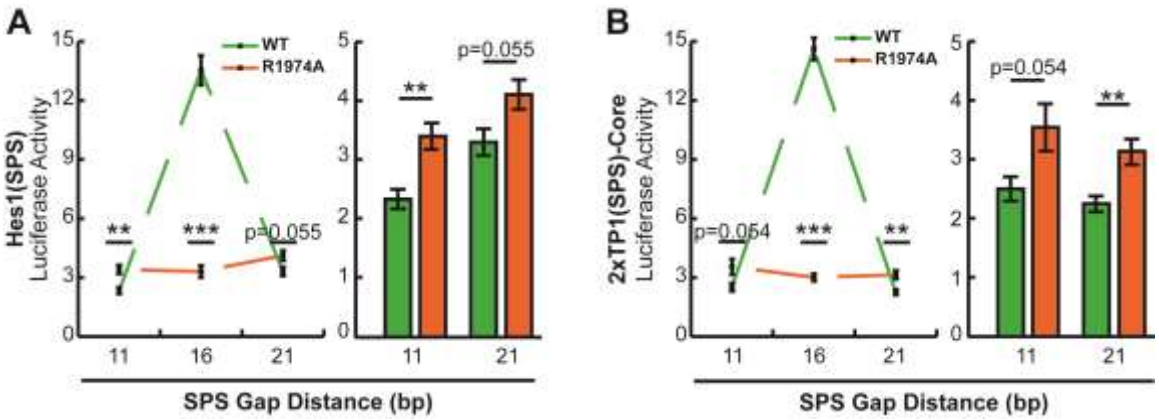

Figure 3.5: Non-optimal SPS sites select against dimer-dependent NICD transcriptional activation

(A and B) 293T cells were transfected with 11, 16, or 21 bp gap versions of the (A) Hes1(SPS) or (B) 2xTP1(SPS)-Core reporters and WT or ankyrin mutated N1ICD. Shown is the average +/- SE of n = 6 experiments. In all panels, a student's t-test was performed to compare the activation between WT and ankyrin mutated NICDs, where P-values are reported as * <0.05, ** <0.01, *** <0.001.

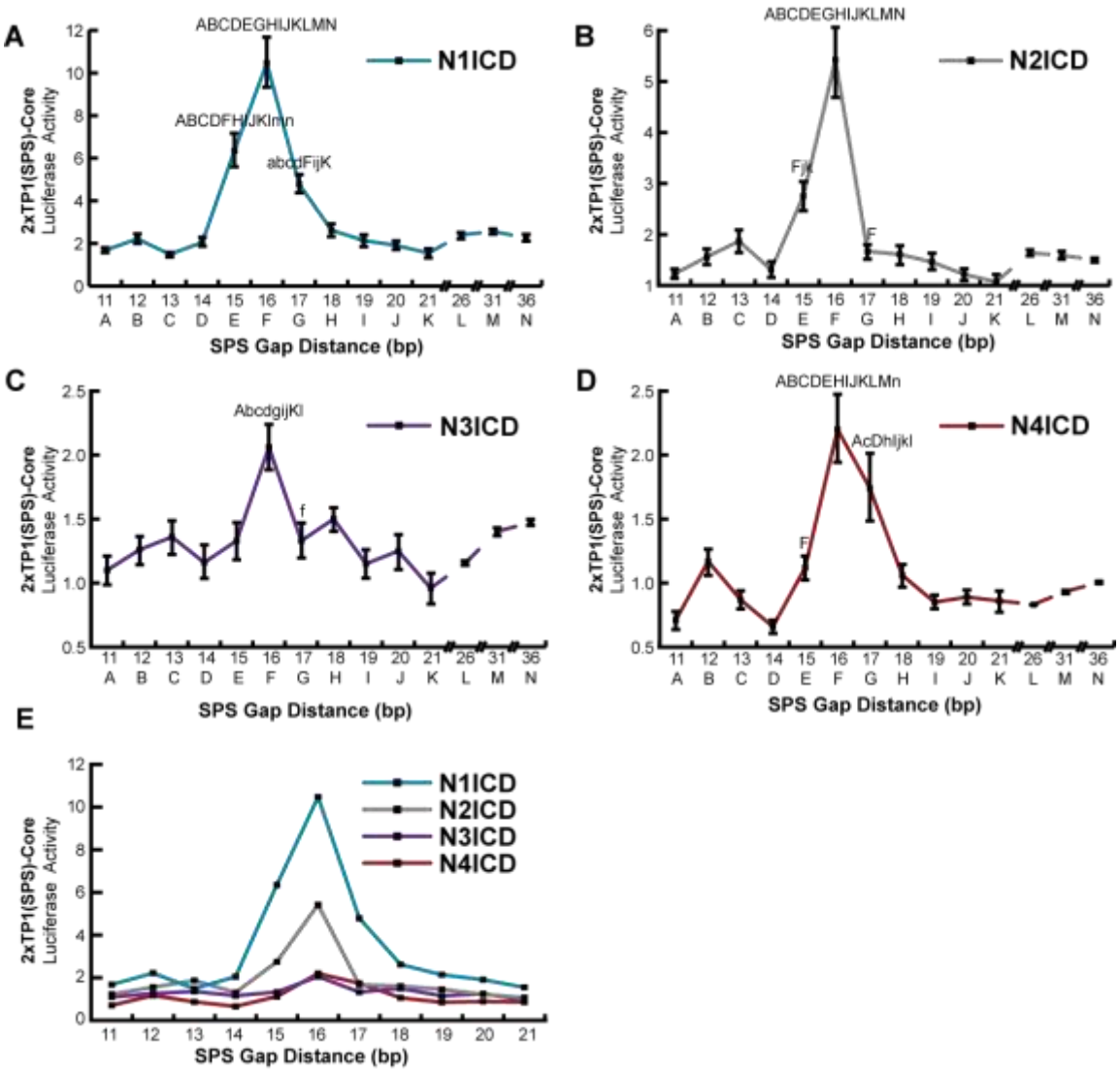

Figure 3.6: Notch homodimers do not tolerate alternative gap distances

(A-D) HEK293T cells were co-transfected with various NICD expression plasmids and 2xTP1(SPS)-Core promoter with varying SPS gap lengths from 11-21 bp, in one bp increments, or 21-36 bp, in 5 bp increments. For all luciferase studies, an empty expression vector was used to equate the amount of DNA transfected across samples. Fold differences are represented as the NICD-induced activity compared to the basal activity levels. Shown are the average +/- SE of n = 5 independent experiments. (E) Overlay of data in panels A-D to emphasize different transcriptional strengths of the

various NICDs. Statistical analysis was performed by using a one-way analysis of variance (ANOVA), followed by a Tukey-Kramer's HSD post-hoc test. Only points that were statistically different from other points are indicated in each graph where capital letters indicate P values < 0.001, whereas small case letters indicate $P < 0.05$ on a point-by-point basis.

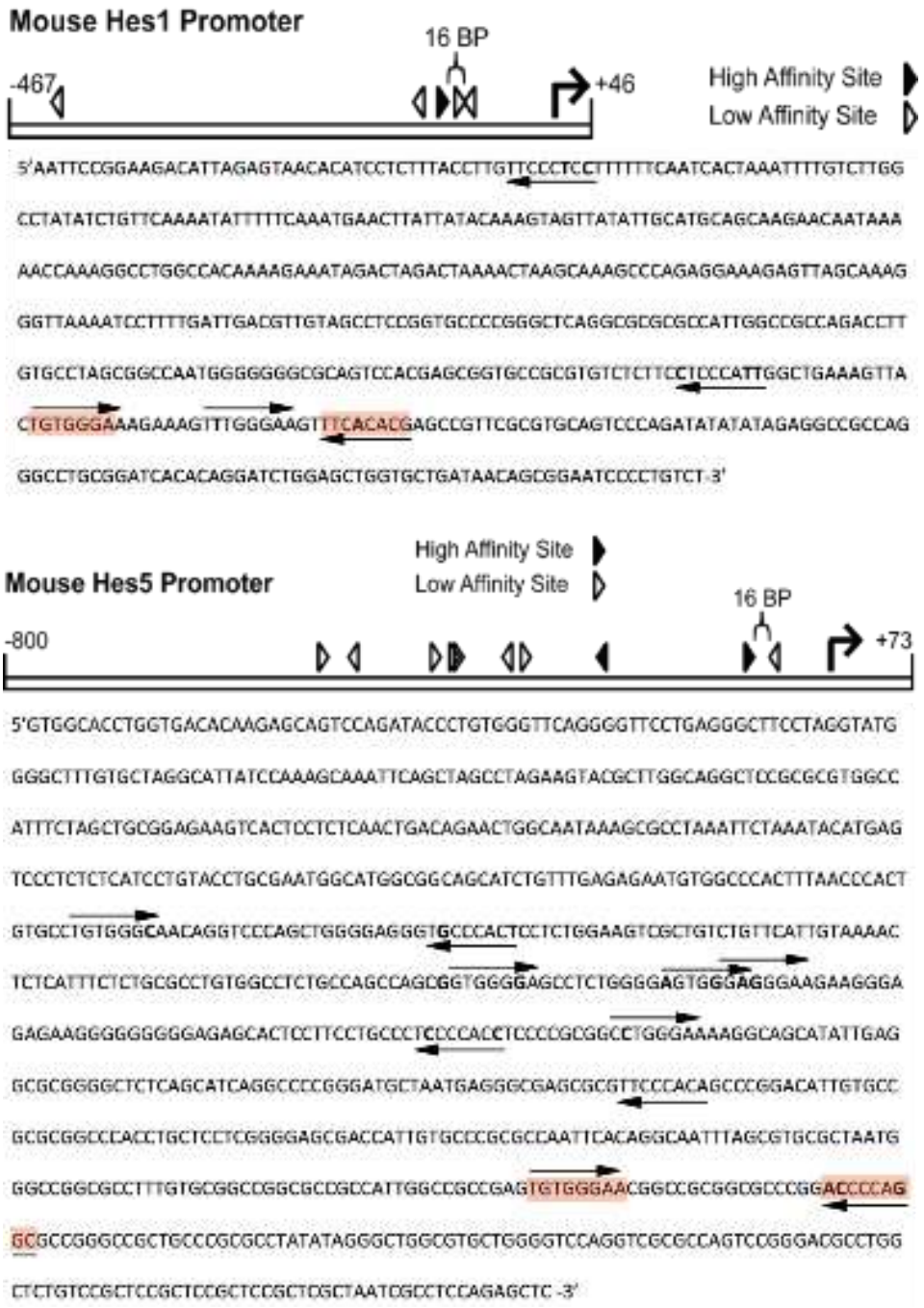

Figure S3.1: Identification of low and high affinity SPS sites in Hes1 and Hes5 promoters

DNA sequences are as reported for AddGene products Hes1-luciferase (#41723) and Hes5-luciferase (#41724) vectors. Possible high and low affinity sites (as described in material and methods) are indicated by forward or reverse arrows. High affinity sites

confirmed to serve as RBPJ binding sites are indicated with red shading. Nucleotides that diverge from the core TP1 element as originally defined (C/tGTGGGAA) are indicated by bolded letters.

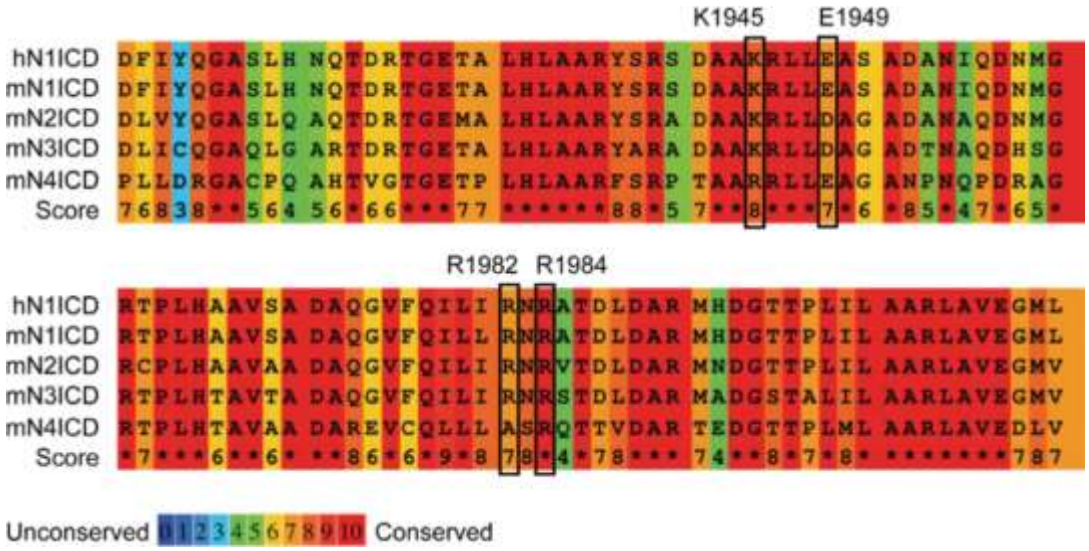

Figure S3.2: Sequence comparison of human N1ICD and mouse NICD dimerization domains

Amino acids previously identified as important for dimerization of N1ICD ankyrin domains are indicated [30]. Amino acid numbers are based on equivalent positions in human N1ICD. R1984A equivalents were used throughout this work to attempt to make generate dimer-incompetent NICD variants.

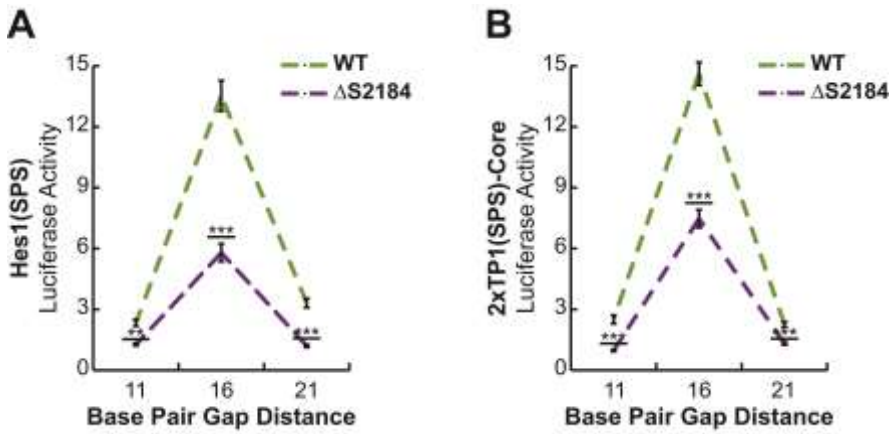

Figure S3.3: N1ICD C-terminus does not impact NICD dimerization

HEK293T cells were transfected with 11, 16, or 21 bp versions of Hes1(SPS) or 2xTP1(SPS)-Core luciferase reporters and either full-length N1ICD or ΔS2184 N1ICD (which deletes residues C-terminal of the N1ICD ankyrin domain). Shown is the average +/- SE of four independent experiments.

Supplementary Table 3.1 Plasmid and Sequence Information for the NICD-Activated Sequence-Paired Sites

Hes1

Plasmid Number	Description	Sequence (5'→3')
344 AddGene #41723	Full Length (mouse sequence)	Construct contains the sequence -467 to +46 around the transcriptional start site.
339	Human/Mouse SPS Region (16 BP Gap)	GTTAC**TGTGGGAA**AGAAAGTTTGGGAAGT**TTCACACG**AGCC
338	11 BP Gap	GTTAC**TGTGGGAA**AGAAAGTT-----AGT**TTCACACG**AGCC
340	21 BP Gap	GTTAC**TGTGGGAA**AGAAAGTT[GGAAT]TGGGAAGT**TTCACACG**AGCC
341	26 BP Gap	GTTAC**TGTGGGAA**AGAAAGTT[GGAAT][GGAAT]TGGGAAGT**TTCACACG**AGCC
342	31 BP Gap	GTTAC**TGTGGGAA**AGAAAGTT[GGAAT][GGAAT][GGAAT]TGGGAAGT**TTCACACG**AGCC
343	36 BP Gap	GTTAC**TGTGGGAA**AGAAAGTT[GGAAT][GGAAT][GGAAT][GGAAT]TGGGAAGT**TTCACACG**AGCC

Hes5

Plasmid Number	Description	Sequence (5'→3')
196 AddGene #41724	Full Length (mouse sequence)	Construct contains the sequence -800 to +73 around the transcriptional start site.
314	Human SPS Region	CGGAG**TGTGGGAA**CGGCCGCGGCGCCCGG**ACTCCAGG**CGCC
315	Mouse SPS Region (16 BP Gap)	CCGAG**TGTGGGAA**CGGCCGCGGCGCCCGG**ACCCCAGG**CGCC
317	11 BP Gap	CCGAG**TGTGGGAA**CGG-----GCGCCCGG**ACCCCAGG**CGCC
318	21 BP Gap	CCGAG**TGTGGGAA**CGGCCGCG**[**GGCCC**]**GCGCCCGG**ACCCCAGG**CGCC

Plasmid Number	Description	Sequence (5'→3')
319	26 BP Gap	CCGAG**TGTGGGAA**CGGCCGCG**[**GGCCC**][**GGCCC**]**GCGCCCGG**ACCCCAGG**CGCC
320	31 BP Gap	CCGAG**TGTGGGAA**CGGCCGCG**[**GGCCC**][**GGCCC**][**GGCCC**]**GCGCCCGG**ACCCCAGG**CGCC
321	36 BP Gap	CCGAG**TGTGGGAA**CGGCCGCG**[**GGCCC**][**GGCCC**][**GGCCC**][**GGCCC**]**GCGCCCGG**ACCCCAGG**CGCC

2xTP1 (Head-to-Head)

Plasmid Number	Description	Sequence (5'→3')
323	Complete TP1 Site	CGACT**CGTGGGAAAAT**GGGCGGAAGGGCACGG**ATTTTCCCACG**AGTA
329	Core TP1 Site (16 BP Gap)	CGAC**TGTGGGAA**GGGCGGAAGGGCACGG**TTCCCACA**GTA
324	11 BP Gap	CGAC**TGTGGGAA**GGGCGGAA-----CGG**TTCCCACA**GTA
325	12 BP Gap	CGAC**TGTGGGAA**GGGCGGAA----ACGG**TTCCCACA**GTA
326	13 BP Gap	CGAC**TGTGGGAA**GGGCGGAA---CACGG**TTCCCACA**GTA
327	14 BP Gap	CGAC**TGTGGGAA**GGGCGGAA--GCACGG**TTCCCACA**GTA
328	15 BP Gap	CGAC**TGTGGGAA**GGGCGGAA-GGCACGG**TTCCCACA**GTA
330	17 BP Gap	CGAC**TGTGGGAA**GGGCGGAA**[**G**]**GGGCACGG**TTCCCACA**GTA
331	18 BP Gap	CGAC**TGTGGGAA**GGGCGGAA**[**GA**]**GGGCACGG**TTCCCACA**GTA
332	19 BP Gap	CGAC**TGTGGGAA**GGGCGGAA**[**GAG**]**GGGCACGG**TTCCCACA**GTA
333	20 BP Gap	CGAC**TGTGGGAA**GGGCGGAA**[**GAGG**]**GGGCACGG**TTCCCACA**GTA
334	21 BP Gap	CGAC**TGTGGGAA**GGGCGGAA**[**GAGGC**]**GGGCACGG**TTCCCACA**GTA
335	26 BP Gap	CGAC**TGTGGGAA**GGGCGGAA**[**GAGGC**][**GAGGC**]**GGGCACGG**TTCCCACA**GTA
336	31 BP Gap	CGAC**TGTGGGAA**GGGCGGAA**[**GAGGC**][**GAGGC**][**GAGGC**]**GGGCACGG**TTCCCACA**GTA
337	36 BP Gap	CGAC**TGTGGGAA**GGGCGGAA**[**GAGGC**][**GAGGC**][**GAGGC**][**GAGGC**]**GGGCACGG**TTCCCACA**GTA

2xTP1 (Head-to-Tail)

Plasmid Number	Description	Sequence (5'→3')
261	Two TP1 Binding Elements, Head-to-Tail Arrangement	CGACT**CGTGGGAAAAT**GGGCGGAAGGGCAC**CGTGGGAAAAT**AGTA

4xTP1 (Head-to-Tail)

Plasmid Number	Description	Sequence (5'→3')
197 AddGene #41726	Four TP1 Binding Elements, Head-to-Tail Arrangement	TTCGC**CGTGGGAAAAT**CGC**CGTGGGAAAAT**CGC**CGTGGGAAAAT**CGC**CGTGGGAAAAT**TCGA

REFERENCES

1. King N, Westbrook MJ, Young SL, et al. The genome of the choanoflagellate Monosiga brevicollis and the origin of metazoans. *Nature*. 2008;451(7180):783-788. doi:10.1038/nature06617

2. Gazave E, Lapébie P, Richards GS, et al. Origin and evolution of the Notch signalling pathway: an overview from eukaryotic genomes. *BMC Evol Biol*. 2009;9(249). doi:10.1186/1471-2148-9-249

3. LaFoya B, Munroe JA, Mia MM, et al. Notch: A multi-functional integrating system of microenvironmental signals. *Dev Biol*. 2016;418(2):227-241. doi:10.1016/j.ydbio.2016.08.023

4. Siebel C, Lendahl U. Notch signaling in development, tissue homeostasis, and disease. *Physiol Rev*. 2017;97(4):1235-1294. doi:10.1152/physrev.00005.2017

5. Morgan TH. The Origin of Nine Wing Mutations in Drosophila. *Science*. 1911;33(848):496-499. doi:10.1126/science.33.848.496

6. Dexter JS. The Analysis of a Case of Continuous Variation in Drosophila by a Study of its Linkage Relations. *Am Nat*. 1914;48(576):712-758.

7. Kidd S, Kelley MR, Young MW. Sequence of the notch locus of Drosophila melanogaster: relationship of the encoded protein to mammalian clotting and growth factors. *Mol Cell Biol*. 1986;6(9):3094-3108. doi:10.1128/mcb.6.9.3094

8. Kidd S, Lockett TJ, Young MW. The Notch locus of Drosophila melanogaster. *Cell*. 1983;34(2):421-433. doi:10.1016/0092-8674(83)90376-8

9. Wharton KA, Johansen KM, Xu T, Artavanis-Tsakonas S. Nucleotide sequence from the neurogenic locus Notch implies a gene product that shares homology with proteins containing EGF-like repeats. *Cell*. 1985;43(3 PART 2):567-581. doi:10.1016/0092-8674(85)90229-6

10. Artavanis-Tsakonas S, Muskavitch MAT, Yedvobnick B. Molecular cloning of Notch, a locus affecting neurogenesis in Drosophila melanogaster. *Proc Natl Acad Sci U S A*. 1983;80(7):1977-1981. doi:10.1073/pnas.80.7.1977

11. Breeden L, Nasmyth K. Similarity between cell-cycle genes of budding yeast and fission yeast and the Notch gene of Drosophila. *Nature*. 1987;329(6140):651-654. doi:10.1038/329651a0

12. Lux SE, John KM, Bennett V. Analysis of cDNA for human erythrocyte ankyrin indicates a repeated structure with homology to tissue-differentiation and cell-cycle control proteins. *Nature*. 1990;344(6261):36-42. doi:10.1038/344036a0

13. Rebay I, Fleming RJ, Fehon RG, Cherbas L, Cherbas P, Artavanis-Tsakonas S. Specific EGF repeats of Notch mediate interactions with Delta and serrate: Implications for notch as a multifunctional receptor. *Cell*. 1991;67(4):687-699. doi:10.1016/0092-8674(91)90064-6

14. Weinmaster G, Roberts VJ, Lemke G. A homolog of Drosophila Notch expressed during mammalian development. *Development*. 1991;113(1):199-205.

15. Rebay I, Fehon RG, Artavanis-Tsakonas S. Specific truncations of Drosophila Notch define dominant activated and dominant negative forms of the receptor. *Cell*. 1993;74(2):319-329. doi:10.1016/0092-8674(93)90423-N

16. Lieber T, Kidd S, Alcamo E, Corbin V, Young MW. Antineurogenic phenotypes induced by truncated Notch proteins indicate a role in signal transduction and may point to a novel function for Notch in nuclei. *Genes Dev*. 1993;7(10):1949-1965. doi:10.1101/gad.7.10.1949

17. Tun T, Hamaguchi Y, Matsunami N, Furukawa T, Honjo T, Kawaichi M. Recognition sequence of a highly conserved DNA binding protein RBP-Jk. *Nucleic Acids Res*. 1994;22(6):965-971. doi:10.1093/nar/22.6.965

18. Jarriault S, Brou C, Logeat F, Schroeter EH, Kopan R, Israel A. Signalling downstream of activated mammalian Notch. *Nature*. 1995;377(6547):355-358. doi:10.1038/377355a0

19. Bailey AM, Posakony JW. Suppressor of hairless directly activates transcription

of Enhancer of split complex genes in response to Notch receptor activity. *Genes Dev*. 1995;9(21):2609-2622. doi:10.1101/gad.9.21.2609

20. Tamura K, Taniguchi Y, Minoguchi S, et al. Physical interaction between a novel domain of the receptor Notch and the transcription factor RBP-Jκ/Su(H). *Curr Biol*. 1995;5(12):1416-1423. doi:10.1016/S0960-9822(95)00279-X

21. Kato H, Sakai T, Tamura K, et al. Functional conservation of mouse Notch receptor family members. *FEBS Lett*. 1996;395(2-3):221-224. doi:10.1016/0014-5793(96)01046-0

22. Kopan R, Schroeter EH, Weintraub H, Nye JS. Signal transduction by activated mNotch: Importance of proteolytic processing and its regulation by the extracellular domain. *Proc Natl Acad Sci U S A*. 1996;93(4):1683-1688. doi:10.1073/pnas.93.4.1683

23. Schroeter EH, Kisslinger JA, Kopan R. Notch-1 signalling requires ligand-induced proteolytic release of intracellular domain. *Nature*. 1998;393(6683):382-386. doi:10.1038/30756

24. Nellesen DT, Lai EC, Posakony JW. Discrete enhancer elements mediate selective responsiveness of Enhancer of split complex genes to common transcriptional activators. *Dev Biol*. 1999;213(1):33-53. doi:10.1006/dbio.1999.9324

25. Wu L, Aster JC, Blacklow SC, Lake R, Artavanis-Tsakonas S, Griffin JD. MAML1, a human homologue of Drosophila mastermind, is a transcriptional co-activator for NOTCH receptors. *Nat Genet*. 2000;26(4):484-489. doi:10.1038/82644

26. Kitagawa M, Oyama T, Kawashima T, et al. A Human Protein with Sequence Similarity to Drosophila Mastermind Coordinates the Nuclear Form of Notch and a CSL Protein To Build a Transcriptional Activator Complex on Target Promoters. *Mol Cell Biol*. 2001;21(13):4337-4346. doi:10.1128/mcb.21.13.4337-4346.2001

27. Cave JW, Loh F, Surpris JW, Xia L, Caudy MA. A DNA Transcription Code for

Cell-Specific Gene Activation by Notch Signaling. *Curr Biol*. 2005;15:94-104. doi:10.1016/j

28. Ong CT, Cheng HT, Chang LW, et al. Target selectivity of vertebrate notch proteins: Collaboration between discrete domains and CSL-binding site architecture determines activation probability. *J Biol Chem*. 2006;281(8):5106-5119. doi:10.1074/jbc.M506108200

29. Nam Y, Sliz P, Pear WS, Aster JC, Blacklow SC. Cooperative assembly of higher-order Notch complexes functions as a switch to induce transcription. *Proc Natl Acad Sci U S A*. 2007;104(7):2103-2108. doi:10.1073/pnas.0611092104

30. Arnett KL, Hass M, McArthur DG, et al. Structural and mechanistic insights into cooperative assembly of dimeric Notch transcription complexes. *Nat Struct Mol Biol*. 2010;17(11):1312-1317. doi:10.1038/nsmb.1938

31. Liu H, Chi AWS, Arnett KL, et al. Notch dimerization is required for leukemogenesis and T-cell development. *Genes Dev*. 2010;24(21):2395-2407. doi:10.1101/gad.1975210

32. Vasquez-Del Carpio R, Kaplan FM, Weaver KL, et al. Assembly of a Notch Transcriptional Activation Complex Requires Multimerization. *Mol Cell Biol*. 2011;31(7):1396-1408. doi:10.1128/MCB.00360-10

33. Castel D, Mourikis P, Bartels SJJ, Brinkman AB, Tajbakhsh S, Stunnenberg HG. Dynamic binding of RBPJ is determined by notch signaling status. *Genes Dev*. 2013;27(9):1059-1071. doi:10.1101/gad.211912.112

34. Hass M, Liow H, Chen X, et al. SpDamID: Marking DNA Bound by Protein Complexes Identifies Notch-Dimer Responsive Enhancers. *Mol Cell*. 2015;59(4):685-697. doi:10.1016/j.molcel.2015.07.008

35. Severson E, Arnett KL, Wang H, et al. Genome-wide identification and characterization of Notch transcription complex–binding sequence-paired sites in leukemia cells. *Sci Signal*. 2017;10(477). doi:10.1111/cpr.12282

36. Blaumueller CM, Qi H, Zagouras P, Artavanis-Tsakonas S. Intracellular Cleavage of Notch Leads to a Heterodimeric Receptor on the Plasma Membrane. *Cell*.

1997;90(2):281-291. doi:10.1016/S0092-8674(00)80336-0

37. Logeat F, Bessia C, Brou C, et al. The Notch1 receptor is cleaved constitutively by a furin-like convertase. *Proc Natl Acad Sci U S A*. 1998;95(14):8108-8112. doi:10.1073/pnas.95.14.8108

38. Gordon WR, Vardar-Ulu D, L'Heureux S, et al. Effects of S1 Cleavage on the Structure, Surface Export, and Signaling Activity of Human Notch1 and Notch2. *PLoS One*. 2009;4(8). doi:10.1371/journal.pone.0006613

39. Gordon WR, Roy M, Vardar-Ulu D, et al. Structure of the Notch1-negative regulatory region: implications for normal activation and pathogenic signaling in T-ALL. *Blood*. 2009;113(18):4381-4390. doi:10.1182/blood-2008-08-174748

40. Sanchez-Irizarry C, Carpenter AC, Weng AP, Pear WS, Aster JC, Blacklow SC. Notch Subunit Heterodimerization and Prevention of Ligand-Independent Proteolytic Activation Depend, Respectively, on a Novel Domain and the LNR Repeats. *Mol Cell Biol*. 2004;24(21):9265-9273. doi:10.1128/mcb.24.21.9265-9273.2004

41. Gordon WR, Vardar-Ulu D, Histen G, Sanchez-Irizarry C, Aster JC, Blacklow SC. Structural basis for autoinhibition of Notch. *Nat Struct Mol Biol*. 2007;14(4):295-300. doi:10.1038/nsmb1227

42. Harvey BM, Haltiwanger RS. Regulation of Notch Function by O-Glycosylation. *Adv Exp Med Biol*. 2018;1066:59-78. doi:10.1007/978-3-319-89512-3

43. Gordon WR, Arnett KL, Blacklow SC. The molecular logic of Notch signaling - a structural and biochemical perspective. *J Cell Sci*. 2008;121(19):3109-3119. doi:10.1242/jcs.035683

44. Tagami S, Okochi M, Yanagida K, et al. Regulation of Notch Signaling by Dynamic Changes in the Precision of S3 Cleavage of Notch-1. *Mol Cell Biol*. 2008;28(1):165-176. doi:10.1128/mcb.00863-07

45. Schnute B, Troost T, Klein T. Endocytic Trafficking of the Notch Receptor. *Adv Exp Med Biol*. 2018;1066:99-122. doi:10.1007/978-3-319-89512-3_6

46. Okochi M, Steiner H, Fukumori A, et al. Presenilins mediate a dual intramembranous γ-secretase cleavage of Notch-1. *EMBO J*. 2002;21(20):5408-5416. doi:10.1093/emboj/cdf541

47. Okochi M, Fukumori A, Jiang J, et al. Secretion of the Notch-1 Aβ-like Peptide during Notch Signaling. *J Biol Chem*. 2006;281(12):7890-7898. doi:10.1074/jbc.M513250200

48. Kato H, Taniguchi Y, Kurooka H, et al. Involvement of RBP-J in biological functions of mouse Notch1 and its derivatives. *Development*. 1997;124(20):4133-4141.

49. Zweifel ME, Leahy DJ, Hughson FM, Barrick D. Structure and stability of the ankyrin domain of the Drosophila Notch receptor. *Protein Sci*. 2009;12(11):2622-2632. doi:10.1110/ps.03279003

50. Kopan R, Nye JS, Weintraub H. The intracellular domain of mouse Notch: A constitutively activated repressor of myogenesis directed at the basic helix-loop-helix region of MyoD. *Development*. 1994;120(9):2385-2396.

51. Nam Y, Weng AP, Aster JC, Blacklow SC. Structural requirements for assembly of the CSL-intracellular Notch1-Mastermind-like 1 transcriptional activation complex. *J Biol Chem*. 2003;278(23):21232-21239. doi:10.1074/jbc.M301567200

52. Kurooka H, Kuroda K, Honjo T. Roles of the ankyrin repeats and C-terminal region of the mouse Notch1 intracellular region. *Nucleic Acids Res*. 1998;26(23):5448-5455. doi:10.1093/nar/26.23.5448

53. Aster JC, Xu L, Karnell FG, Patriub V, Pui JC, Pear WS. Essential Roles for Ankyrin Repeat and Transactivation Domains in Induction of T-Cell Leukemia by Notch1. *Mol Cell Biol*. 2000;20(20):7505-7515. doi:10.1128/mcb.20.20.7505-7515.2000

54. Gerhardt DM, Pajcini K V., D'altri T, et al. The Notch1 transcriptional activation domain is required for development and reveals a novel role for Notch1 signaling in fetal hematopoietic stem cells. *Genes Dev*. 2014;28(6):576-593. doi:10.1101/gad.227496.113

55. Kurooka H, Honjo T. Functional Interaction between the Mouse Notch1 Intracellular Region and Histone Acetyltransferases PCAF and GCN5. *J Biol Chem*. 2000;275(22):17211-17220. doi:10.1074/jbc.M000909200

56. Wallberg AE, Pedersen K, Lendahl U, Roeder RG. p300 and PCAF Act Cooperatively To Mediate Transcriptional Activation from Chromatin Templates by Notch Intracellular Domains In Vitro. *Mol Cell Biol*. 2002;22(22):7812-7819. doi:10.1128/mcb.22.22.7812-7819.2002

57. Antfolk D, Antila C, Kemppainen K, Landor SKJ, Sahlgren C. Decoding the PTM-switchboard of Notch. *Biochim Biophys Acta - Mol Cell Res*. 2019;1866(12):118507. doi:10.1016/j.bbamcr.2019.07.002

58. Stifani S, Blaumueller CM, Redhead NJ, Hill RE, Artavanis-Tsakonas S. Human homologs of a Drosophila Enhancer of Split gene product define a novel family of nuclear proteins. *Nat Genet*. 1992;2(2):119-127. doi:10.1038/ng1092-119

59. Öberg C, Li J, Pauley A, Wolf E, Gurney M, Lendahl U. The Notch Intracellular Domain is Ubiquitinated and Negatively Regulated by the Mammalian Sel-10 Homolog. *J Biol Chem*. 2001;276(38):35847-35853. doi:10.1074/jbc.M103992200

60. Gupta-Rossi N, Le Bail O, Gonen H, et al. Functional Interaction between SEL-10, an F-box Protein, and the Nuclear Form of Activated Notch1 Receptor. *J Biol Chem*. 2001;276(37):34371-34378. doi:10.1074/jbc.M101343200

61. Oswald F, Täuber B, Dobner T, et al. p300 Acts as a Transcriptional Coactivator for Mammalian Notch-1. *Mol Cell Biol*. 2001;21(22):7761-7774. doi:10.1128/mcb.21.22.7761-7774.2001

62. Masuda S, Kumano K, Shimizu K, et al. Notch 1 oncoprotein antagonizes TGF-β/Smad-mediated cell growth suppression via sequestration of coactivator p300. *Cancer Sci*. 2005;96(5):274-282. doi:10.1111/j.1349-7006.2005.00048.x

63. Lubman OY, Korolev S V., Kopan R. Anchoring Notch genetics and biochemistry: Structural analysis of the ankyrin domain sheds light on existing data. *Mol Cell*. 2004;13(5):619-626. doi:10.1016/S1097-2765(04)00120-0

64. Zweifel ME, Barrick D. Studies of the ankyrin repeats of the Drosophila melanogaster Notch receptor. 2. Solution stability and cooperativity of unfolding. *Biochemistry*. 2001;40(48):14357-14367. doi:10.1021/bi011436+

65. Hozumi K. Distinctive properties of the interactions between Notch and Notch ligands. *Dev Growth Differ*. 2020;62(1):49-58. doi:10.1111/dgd.12641

66. Artavanis-Tsakonas S, Matsuno K, Fortini ME. Notch signaling. *Science*. 1995;268(5208):225-232. doi:10.1126/science.7716513

67. Uyttendaele H, Marazzi G, Wu G, Yan Q, Sassoon D, Kitajewski J. Notch4/int-3, a mammary proto-oncogene, is an endothelial cell-specific mammalian Notch gene. *Development*. 1996;122(7):2251-2259.

68. Fleming RJ. Structural conservation of Notch receptors and ligands. *Semin Cell Dev Biol*. 1998;9(6):599-607. doi:10.1006/scdb.1998.0260

69. Weinmaster G, Roberts VJ, Lemke G. Notch2: a second mammalian Notch gene. *Development*. 1992;116(4):931-941.

70. James AC, Szot JO, Iyer K, et al. Notch4 reveals a novel mechanism regulating Notch signal transduction. *Biochim Biophys Acta*. 2014;1843(7):1272-1284. doi:10.1016/j.bbamcr.2014.03.015

71. Uyttendaele H, Closson V, Wu G, Roux F, Weinmaster G, Kitajewski J. Notch4 and Jagged-1 induce microvessel differentiation of rat brain endothelial cells. *Microvasc Res*. 2000;60(2):91-103. doi:10.1006/mvre.2000.2254

72. Shawber CJ, Das I, Francisco E, Kitajewski J. Notch Signaling in Primary Endothelial Cells. *Ann N Y Acad Sci*. 2003;995:162-170. doi:10.1111/j.1749-6632.2003.tb03219.x

73. Shawber CJ, Funahashi Y, Francisco E, et al. Notch alters VEGF responsiveness in human and murine endothelial cells by direct regulation of VEGFR-3 expression. *J Clin Invest*. 2007;117(11):3369-3382. doi:10.1172/JCI24311

74. Weng AP, Adolfo FA, Lee W, et al. Activating Mutations of NOTCH1 in Human T Cell Acute Lymphoblastic Leukemia Downloaded from. *Science*.

2004;306(5694):269-271. doi:10.1126/science.1102160

75. Berry LW, Westlund B, Schedl T. Germ-line tumor formation caused by activation of glp-1, a Caenorhabditis elegans member of the Notch family of receptors. *Development*. 1997;124(4):925-936.

76. Chapman G, Sparrow DB, Kremmer E, Dunwoodie SL. Notch inhibition by the ligand Delta-Like 3 defines the mechanism of abnormal vertebral segmentation in spondylocostal dysostosis. *Hum Mol Genet*. 2011;20(5):905-916. doi:10.1093/hmg/ddq529

77. Ladi E, Nichols JT, Ge W, et al. The divergent DSL ligand Dll3 does not activate Notch signaling but cell autonomously attenuates signaling induced by other DSL ligands. *J Cell Biol*. 2005;170(6):983-992. doi:10.1083/jcb.200503113

78. Henderson ST, Gao D, Christensen S, Kimble J. Functional Domains of LAG-2, a Putative Signaling Ligand for LIN-12 and GLP-1 Receptors in Caenorhabditis elegans. *Mol Biol Cell*. 1997;8(9):1751-1762. doi:10.1091/mbc.8.9.1751

79. Chillakuri CR, Sheppard D, Ilagan MXG, et al. Structural Analysis Uncovers Lipid-Binding Properties of Notch Ligands. *Cell Rep*. 2013;5(4):861-867. doi:10.1016/j.celrep.2013.10.029

80. Henderson ST, Gao D, Lambie EJ, Kimble J. lag-2 may encode a signaling ligand for the GLP-1 and LIN-12 receptors of C. elegans. *Development*. 1994;120(10):2913-2924.

81. Handford PA, Korona B, Suckling R, Redfield C, Lea SM. Structural Insights into Notch Receptor-Ligand Interactions. *Adv Exp Med Biol*. 2018;1066:33-46. doi:10.1007/978-3-319-89512-3_2

82. Xu A, Lei L, Irvine KD. Regions of Drosophila Notch that Contribute to Ligand Binding and the Modulatory Influence of Fringe. *J Biol Chem*. 2005;280(34):30158-30165. doi:10.1074/jbc.M505569200

83. Kakuda S, Haltiwanger RS. Deciphering the Fringe-Mediated Notch Code: Identification of Activating and Inhibiting Sites Allowing Discrimination between Ligands. *Dev Cell*. 2017;40(2):193-201. doi:10.1016/j.devcel.2016.12.013

84. Pandey A, Harvey BM, Lopez MF, Ito A, Haltiwanger RS, Jafar-Nejad H. Glycosylation of Specific Notch EGF Repeats by O-Fut1 and Fringe Regulates Notch Signaling in Drosophila. *Cell Rep*. 2019;29(7):2054-2066.e6. doi:10.1016/j.celrep.2019.10.027

85. Schneider M, Kumar V, Nordstrøm LU, et al. Inhibition of Delta-induced Notch signaling using fucose analogs. *Nat Chem Biol*. 2018;14(1):65-71. doi:10.1038/nchembio.2520

86. Luca VC, Kim BC, Ge C, et al. Notch-Jagged complex structure implicates a catch bond in tuning ligand sensitivity. *Science*. 2017;355(6331):1320-1324. doi:10.1126/science.aaf9739

87. Yamamoto S, Charng WL, Rana NA, et al. A Mutation in EGF Repeat-8 of Notch Discriminates Between Serrate/Jagged and Delta Family Ligands. *Science*. 2012;338(6111):1229-1232. doi:10.1126/science.1228745

88. Andrawes MB, Xu X, Liu H, et al. Intrinsic Selectivity of Notch1 for Delta-like 4 over Delta-like 1. *J Biol Chem*. 2013;288(35):25477-25489. doi:10.1074/jbc.M113.454850

89. Luca VC, Jude KM, Pierce NW, Nachury M V., Fischer S, Garcia KC. Structural basis for Notch1 engagement of Delta-like 4. *Science*. 2015;347(6224):847-853. doi:10.1126/science.1261093

90. Chen H, Fre S, Slepnev VI, et al. Epsin is an EH-domain-binding protein implicated in clathrin-mediated endocytosis. *Nature*. 1998;394(6695):793-797. doi:10.1038/29555

91. Langridge PD, Struhl G. Epsin-Dependent Ligand Endocytosis Activates Notch by Force. *Cell*. 2017;171(6):1383-1396.e12. doi:10.1016/j.cell.2017.10.048

92. Hansson EM, Lanner F, Das D, et al. Control of Notch-ligand endocytosis by ligand-receptor interaction. *J Cell Sci*. 2010;123(17):2931-2942. doi:10.1242/jcs.073239

93. Musse AA, Meloty-Kapella L, Weinmaster G. Notch ligand endocytosis: Mechanistic basis of signaling activity. *Semin Cell Dev Biol*. 2012;23(4):429-436.

doi:10.1016/j.semcdb.2012.01.011

94. Parks AL, Klueg KM, Stout JR, Muskavitch MAT. Ligand endocytosis drives receptor dissociation and activation in the Notch pathway. *Development*. 2000;127(7):1373-1385.

95. Nichols JT, Miyamoto A, Olsen SL, D'Souza B, Yao C, Weinmaster G. DSL ligand endocytosis physically dissociates Notch1 heterodimers before activating proteolysis can occur. *J Cell Biol*. 2007;176(4):445-458. doi:10.1083/jcb.200609014

96. Lovendahl KN, Blacklow SC, Gordon WR. The Molecular Mechanism of Notch Activation. *Adv Exp Med Biol*. 2018;1066:47-58. doi:10.1007/978-3-319-89512-3_3

97. Stephenson NL, Avis JM. Direct observation of proteolytic cleavage at the S2 site upon forced unfolding of the Notch negative regulatory region. *Proc Natl Acad Sci U S A*. 2012;109(41). doi:10.1073/pnas.1205788109

98. Mumm JS, Schroeter EH, Saxena MT, et al. A Ligand-Induced Extracellular Cleavage Regulates γ-Secretase-like Proteolytic Activation of Notch1. *Mol Cell*. 2000;5(2):197-206. doi:10.1016/S1097-2765(00)80416-5

99. Bozkulak EC, Weinmaster G. Selective Use of ADAM10 and ADAM17 in Activation of Notch1 Signaling. *Mol Cell Biol*. 2009;29(21):5679-5695. doi:10.1128/mcb.00406-09

100. Delwig A, Rand MD. Kuz and TACE can activate Notch independent of ligand. *Cell Mol Life Sci*. 2008;65(14):2232-2243. doi:10.1007/s00018-008-8127-x

101. Hartmann D, Strooper B de, Serneels L, et al. The disintegrin/metalloprotease ADAM 10 is essential for Notch signalling but not for α-secretase activity in fibroblasts. *Hum Mol Genet*. 2002;11(21):2615-2624. doi:10.1093/hmg/11.21.2615

102. van Tetering G, van Diest P, Verlaan I, van der Wall E, Kopan R, Vooijs M. Metalloprotease ADAM10 is Required for Notch1 Site 2 Cleavage. *J Biol Chem*. 2009;284(45):31018-31027. doi:10.1074/jbc.M109.006775

103. Brou C, Logeat F, Gupta N, et al. A Novel Proteolytic Cleavage Involved in Notch Signaling: The Role of the Disintegrin-Metalloprotease TACE. *Mol Cell*. 2000;5(2):207-216. doi:10.1016/S1097-2765(00)80417-7

104. Jorissen E, De Strooper B. γ-Secretase and the Intramembrane Proteolysis of Notch. *Curr Top Dev Biol*. 2010;92:201-230. doi:10.1016/S0070-2153(10)92006-1

105. De Strooper B, Annaert W, Cupers P, et al. A presenilin-1-dependent γ-secretase-like protease mediates release of notch intracellular domain. *Nature*. 1999;398(6727):518-522. doi:10.1038/19083

106. Struhl G, Greenwald I. Presenilin is required for activity and nuclear access of Notch in Drosophila. *Nature*. 1999;398(6727):522-525. doi:10.1038/19091

107. Struhl G, Adachi A. Requirements for Presenilin-Dependent Cleavage of Notch and Other Transmembrane Proteins. *Mol Cell*. 2000;6(3):625-636. doi:10.1016/S1097-2765(00)00061-7

108. Chandu D, Huppert SS, Kopan R. Analysis of transmembrane domain mutants is consistent with sequential cleavage of Notch by γ-secretase. *J Neurochem*. 2006;96(1):228-235. doi:10.1111/j.1471-4159.2005.03547.x

109. Zheng L, Saunders CA, Sorensen EB, Waxmonsky NC, Conner SD. Notch signaling from the endosome requires a conserved dileucine motif. *Mol Biol Cell*. 2013;24(3):297-307. doi:10.1091/mbc.E12-02-0081

110. Conner SD. *Regulation of Notch Signaling Through Intracellular Transport*. Vol 323. Elsevier Inc.; 2016. doi:10.1016/bs.ircmb.2015.12.002

111. Baron M. Endocytic routes to Notch activation. *Semin Cell Dev Biol*. 2012;23(4):437-442. doi:10.1016/j.semcdb.2012.01.008

112. Yamamoto S, Charng WL, Bellen HJ. Endocytosis and Intracellular Trafficking of Notch and its Ligands. *Curr Top Dev Biol*. 2010;92:165-200. doi:10.1016/S0070-2153(10)92005-X

113. Sachan N, Mishra AK, Mutsuddi M, Mukherjee A. The Drosophila Importin-α3 Is

Required for Nuclear Import of Notch In Vivo and It Displays Synergistic Effects with Notch Receptor on Cell Proliferation. *PLoS One*. 2013;8(7). doi:10.1371/journal.pone.0068247

114. Huenniger K, Krämer A, Soom M, et al. Notch1 signaling is mediated by importins alpha 3, 4, and 7. *Cell Mol Life Sci*. 2010;67(18):3187-3196. doi:10.1007/s00018-010-0378-7

115. Kovall RA, Hendrickson WA. Crystal structure of the nuclear effector of Notch signaling, CSL, bound to DNA. *EMBO J*. 2004;23(17):3441-3451. doi:10.1038/sj.emboj.7600349

116. Kovall RA, Blacklow SC. Mechanistic Insights into Notch Receptor Signaling from Structural and Biochemical Studies. *Curr Top Dev Biol*. 2010;92:31-71. doi:10.1016/S0070-2153(10)92002-4

117. Wilson JJ, Kovall RA. Crystal Structure of the CSL-Notch-Mastermind Ternary Complex Bound to DNA. *Cell*. 2006;124(5):985-996. doi:10.1016/j.cell.2006.01.035

118. Waltzer L, Bourillot PY, Sergeant A, Manet E. RBP-Jk repression activity is mediated by a co-repressor and antagonized by the Epstein-Barr virus transcription factor EBNA2. *Nucleic Acids Res*. 1995;23(24):4939-4945. doi:10.1093/nar/23.24.4939

119. Oswald F, Kovall RA. CSL-Associated Corepressor and Coactivator Complexes. *Adv Exp Med Biol*. 2018;1066:279-295. doi:10.1007/978-3-319-89512-3

120. Contreras-Cornejo H, Saucedo-Correa G, Oviedo-Boyso J, et al. The CSL proteins, versatile transcription factors and context dependent corepressors of the notch signaling pathway. *Cell Div*. 2016;11(1):1-11. doi:10.1186/s13008-016-0025-2

121. Borggrefe T, Oswald F. The Notch signaling pathway: Transcriptional regulation at Notch target genes. *Cell Mol Life Sci*. 2009;66(10):1631-1646. doi:10.1007/s00018-009-8668-7

122. Fortini ME, Artavanis-Tsakonas S. The Suppressor of Hairless Protein

Participates in Notch Receptor Signaling. *Cell*. 1994;79(2):273-282. doi:10.1016/0092-8674(94)90196-1

123. Lecourtois M, Schweisguth F. The neurogenic suppressor of hairless DNA-binding protein mediates the transcriptional activation of the enhancer of split complex genes triggered by Notch signaling. *Genes Dev*. 1995;9(21):2598-2608. doi:10.1101/gad.9.21.2598

124. Furukawa T, Tamura K, Kawaichi M, et al. Suppressor of Hairless, the Drosophila homologue of RBP-Jκ, transactivates the neurogenic gene E(spl)m8. *Japanese J Genet*. 1995;70(4):505-524. doi:10.1266/jjg.70.505

125. Lubman OY, Ilagan MXG, Kopan R, Barrick D. Quantitative Dissection of the Notch:CSL Interaction: Insights into the Notch-mediated Transcriptional Switch. *J Mol Biol*. 2007;365(3):577-589. doi:10.1016/j.jmb.2006.09.071

126. Nam Y, Sliz P, Song L, Aster JC, Blacklow SC. Structural Basis for Cooperativity in Recruitment of MAML Coactivators to Notch Transcription Complexes. *Cell*. 2006;124(5):973-983. doi:10.1016/j.cell.2005.12.037

127. Del Bianco C, Aster JC, Blacklow SC. Mutational and Energetic Studies of Notch1 Transcription Complexes. *J Mol Biol*. 2008;376(1):131-140. doi:10.1016/j.jmb.2007.11.061

128. Friedmann DR, Wilson JJ, Kovall RA. RAM-induced Allostery Facilitates Assembly of a Notch Pathway Active Transcription Complex. *J Biol Chem*. 2008;283(21):14781-14791. doi:10.1074/jbc.M709501200

129. Lin S-E, Oyama T, Nagase T, Harigaya K, Kitagawa M. Identification of New Human Mastermind Proteins Defines a Family That Consists of Positive Regulators for Notch Signaling. *J Biol Chem*. 2002;277(52):50612-50620. doi:10.1074/jbc.M209529200

130. Kitagawa M. Notch signalling in the nucleus: roles of Mastermind-like (MAML) transcriptional coactivators. *J Biochem*. 2015;159(3):287-294. doi:10.1093/jb/mvv123

131. Fryer CJ, Lamar E, Turbachova I, Kintner C, Jones KA. Mastermind mediates

chromatin-specific transcription and turnover of the notch enhancer complex. *Genes Dev*. 2002;16(11):1397-1411. doi:10.1101/gad.991602

132. Saint Just Ribeiro M, Hansson ML, Wallberg AE. A proline repeat domain in the Notch co-activator MAML1 is important for the p300-mediated acetylation of MAML1. *Biochem J*. 2007;404(2):289-298. doi:10.1042/BJ20061900

133. Weaver KL, Alves-Guerra MC, Jin K, et al. NACK Is an Integral Component of the Notch Transcriptional Activation Complex and Is Critical for Development and Tumorigenesis. *Cancer Res*. 2014;74(17):4741-4751. doi:10.1158/0008-5472.CAN-14-1547

134. Jin K, Zhou W, Han X, et al. Acetylation of Mastermind-like 1 by p300 Drives the Recruitment of NACK to Initiate Notch-Dependent Transcription. *Cancer Res*. 2017;77(16):4228-4237. doi:10.1158/0008-5472.CAN-16-3156

135. Carrieri FA, Dale JK. Turn It Down a Notch. *Front Cell Dev Biol*. 2017;4(151):1-9. doi:10.3389/fcell.2016.00151

136. Carrieri FA, Murray PJ, Ditsova D, Ferris MA, Davies P, Dale JK. CDK 1 and CDK 2 regulate NICD1 turnover and the periodicity of the segmentation clock. *EMBO Rep*. 2019;20(7):1-22. doi:10.15252/embr.201846436

137. Fryer CJ, White JB, Jones KA, Jolla L. Mastermind Recruits CycC:CDK8 to Phosphorylate the Notch ICD and Coordinate Activation with Turnover. *Molcular Cell*. 2004;16(4):509-520. doi:10.1016/j.molcel.2004.10.014

138. Jin YH, Kim H, Oh M, Ki H, Kim K. Regulation of Notch1/NICD and Hes1 Expressions by GSK-3α/β. *Mol Cells*. 2009;27(1):15-19. doi:10.1007/s10059-009-0001-7

139. Espinosa L, Inglés-Esteve J, Aguilera C, Bigas A. Phosphorylation by Glycogen Synthase Kinase-3β Down-regulates Notch Activity, a Link for Notch and Wnt Pathways. *J Biol Chem*. 2003;278(34):32227-32235. doi:10.1074/jbc.M304001200

140. Kim WY, Wang X, Wu Y, et al. GSK-3 is a master regulator of neural progenitor homeostasis. *Nat Neurosci*. 2009;12(11):1390-1397. doi:10.1038/nn.2408

141. Orlicky S, Tang X, Willems A, Tyers M, Sicheri F. Structural Basis for Phosphodependent Substrate Selection and Orientation by the SCF/Cdc4 Ubiquitin Ligase. *Cell*. 2003;112(2):243-256. doi:10.1016/S0092-8674(03)00034-5

142. Wu G, Lyapina S, Das I, et al. SEL-10 Is an Inhibitor of Notch Signaling That Targets Notch for Ubiquitin-Mediated Protein Degradation. *Mol Cell Biol*. 2001;21(21):7403-7415. doi:10.1128/mcb.21.21.7403-7415.2001

143. Tsunematsu R, Nakayama K, Oike Y, et al. Mouse Fbw7/Sel-10/Cdc4 Is Required for Notch Degradation during Vascular Development. *J Biol Chem*. 2004;279(10):9417-9423. doi:10.1074/jbc.M312337200

144. O'Neil J, Grim J, Strack P, et al. FBW7 mutations in leukemic cells mediate NOTCH pathway activation and resistance to γ-secretase inhibitors. *J Exp Med*. 2007;204(8):1813-1824. doi:10.1084/jem.20070876

145. Tetzlaff MT, Yu W, Li M, et al. Defective cardiovascular development and elevated cyclin E and Notch proteins in mice lacking the Fbw7 F-box protein. *Proc Natl Acad Sci U S A*. 2004;101(10):3338-3345. doi:10.1073/pnas.0307875101

146. Hubbard EJA, Wu G, Kitajewski J, Greenwald I. sel-10, a negative regulator of lin-12 activity in Caenorhabditis elegans, encodes a member of the CDC4 family of proteins. *Genes Dev*. 1997;11(23):3182-3193. doi:10.1101/gad.11.23.3182

147. Chiang MY, Xu ML, Histen G, et al. Identification of a Conserved Negative Regulatory Sequence That Influences the Leukemogenic Activity of NOTCH1. *Mol Cell Biol*. 2006;26(16):6261-6271. doi:10.1128/mcb.02478-05

148. Broadus MR, Chen TW, Neitzel LR, et al. Identification of a Paralog-Specific Notch1 Intracellular Domain Degron. *Cell Rep*. 2016;15(9):1920-1929. doi:10.1016/j.celrep.2016.04.070

149. Qiu L, Joazeiro C, Fang N, et al. Recognition and ubiquitination of Notch by Itch, a Hect-type E3 ubiquitin ligase. *J Biol Chem*. 2000;275(46):35734-35737. doi:10.1074/jbc.M007300200

150. Cornell M, Evans DAP, Mann R, et al. The Drosophila melanogaster Suppressor of deltex Gene, a Regulator of the Notch Receptor Signaling Pathway, Is an E3 Class Ubiquitin Ligase. *Genetics*. 1999;152(2):567-576.

151. Chastagner P, Israel A, Brou C. AIP4/Itch Regulates Notch Receptor Degradation in the Absence of Ligand. *PLoS One*. 2008;3(7):e2735. doi:10.1371/journal.pone.0002735

152. McGill MA, McGlade CJ. Mammalian Numb Proteins Promote Notch1 Receptor Ubiquitination and Degradation of the Notch1 Intracellular Domain. *J Biol Chem*. 2003;278(25):23196-23203. doi:10.1074/jbc.M302827200

153. Puca L, Chastagner P, Meas-Yedid V, Israël A, Brou C. α-arrestin 1 (ARRDC1) and β-arrestins cooperate to mediate Notch degradation in mammals. *J Cell Sci*. 2013;126(19):4457-4468. doi:10.1242/jcs.130500

154. Mo J-S, Kim M-Y, Han S-O, et al. Integrin-Linked Kinase Controls Notch1 Signaling by Down-Regulation of Protein Stability through Fbw7 Ubiquitin Ligase. *Mol Cell Biol*. 2007;27(15):5565-5574. doi:10.1128/mcb.02372-06

155. Rallis C, Pinchin SM, Ish-Horowicz D. Cell-autonomous integrin control of Wnt and Notch signalling during somitogenesis. *Development*. 2010;137(21):3591-3601. doi:10.1242/dev.050070

156. Sutherland C, Leighton IA, Cohen P. Inactivation of glycogen synthase kinase-3β by phosphorylation: new kinase connections in insulin and growth-factor signalling. *Biochem J*. 1993;296(1):15-19. doi:10.1042/bj2960015

157. Lafoya B, Munroe JA, Pu X, Albig AR. Src kinase phosphorylates Notch1 to inhibit MAML binding. *Sci Rep*. 2018;8(1):1-12. doi:10.1038/s41598-018-33920-y

158. Davis RL, Turner DL. Vertebrate hairy and Enhancer of split related proteins: transcriptional repressors regulating cellular differentiation and embryonic patterning. *Oncogene*. 2001;20(58):8342-8357. doi:10.1038/sj.onc.1205094

159. Fischer A, Gessler M. Delta-Notch-and then? Protein interactions and proposed modes of repression by Hes and Hey bHLH factors. *Nucleic Acids Res*.

2007;35(14):4583-4596. doi:10.1093/nar/gkm477

160. Friedmann DR, Kovall RA. Thermodynamic and structural insights into CSL-DNA complexes. *Protein Sci*. 2010;19(1):34-46. doi:10.1002/pro.280

161. Del Bianco C, Vedenko A, Choi SH, et al. Notch and MAML-1 complexation do not detectably alter the DNA binding specificity of the transcription factor CSL. *PLoS One*. 2010;5(11). doi:10.1371/journal.pone.0015034

162. Shimizu K, Chiba S, Saito T, et al. Functional Diversity among Notch1, Notch2, and Notch3 Receptors. *Biochem Biophys Res Commun*. 2002;291(4):775-779. doi:10.1006/bbrc.2002.6528

163. Ehebauer MT, Chirgadze DY, Hayward P, Martinez Arias A, Blundell TL. High-resolution crystal structure of the human Notch 1 ankyrin domain. *Biochem J*. 2005;392(1):13-20. doi:10.1042/bj20050515

164. Reynolds CR, Islam SA, Sternberg MJE. EzMol: A Web Server Wizard for the Rapid Visualization and Image Production of Protein and Nucleic Acid Structures. *J Mol Biol*. 2018;430(15):2244-2248. doi:10.1016/j.jmb.2018.01.013

165. Koch U, Radtke F. Mechanisms of T Cell Development and Transformation. *Annu Rev Cell Dev Biol*. 2011;27(1):539-562. doi:10.1146/annurev-cellbio-092910-154008

166. Radtke F, Fasnacht N, MacDonald HR. Notch Signaling in the Immune System. *Immunity*. 2010;32(1):14-27. doi:10.1016/j.immuni.2010.01.004

167. McCarter AC, Wang Q, Chiang M. Notch in Leukemia. *Adv Exp Med Biol*. 2018;1066:355-394. doi:10.1007/978-3-319-89512-3

168. Reizis B, Leder P. Direct induction of T lymphocyte-specific gene expression by the mammalian Notch signaling pathway. *Genes Dev*. 2002;16(3):295-300. doi:10.1101/gad.960702

169. Yashiro-Ohtani Y, Wang H, Zang C, et al. Long-range enhancer activity determines Myc sensitivity to Notch inhibitors in T cell leukemia. *Proc Natl Acad Sci U S A*. 2014;111(46):E4946-E4953. doi:10.1073/pnas.1407079111

170. Wang H, Zou J, Zhao B, et al. Genome-wide analysis reveals conserved and divergent features of Notch1/RBPJ binding in human and murine T-lymphoblastic leukemia cells. *Proc Natl Acad Sci U S A*. 2011;108(36):14908-14913. doi:10.1073/pnas.1109023108

171. Li Y, Hibbs MA, Gard AL, Shylo NA, Yun K. Genome-Wide Analysis of N1ICD/RBPJ Targets in Vivo Reveals Direct Transcriptional Regulation of Wnt, SHH, and Hippo Pathway Effectors by Notch1. *Stem Cells*. 2012;30(4):741-752. doi:10.1002/stem.1030

172. van Heeringen SJ, Veenstra GJC. GimmeMotifs: a de novo motif prediction pipeline for ChIP-sequencing experiments. *Bioinformatics*. 2011;27(2):270-271. doi:10.1093/bioinformatics/btq636

173. van Steensel B, Henikoff S. Identification of in vivo DNA targets of chromatin proteins using tethered Dam methyltransferase. *Nat Biotechnol*. 2000;18(4):424-428. doi:10.1038/74487

174. Heinz S, Benner C, Spann N, et al. Simple Combinations of Lineage-Determining Transcription Factors Prime cis-Regulatory Elements Required for Macrophage and B Cell Identities. *Mol Cell*. 2010;38(4):576-589. doi:10.1016/j.molcel.2010.05.004

175. Wang H, Zang C, Taing L, et al. NOTCH1-RBPJ complexes drive target gene expression through dynamic interactions with superenhancers. *Proc Natl Acad Sci U S A*. 2014;111(2):705-710. doi:10.1073/pnas.1315023111

176. Palomero T, Barnes KC, Real PJ, et al. CUTLL1, a novel human T-cell lymphoma cell line with t(7;9) rearrangement, aberrant NOTCH1 activation and high sensitivity to γ-secretase inhibitors. *Leukemia*. 2006;20(7):1279-1287. doi:10.1038/sj.leu.2404258

177. Cuddapah S, Jothi R, Schones DE, Roh TY, Cui K, Zhao K. Global analysis of the insulator binding protein CTCF in chromatin barrier regions reveals demarcation of active and repressive domains. *Genome Res*. 2009;19(1):24-32. doi:10.1101/gr.082800.108

178. Handoko L, Xu H, Li G, et al. CTCF-mediated functional chromatin interactome in pluripotent cells. *Nat Genet*. 2011;43(7):630-638. doi:10.1038/ng.857

179. Hawkins RD, Hon GC, Yang C, et al. Dynamic chromatin states in human ES cells reveal potential regulatory sequences and genes involved in pluripotency. *Cell Res*. 2011;21(10):1393-1409. doi:10.1038/cr.2011.146

180. Braccioli L, De Wit E. CTCF: A Swiss-army knife for genome organization and transcription regulation. *Essays Biochem*. 2019;63(1):157-165. doi:10.1042/EBC20180069

181. Pear WS, Aster JC, Scott ML, et al. Exclusive Development of T cell Neoplasms in Mice Transplanted with Bone Marrow Expressing Activated Notch Alleles. *J Exp Med*. 1996;183(5):2283-2291. doi:10.1084/jem.183.5.2283

182. Weng AP, Nam Y, Wolfe MS, et al. Growth Suppression of Pre-T Acute Lymphoblastic Leukemia Cells by Inhibition of Notch Signaling. *Mol Cell Biol*. 2003;23(2):655-664. doi:10.1128/mcb.23.2.655-664.2003

183. Jeffries S, Robbins DJ, Capobianco AJ. Characterization of a High-Molecular-Weight Notch Complex in the Nucleus of NotchIC-Transformed RKE Cells and in a Human T-Cell Leukemia Cell Line. *Mol Cell Biol*. 2002;22(11):3927-3941. doi:10.1128/mcb.22.11.3927-3941.2002

184. Zhou S, Fujimuro M, Hsieh JJ-D, et al. SKIP, a CBF1-Associated Protein, Interacts with the Ankyrin Repeat Domain of NotchIC To Facilitate NotchIC Function. *Mol Cell Biol*. 2000;20(7):2400-2410. doi:10.1128/mcb.20.7.2400-2410.2000

185. Brès V, Gomes N, Pickle L, Jones KA. A human splicing factor, SKIP, associates with P-TEFb and enhances transcription elongation by HIV-1 Tat. *Genes Dev*. 2005;19(10):1211-1226. doi:10.1101/gad.1291705

186. Aster JC, Pear WS. Notch signaling in leukemia. *Curr Opin Hematol*. 2001;8(4):237-244. doi:10.1097/00062752-200107000-00010

187. Yatim A, Benne C, Sobhian B, et al. NOTCH1 Nuclear Interactome Reveals Key Regulators of Its Transcriptional Activity and Oncogenic Function. *Mol Cell*.

2012;48(3):445-458. doi:10.1016/j.molcel.2012.08.022

188. Xiang J, Ouyang Y, Cui Y, et al. Silencing of Notch3 Using shRNA Driven by Survivin Promoter Inhibits Growth and Promotes Apoptosis of Human T-Cell Acute Lymphoblastic Leukemia Cells. *Clin Lymphoma, Myeloma Leuk*. 2012;12(1):59-65. doi:10.1016/j.clml.2011.07.005

189. Krebs LT, Xue Y, Norton CR, et al. Notch signaling is essential for vascular morphogenesis in mice. *Genes Dev*. 2000;14(11):1343-1352. doi:10.1101/gad.14.11.1343

190. Sweeney C, Morrow D, Birney YA, et al. Notch 1 and 3 receptors modulate vascular smooth muscle cell growth, apoptosis and migration via a CBF-1/RBP-Jk dependent pathway. *FASEB J*. 2004;18(12):1421-1423.

191. Aster JC, Bodnar N, Xu L, et al. Notch ankyrin repeat domain variation influences leukemogenesis and Myc transactivation. *PLoS One*. 2011;6(10). doi:10.1371/journal.pone.0025645

192. Jarrett SM, Seegar TCM, Andrews M, et al. Extension of the Notch intracellular domain ankyrin repeat stack by NRARP promotes feedback inhibition of Notch signaling. *Sci Signal*. 2019;12(606):1-11. doi:10.1126/scisignal.aay2369

193. Nandagopal N, Santat LA, LeBon L, Sprinzak D, Bronner ME, Elowitz MB. Dynamic Ligand Discrimination in the Notch Signaling Pathway. *Cell*. 2018;172(4):869-880.e19. doi:10.1016/j.cell.2018.01.002

194. Nandagopal N, Santat LA, Elowitz MB. Cis-activation in the Notch signaling pathway. *Elife*. 2019;8(e37880):1-34. doi:10.7554/eLife.37880

195. Bray SJ. Notch signalling in context. *Nat Rev Mol Cell Biol*. 2016;17(11):722-735. doi:10.1038/nrm.2016.94

196. Bellavia D, Checquolo S, Campese AF, Felli MP, Gulino A, Screpanti I. Notch3: from subtle structural differences to functional diversity. *Oncogene*. 2008;27(38):5092-5098. doi:10.1038/onc.2008.230

197. Shimizu K, Chiba S, Kumano K, et al. Mouse Jagged1 Physically Interacts with

Notch2 and Other Notch Receptors. *J Biol Chem*. 1999;274(46):32961-32969. doi:10.1074/jbc.274.46.32961

198. Zhang R, Engler A, Taylor V. Notch: an interactive player in neurogenesis and disease. *Cell Tissue Res*. 2018;371(1):73-89. doi:10.1007/s00441-017-2641-9

199. Gridley T. Notch signaling in vascular development and physiology. *Development*. 2007;134(15):2709-2718. doi:10.1242/dev.004184

200. Gridley T. Notch signaling in the vasculature. *Curr Top Dev Biol*. 2010;92:277-309. doi:10.1016/S0070-2153(10)92009-7

201. Andersson ER, Lendahl U. Therapeutic modulation of Notch signalling-are we there yet? *Nat Rev Drug Discov*. 2014;13(5):357-378. doi:10.1038/nrd4252

202. Aster JC. In Brief: Notch signalling in health and disease. *J Pathol*. 2014;232(1):1-3. doi:10.1002/path.4291

203. Kopan R, Ilagan MXG. The Canonical Notch Signaling Pathway: Unfolding the Activation Mechanism. *Cell*. 2009;137(2):216-233. doi:10.1016/j.cell.2009.03.045

204. Chowdhury F, Li ITS, Ngo TTM, et al. Defining single molecular forces required for Notch activation using nano yoyo. *Nano Lett*. 2016;16(6):3892-3897. doi:10.1021/acs.nanolett.6b01403

205. Kadesch T. Notch signaling: the demise of elegant simplicity. *Curr Opin Genet Dev*. 2004;14(5):506-512. doi:10.1016/j.gde.2004.07.007

206. Mattingly RR, Macara IG. Phosphorylation-dependent activation of the Ras-GRF-CDC25Mm exchange factor by muscarinic receptors and G-protein By subunits. *Nature*. 1996;382:268-272.

207. Carey MF, Peterson CL, Smale ST. Chromatin Immunoprecipitation (ChIP). *Cold Spring Harb Protoc*. 2009;4(9):1-9. doi:10.1101/pdb.prot5279

208. Wolberger C. Multiprotein-DNA Complexes in Transcriptional Regulation. *Annu Rev Biophys Biomol Struct*. 1999;28:29-56. doi:10.1146/annurev.biophys.28.1.29

209. Blain J, Bédard J, Thompson M, Boisvert FM, Boucher MJ. C-terminal deletion

of NOTCH1 intracellular domain (N1ICD) increases its stability but does not amplify and recapitulate N1ICD-dependent signalling. *Sci Rep*. 2017;7(1):1-11. doi:10.1038/s41598-017-05119-0

210. Murtaugh LC, Stanger BZ, Kwan KM, Melton DA. Notch signaling controls multiple steps of pancreatic differentiation. *Proc Natl Acad Sci U S A*. 2003;100(25):14920-14925. doi:10.1073/pnas.2436557100

211. Mumm JS, Schroeter EH, Saxena MT, et al. A ligand-induced extracellular cleavage regulates gamma-secretase-like proteolytic activation of Notch1. *Mol Cell*. 2000;5(2):197-206. doi:10.1016/s1097-2765(00)80416-5

212. Hsieh JJ, Henkel T, Salmon P, Robey E, Peterson MG, Hayward SD. Truncated mammalian Notch1 activates CBF1/RBPJk-repressed genes by a mechanism resembling that of Epstein-Barr virus EBNA2. *Mol Cell Biol*. 1996;16(3):952-959. doi:10.1128/mcb.16.3.952

213. Meitinger C, Strobl LJ, Marschall G, Bornkamm GW, Zimber-Strobl U. Crucial Sequences within the Epstein-Barr Virus TP1 Promoter for EBNA2-Mediated Transactivation and Interaction of EBNA2 with Its Responsive Element. *J Virol*. 1994;68(11):7497-7506. doi:10.1128/JVI.68.11.7497-7506.1994

214. Strobl LJ, Höfelmayr H, Stein C, et al. Both Epstein-Barr viral nuclear antigen 2 (EBNA2) and activated notch 1 transactivate genes by interacting with the cellular protein RBP-Jκ. *Immunobiology*. 1997;198(1-3):299-306. doi:10.1016/S0171-2985(97)80050-2

215. Nishimura M, Isaka F, Ishibashi M, et al. Structure, Chromosomal Locus, and Promoter of Mouse Hes2 Gene, a Homologue of Drosophila hairy and Enhancer of split. *Genomics*. 1998;49(1):69-75. doi:10.1006/geno.1998.5213

216. Saxena MT, Schroeter EH, Mumm JS, Kopan R. Murine Notch Homologs (N1-4) Undergo Presenilin-dependent Proteolysis. *J Biol Chem*. 2001;276(43):40268-40273. doi:10.1074/jbc.M107234200

217. Dhanesh SB, Subashini C, James J. Hes1: the maestro in neurogenesis. *Cell Mol Life Sci*. 2016;73(21):4019-4042. doi:10.1007/s00018-016-2277-z

218. Takebayashi K, Akazawa C, Nakanaishi S, Kageyama R. Structure and Promoter Analysis of the Gene Encoding the Mouse Helix-Loop-Helix Factor Hes-5. *J Biol Chem*. 1995;270(3):1342-1349. doi:10.1074/jbc.270.3.1342

219. Takebayashi K, Sasai Y, Sakai Y, Watanabe T, Nakanishi S, Kageyama R. Structure, chromosomal locus, and promoter analysis of the gene encoding the mouse helix-loop-helix factor HES-1. *J Biol Chem*. 1994;269(7):5150-5156.

220. Akazawa C, Sasai Y, Nakanishi S, Kageyama R. Molecular characterization of a rat negative regulator with a basic helix- loop-helix structure predominantly expressed in the developing nervous system. *J Biol Chem*. 1992;267(30):21879-21885.

221. Raffetseder U, Rauen T, Boor P, et al. Extracellular YB-1 blockade in experimental nephritis upregulates Notch-3 receptor expression and signaling. *Nephron - Exp Nephrol*. 2011;118(4):100-108. doi:10.1159/000324209

222. Hansson EM, Teixeira AI, Gustafsson M V, et al. Recording Notch Signaling in Real Time. *Dev Neurosci*. 2006;28(1-2):118-127. doi:10.1159/000090758

223. Hirata H, Yoshiura S, Ohtsuka T, et al. Oscillatory expression of the bHLH factor Hes1 regulated by a negative feedback loop. *Science*. 2002;298(840):840-843. doi:10.1126/science.1074560